Reliability of Concrete-Filled HSS Beam-Column Design Provisions

by

Sadaf Rahbari Manesh

Submitted in partial fulfilment of the requirements
for the degree of Master of Applied Science

at

Dalhousie University
Halifax, Nova Scotia
September 2022

TABLE OF CONTENTS

LIST OF TABLES

LIST OF FIGURES

ABSTRACT

Revisions were recently proposed by Tousignant & Packer (2022a,b) to the way in which concrete-filled hollow structural section (HSS) members are handled in CSA S16. These revisions were based on previous research, comparisons to experiments, and a first-order reliability method (FORM) analysis of existing provisions for compression and flexural members. Herein, this topic is further expanded by using Monte Carlo Simulations (MCS) to determine the inherent reliability of existing and recommended design rules for concrete-filled rectangular hollow section (RHS) and circular hollow section (CHS) beam-columns.

A review is given of the methods in use for determining the structural reliability of steel members and connections. Based on this, a reliability study is performed on the current CSA S16:19, AISC 360-16 and proposed design provisions by Tousignant & Packer (2022a,b).

A representative set of concrete-filled RHS and CHS members are analyzed with variations in concrete strength, wall slenderness, effective length, and loading eccentricity. Using MCS, the reliability index (β^+) of each is determined over a range of live-to-dead load (L/D) ratios. Inherent β^+-values are compared to the code-specified target (i.e., $\beta^+ = 3.0$ per Annex B of CSA S16:19 and Section B3.1 of the AISC Commentary). The effect of various member and loading parameters on the structural reliability is determined.

LIST OF ABBREVIATIONS AND SYMBOLS

AISC	=	American Institute of Steel Construction
ASCE	=	American Society of Civil Engineers
CIDECT	=	International Committee for the Development and Study of Tubular Construction
CISC	=	Canadian Institute of Steel Construction
CHS	=	Circular Hollow Steel section
COV	=	Coefficient of Variation
CSA	=	Canadian Standards Association
ERW	=	electric resistance welded
FORM	=	First Order Reliability Method
HSS	=	Hollow Structural Section
LRFD	=	Load and Resistance Factor Design
LSD	=	Limit State Design
MCS	=	Monte Carlo Simulations
RHS	=	Rectangular Hollow Steel section
ULS	=	Ultimate Limit State

A_g	=	gross cross-sectional area of composite section
A_c	=	cross-sectional area of concrete
A_s	=	cross-sectional area of steel
A_{sr}	=	cross-sectional area of steel reinforcement
A_{st}	=	area of steel section in tension
A_{srb}	=	area of steel reinforcement in bottom region
A_{src}	=	area of steel reinforcement in central region
A_{srt}	=	area of steel reinforcement in top region
C_2	=	ratio of average concrete stress to f_c' accounting for confinement effect
C_{ec}	=	Euler buckling strength
C_f	=	factored compressive force
C_{fs}	=	factored sustained axial load
C_p	=	nominal compressive resistance

C_r	=	compressive resistance of steel above neutral axis (in CSA S16:19 Clause 18.2.2)
C_r'	=	compressive resistance of concrete above neutral axis (in CSA S16:19 Clause 18.2.2)
C_{rc}	=	factored compressive resistance of composite section
C_{rcm}	=	factored compressive resistance that can coexist with M_{rc} when all of the cross section is in compression
C_{rco}	=	compressive resistance with $\lambda = 0$
D	=	dead load
E_s	=	modulus of elasticity of steel
E_{sr}	=	modulus of elasticity of steel reinforcement
E_c	=	modulus of elasticity of concrete
EI_e	=	effective flexural stiffness
F_y	=	yield stress of steel section
F_{yr}	=	yield strength of steel reinforcement
G	=	Safety margin
G_m	=	mean of the safety margin
I_c	=	moment of inertia of concrete
I_s	=	moment of inertia of steel
I_{sr}	=	moment of inertia of steel reinforcement
KL	=	effective length
L	=	live load; length of member
M_f	=	factored moment
M_n	=	nominal flexural strength
M_p	=	moment corresponding to plastic stress distribution over the composite cross-section
M_{rc}	=	factored bending resistance of composite section
M_{rr}	=	factored bending resistance of steel reinforcement
R	=	resistance
R_m	=	mean resistance
R_n	=	nominal resistance
S	=	load effect
S_m	=	mean load effect
T_r	=	tensile resistance of steel below neutral axis
V	=	coefficient of variation
V_G	=	coefficient of variation for geometric properties
V_M	=	coefficient of variation for material properties
V_P	=	coefficient of variation for professional factor
V_r	=	coefficient of variation for resistance

V_s	=	coefficient of variation for load effect
U_1	=	factor to account for moment gradient and for second order effect of axial force acting on deformed member
Z_c	=	plastic modulus of concrete
Z_s	=	plastic modulus of steel section
a	=	depth of concrete compression zone
b	=	width of RHS
b_c	=	width of concrete at the neutral axis
b_i	=	inner width of RHS (= $b - 2t$)
f_c'	=	concrete compressive strength
d	=	outside diameter of CHS
d_i	=	inner diameter of CHS
e	=	eccentricity; lever arm between C_r and T_r (in CSA S16:19 Clause 18.2.2)
e'	=	lever arm between C_r' and T_r
h	=	height of RHS
h_i	=	inner height of RHS (= $h - 2t$)
h_n	=	distance from the plastic neutral axis to cross-section's centre line
n	=	column curve parameter (= 1.80 for concrete-filled HSS) (in CSA S16:19 Clause 18.2.1); number of steel reinforcing bars
p_f	=	Probability of failure
r_i	=	inside corner radius of RHS
r_o	=	outside corner radius of RHS
t	=	wall thickness
α_1	=	ratio of average stress block to f_c'
β	=	coefficient for bending in beam-columns; angle in radians
β^+	=	reliability index
γ_0	=	angular location of the neutral axis
δ	=	bias coefficient
δ_G	=	bias coefficient for geometric properties
δ_M	=	bias coefficient for material properties
δ_P	=	bias coefficient for professional factor
θ	=	angle of the compressive concrete slice measured from the cross-section's centroid
λ	=	non-dimensional slenderness parameter
ρ	=	slenderness factor
σ_G	=	standard deviation of safety margin

τ	=	confinement reduction factor for steel
τ'	=	enhancement factor for concrete strength
ϕ	=	resistance factor
ϕ_a	=	resistance factor for compression (in AISC 360-16 Section I2.1b)
ϕ_b	=	resistance factor for bending (in AISC 360-16 Section I3.4b)
ϕ_c	=	resistance factor for concrete
ω_1	=	coefficient to determine the equivalent uniform bending effect

ACKNOWLEDGMENTS

First, I would like to thank my supervisor, Dr. Kyle Tousignant whose expertise, guidance and encouragement have been beyond valuable, not just in research, but also in my journey to become a young professional. During the past two years, dealing with COVID-19 pandemic made education difficult by causing constant uncertainties in many aspects, but Dr. Tousignant was always optimistic and helped me see the light when I was struggling. I would also like to thank my wonderful research group members and colleagues whose help and support was very heartwarming. Interacting with these bright and smart researchers taught me new ways of looking at challenges and gave me a new perspective to life.

I would like to extend my sincere thanks to my parents, my sister Hana, and my friends who have always been there to support and encourage me throughout my education. Finally, I owe thanks to a very special person, my husband, Alireza, for his continued and unfailing love, support and understanding during this time that made the completion of my education possible.

Chapter 1: INTRODUCTION

1.1. HOLLOW STRUCTURAL SECTIONS

The use of hollow structural sections (HSS) in Canada has expanded significantly over the last 60 years. HSS sections have exceptional structural efficiency in torsion and compression, due to HSS sections being closed members and have high strength-to-weight ratio. Filling HSS with concrete is becoming a common practice to help with reduction in requirements for costly coatings for fire protection, reduction in the quantity of steel required, and achieving less surface area. In terms of strength and compressive behaviour, HSS perform well, but local buckling and compressive strength can be a challenge in large sections with slender walls. Filling HSS with concrete can help overcome these challenges as well.

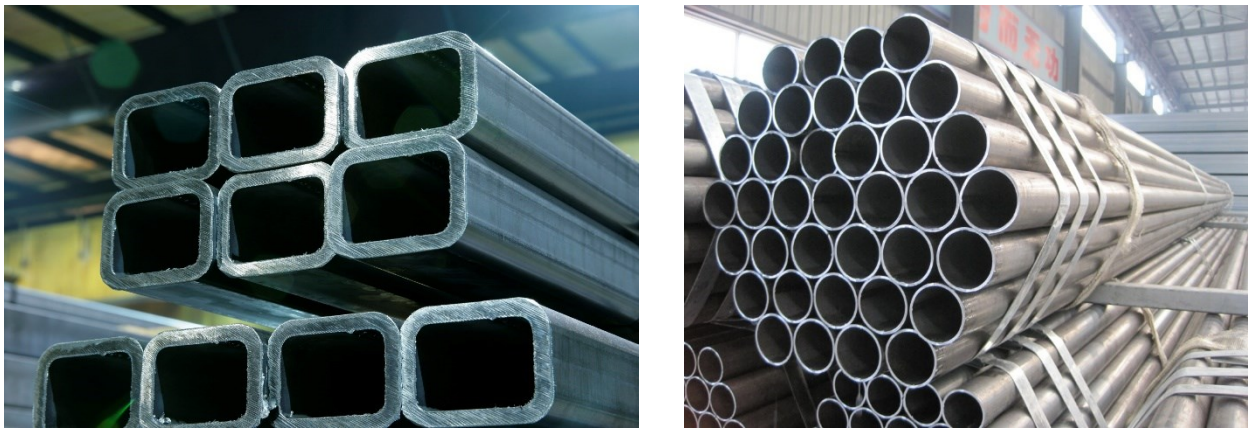

(a) (b)

Figure 1-1. Hollow structural sections (HSS): (a) Rectangular hollow sections (RHS) (courtesy of Steel Tube Institute), (b) Circular hollow sections (CHS)

1.2. CONCRETE-FILLED HSS

Since the advent of HSS in Canada in the 1960s, in the form of both circular hollow sections (CHS) and rectangular hollow sections (RHS), there has been interest in filling the HSS void with concrete. Concrete-filled HSS, in relation to unfilled HSS, offer several advantages (BSC, 1984; Wardenier et al., 2010; Zhao et al., 2019):

- An increase in the load-bearing capacity, in both compression and flexure
- A reduction in the quantity of required steel (hence a lighter HSS), for the same applied load
- A smaller diameter or outside dimension, for the same applied load, resulting in a reduction of the floor space occupied by a column as well as a lower surface area for coatings
- An increase in the fire resistance (either with or without external protection), and especially with the addition of steel reinforcing bars or steel fibres to the concrete
- An increase in the stiffness of columns in building frames
- A potential increase in the strength of connections. This was demonstrated for HSS-to-HSS truss connections by concrete filling of the chord (or "through") member (Packer & Henderson, 1997).
- Formwork will not be required
- A considerable decrease in the occupied floor space
- The omission (in many cases) of reinforcement
- The introduction of off-site fabrication, faster on-site construction
- The introduction of tighter construction tolerances, typical of steel construction

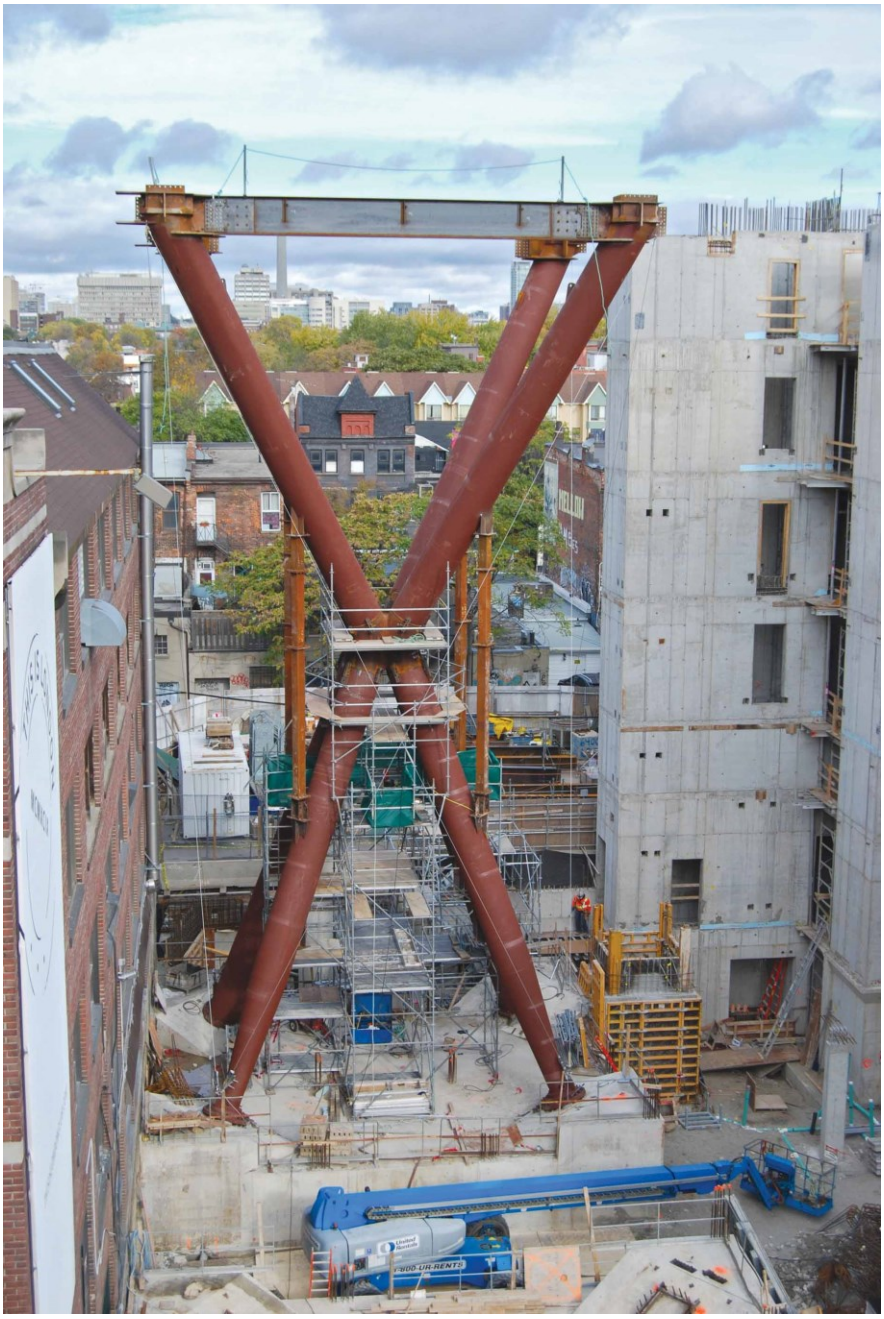

Figure 1-2. Concrete-filled HSS member, Queen Elizabeth Centre West (Courtesy of CastConnex)

1.3. RECENT DEVELOPMENTS

In Canada, design of concrete-filled HSS columns was first covered by the Canadian steel design code, CSA S16, in 1969 (CSA, 1969). Axial compressive strength in this code was taken as summation of the allowable axial load on the steel and concrete portions of cross section, A_s and A_c respectively, with the latter calculated using the slenderness ratio (KL/r) of the steel member. The current Canadian code (CSA, 2019a), is similar to the composite structures design code in Europe, Eurocode 4 (CEN, 2004a). Both codes take into

account the interaction that develops between the steel member and concrete. This enables designers to take advantage of the sectional properties of the composite member and achieve a more efficient design.

CIDECT is an international association of leading manufacturers of structural hollow sections and pipes. Recently, following the completion of CIDECT Design Guide No. 4, 2nd edition (on concrete-filled HSS under static, impact, blast, seismic and fire loading) (Zhao et al., 2019), Tousignant & Packer (2022a,b) conducted a review of the design rules in CSA S16:19 Clause 18.2 (CSA 2019a), which led to proposal of changes in its scope (i.e., material and cross-section classification limitations) and several provisions (i.e., for compressive resistance, flexural resistance, and beam-columns). An overview of these proposed changes is given in Tousignant & Packer (2022c) and Section 2.4 of this thesis.

The proposed changes by Tousignant & Packer (2022a,b) to the CSA S16 design formulae for the compressive resistance and bending resistance of concrete-filled HSS were supported, in part, by approximate first-order reliability method analyses that utilized data from over 450 tests to determine their inherent safety indices over a range of design scenarios (Tousignant & Packer, 2022a,b); however, the impact of these proposed changes on the reliability of the beam-column interaction equation(s) (in Clause 18.2.4 of CSA S16:19) was not directly assessed.

1.4. THESIS OVERVIEW

In this research, the impact of proposed changes by Tousignant & Packer (2022a,b) on the reliability of the CSA S16:19 beam-column interaction equation(s) is investigated. Reliability analysis of the formulae in CSA S16:19, AISC 360-16, and proposed equations by Tousignant & Packer (2022a,b) are performed using Monte Carlo Simulations (MCS) to determine the inherent reliability indices (β^+) of each method for concrete-filled RHS and CHS beam-columns.

Chapter 2 presents relevant research and current design criteria for concrete-filled HSS according to CSA S16, AISC 360, Eurocode, and recent research performed in Canada. Classification of cross sections, axial strength, bending strength, and axial compression plus bending provisions are discussed for each code, and is the recommendations of Tousignant & Packer (2022a,b) are explained extensively. Structural reliability methods, including closed form solutions, the so-called separation factor approach, and Monte Carlo Simulation (MCS), are then discussed.

Chapter 3 discusses the MCS methodology in greater detail. The MCS procedure applied in this work is explained, and simulation inputs – including resistance parameters, load effect parameters, and a database of tests provided by Thai et al. (2019) – are studied for the purpose of determininng the statistical parameters required for the MCS. The selection and strength formulation of representative concrete-filled beam-column RHS and CHS members using the Handbook of Steel Construction (CISC, 2021) is then explained.

Chapter 4 presents the results of the MCS. Reliability indices (β^+) calculated for two of the above-mentioned codes (AISC 360-16 and CSA S16:19) and the proposed design approaches given by Tousignant &

Packer (2022a,b) are compared to the code-specified target (i.e., $\beta^{+} = 3.0$ per Annex B of CSA S16:19 and Section B3.1 of the AISC Commentary). The effects of several parameters on the reliability are studied.

Chapter 5 presents a summary of the results and conclusions of this research, and gives recommendations for future work.

Chapter 2: RELEVANT RESEARCH AND CURRENT DESIGN CRITERIA

2.1. DESIGN OF CONCRETE-FILLED HSS ACCORDING TO CSA S16

CSA S16 provides requirements for the design, fabrication, and erection of steel structures and the structural steel components framed in other building materials. Concrete-filled hollow structural section (HSS) design criteria are covered within Clause 18.2 of CSA S16:19, where general provisions, axial resistance, composite action, bending resistance, and axial compression plus bending provisions are explained. The relevant clauses include:

- Clause 18.2.1.1 General: These provisions include the infill concrete strength limit, width to thickness ration of walls for rectangular hollow sections (RHS), and ratio of outside diameter-to-thickness for circular hollow sections (CHS). These provisions are discussed in Section 2.1.2 of this thesis.
- Clause 18.2.2 Compressive Resistance: This clause contains provisions to calculate the factored compressive resistance (C_{rc}). This clause is discussed in Section 2.1.3 of this thesis.
- Clause 18.2.3 Bending Resistance: This clause contains provisions to calculate the factored bending resistance (M_{rc}). This clause is discussed in Section 2.1.4 of the thesis.
- Clause 18.2.4 Axial Compression and Bending: This clause contains provisions to determine the adequacy of beam-columns using an interaction equation (i.e., by limiting the combined ratios of axial and bending resistance effect to unity). These provisions are discussed in Section 2.1.5 in this thesis.

2.1.1. MATERIAL LIMITATIONS

The intent of Clause 18.2 is for design using manufactured HSS made to CSA G40 (in Class C or Class H) (CSA, 2018), ASTM A500 Grade B/C (ASTM, 2021), or ASTM A1085 (ASTM, 2015). The relative availability of these alternatives varies around Canada, as described in Table 6-8 of the CISC Handbook (CISC, 2021). CSA G40 HSS is produced as cold-formed RHS and CHS from round by electric resistance welding (ERW) process, to a single grade of 350W with a specified minimum yield of 350 MPa. A tolerance of -5% is permitted on wall thickness with a further tolerance on mass (and hence effectively cross-sectional area) of -

3.5%. The cold-formed HSS end product (Class C) can be heat-treated to form an alternative Class H product by heating to 450º C or higher, followed by cooling in air. While Class H enables a higher compressive resistance for unfilled HSS columns, the higher cost associated with Class H is unwarranted for HSS once it is filled with concrete It is important to note that in the CISC Handbook (CISC, 2021), as in design, section properties for ASTM A500 sections are computed using a design wall thickness (t) of 0.90 times the nominal wall thickness. The yield stress (F_y) for all ASTM A500 Grade C HSS shapes has been harmonized to 345 MPa (ASTM, 2021). One further HSS product, ASTM A1085 (ASTM, 2015), is now heavily promoted in North America as a desirable substitute for ASTM A500. A1085 is directly equivalent to the G40 Class C (CSA, 2018) product except that F_y = 345 MPa. Section properties for ASTM A1085 are identical to those for CSA G40. As a consequence, if ASTM A1085 is ordered in Canada, one is directed to substitution with CSA G40 Class C (Tousignant & Packer, 2022a).

The scope of CSA S16:19 Clause 18.2 (CSA, 2019a) covers concrete-strength (f_c') between 20 MPa and 80 MPa for concentrically loaded columns, and between 20 MPa and 40 MPa for columns subjected to axial compression plus bending.

Unlike other national standards [e.g., AISC 360-16 (AISC, 2016) and EN 1994-1-1 (CEN, 2004a)], CSA S16:19 does not cater to the use of longitudinal steel reinforcing bars in concrete-filled HSS strength calculations. They are, however, catered to in strength calculations for partially encased and encased composite columns (Clauses 18.3.2 and 18.4.2, respectively) (CSA, 2019a). The Canadian concrete standard (CSA A23.3:19) (CSA, 2019b) has an upper limit of 500 MPa on yield strength of steel reinforcing bars (F_{yr}), although the most common strength used in Canada is still 400 MPa.

2.1.2. Classification of Cross Sections

In concrete-filled HSS, the concrete is well-known to change the local buckling mode of the HSS wall by only allowing it to buckle outward, for both the cross section and along the length of the HSS. This is reflected in the design provisions for concrete-filled HSS in Canada, via CSA S16:19, which cover Class 1 or 2 cross-sections that can undergo complete plasticisation. CSA S16:19 Clause 18.2 covers concrete-filled with Class 1 and 2 sections. In Clause 18.2.1.1, such sections are identified as those RHS having flat width-to-thickness ratios (b_{el}/t) and CHS with outside diameter-to-thickness ratio (d/t) defined in Table 2-1 and **Error! Reference source not found.** for elements under axial compression and flexural compression, respectively, calculated by assuming an outside corner radius (r_0) = 2t (i.e. $b_{el} = b - 4t$ and $h_{el} = h - 4t$) (Clause 11.3.2).

Table 2-1. Limits for concrete-filled elements in compression in accordance with CSA S16:19

Shape	Element	Limit
RHS	Flanges	$1{,}350/\sqrt{F_y}$
	Webs	$1{,}350/\sqrt{F_y}$
CHS		$28{,}000/F_y$

Table 2-2. Limits for concrete-filled elements in flexural compression in accordance with CSA S16:19

Shape	Element	Limit
RHS	Flanges	$1{,}350/\sqrt{F_y}$
	Webs	$1{,}350/\sqrt{F_y}$
CHS		$28{,}000/F_y$

Note: CSA S16:19 does not provide separate width-to-thickness ratios (or "limits") for elements in direct (axial) compression and flexural compression.

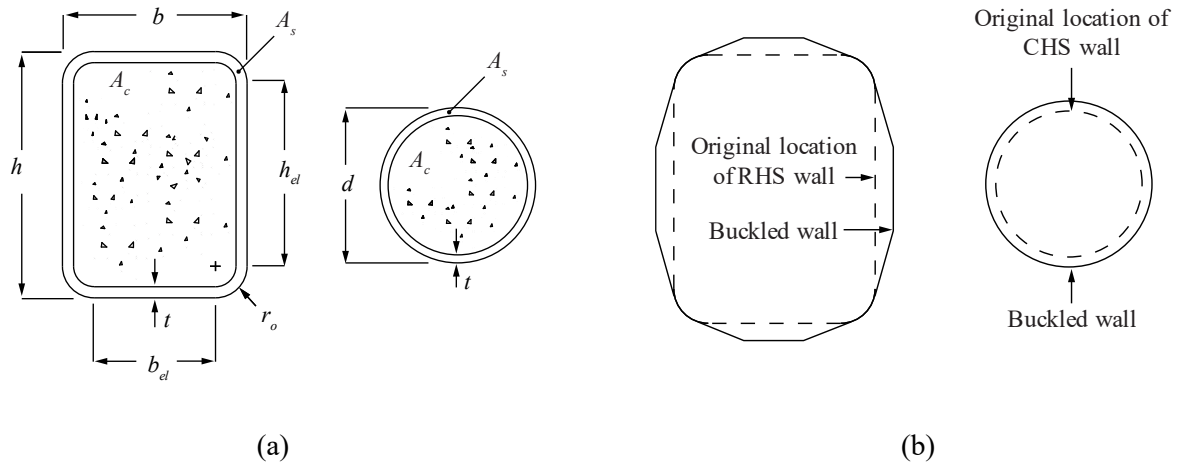

Figure 2-1. Concrete-filled HSS: (a) Nomenclature; (b) Cross-sectional buckling modes

CSA S16:19 proposes higher compressibility limits for concrete-filled HSS compared to regular HSS because the infill concrete is expected to limit the wall local buckling to outward buckling only which results in higher capacity of members against local buckling.

2.1.3. AXIAL COMPRESSION

According to CSA S16:19 Clause 18.2.2, the factored compressive resistance of a composite concrete-filled hollow structural section (C_{rc}) is taken as:

$$C_{rc} = \frac{\left(\tau\phi A_s F_y + \tau'\alpha_1\phi_c A_c f_c'\right)}{\left(1+\lambda^{2n}\right)^{1/n}} \tag{2.1}$$

where A_s and A_c = cross-sectional area of steel and concrete, respectively (Figure 2-1); ϕ = steel resistance factor; ϕ_c = concrete resistance factor; τ = confinement reduction factor for steel (due to tensile hoop stresses that develop to confine the concrete); τ' = enhancement factor for concrete strength due to 3D confinement; α_1 = ratio of average stress in rectangular stress block to f_c' (= 0.85 - 0.0015 $f_c' \geq 0.73$); λ = non-dimensional slenderness parameter; and n = column curve parameter (= 1.80 for concrete-filled HSS). Geometric parameters are displayed in Figure 2-1, and $\tau = \tau' = 1.0$, except for CHS sections with a height-to-diameter ratio (L/D) of less than 25 for which:

$$\tau = \frac{1}{\sqrt{1+\rho+\rho^2}} \tag{2.2}$$

and:

$$\tau' = 1 + \left(\frac{25\rho^2\tau}{d/t}\right)\left(\frac{F_y}{\alpha_1 f_c'}\right) \tag{2.3}$$

where ρ = slenderness factor [= 0.02(25 – L/D)], and:

$$\lambda = \sqrt{\frac{C_p}{C_{ec}}} \tag{2.4}$$

where C_p = nominal compressive resistance computed with $\phi = \phi_c = 1.0$ and $\lambda = 0$, and C_{ec} = Euler buckling strength; i.e.:

$$C_{ec} = \frac{\pi^2 EI_e}{(KL)^2} \tag{2.5}$$

and:

$$EI_e = E_s I_s + \frac{0.6E_c I_c}{1 + C_{fs}/C_f} \tag{2.6}$$

where I_s and I_c = moment of inertia of the steel and concrete areas, respectively, as computed with respect to the centre of gravity of the cross-section; E_s = modulus of elasticity of steel; E_c = modulus of elasticity of concrete; C_{fs} = factored sustained axial load; C_f = total factored axial load.

Eq. 2.1 expresses the total axial compressive capacity of concrete-filled HSS as summation of steel and concrete portions of cross section, plus adjustment factors (τ and τ') to reflect concrete confinement effects in CHS.

As shown above, for CHS, lateral deformation of concrete infill is restrained by the tube (i.e., the CHS "shell" produces a hoop restraining effect around the concrete, subjecting it to a triaxial state of stress; in contrast the CHS "shell" is subjected to bi-axial stress state) (CIDECT, 1979). For RHS, concrete confinement effects are ignored because the RHS corners provide only partial, or discontinuous, confinement.

It is important to note that other national steel standards (i.e., AISC 360-16 and EN 199-1-1) consider the contribution of longitudinal reinforcing bars when calculating C_{rc}, which are beneficial to strength and often included to improve fire endurance, whereas CSA S16:19 (CSA, 2019a) does not.

2.1.4. BENDING

According to CSA S16:19 Clause 18.2.2, the factored bending resistance (M_{rc}) of a composite concrete-filled HSS is taken as:

$$M_{rc} = C_r e + C_r' e' \tag{2.7}$$

where C_r = compressive resistance of steel above the neutral axis (NA); C_r' = compressive resistance of concrete above the NA (over the depth of the concrete compression zone, a); e = lever arm between C_r and T_r; T_r = tensile resistance of steel below the NA (with an area of A_{st}); and e' = lever arm between C_r' and T_r (Figure 2-2).

a) For concrete-filled RHS:

$$C_r = \frac{\phi A_s F_y - C_r'}{2} \tag{2.8}$$

and:

$$C_r' = 1.18\alpha_1\phi_c a(b - 2t) f_c' \tag{2.9}$$

$$C_r + C_r' = T_r = \phi A_{st} F_y \tag{2.10}$$

where a = depth of the concrete compression zone.

A major assumption in these formulae is that at the moment of failure, the steel shell is fully plastic and the concrete is crushing in compression. This assumption is supported by experimental research on concrete-filled RHS members (Kennedy et al., 1994). Kennedy et al. (1994) showed that fully plastic stress blocks are developed in the steel and in the concrete at the time of failure, and that the steel restrains (or confines) the concrete, increasing its compressive resistance to f_c' rather than 0.85 f_c' (which was the historically assumed bearing limit). This is the reason for the 1.18 factor in the C_r' equation (Eq. 2.9).

Another important note about CSA S16:19 bending resistance provisions for concrete-filled RHS is that M_{rc}'s constituent terms are poorly defined. First, the depth of a is not specified. [In CSA S16-01 Clause 18.2.3 and earlier editions, a was noted to be taken as 0.85 times the concrete depth to the neutral axis. However, in later editions, this note was removed. Currently, it is common practice to assume that a extends to one times the depth of the NA measured from the inside face of the RHS (Tousignant & Packer, 2022b)]. Second, the rounded RHS corners are ignored for the calculation of C_r', while apparently, they are not ignored for the calculation of C_r and T_r. The existing M_{rc} expression also does not cater to the use of longitudinal steel reinforcing bars. Derivation of the CSA S16:19 M_{rc} equation for concrete-filled RHS members is further explained in Appendix A:.

b) For concrete-filled CHS:

$$C_r = \phi F_y \beta \frac{dt}{2} \tag{2.11}$$

and:

$$C_r' = 1.18\alpha_1\phi_c f_c' \left[\frac{\beta d^2}{8} - \frac{b_c}{2}\left(\frac{d}{2} - a\right) \right] \tag{2.12}$$

where b_c = width of concrete at the neutral axis; a = depth of concrete compression zone, and:

$$e = b_c \left[\frac{1}{(2\pi - \beta)} + \frac{1}{\beta} \right] \tag{2.13}$$

and:

$$e' = b_c \left[\frac{1}{(2\pi - \beta)} + \frac{b_c^{\,2}}{1.5\beta d^2 - 6b_c(0.5d - a)} \right] \tag{2.14}$$

where:

$$\beta = \frac{\phi A_s F_y + 0.295\alpha_1\phi_c d^2 f_c' \left[\sin(\beta/2)\tan(\beta/4)\right]}{(0.148\alpha_1\phi_c d^2 f_c' + \phi dt F_y)} \tag{2.15}$$

and:

$$b_c = d\sin\left(\frac{\beta}{2}\right) \tag{2.16}$$

and:

$$a = \frac{b_c}{2}\tan\left(\frac{\beta}{4}\right) \tag{2.17}$$

For concrete-filled CHS, force and moment components can be found in a similar manner, by integrating stress blocks over corresponding areas of steel, concrete and reinforcing bars. CSA S16 does this, presently, by assuming "thick-walled" CHS. The resulting expression for M_{rc} requires solving a recursive formula (Eq. 2.15) to determine the angle (β) that describes the location of neutral axis (Figure 2-2). The existing M_{rc} expression also does not cater to the use of longitudinal steel reinforcing bars.

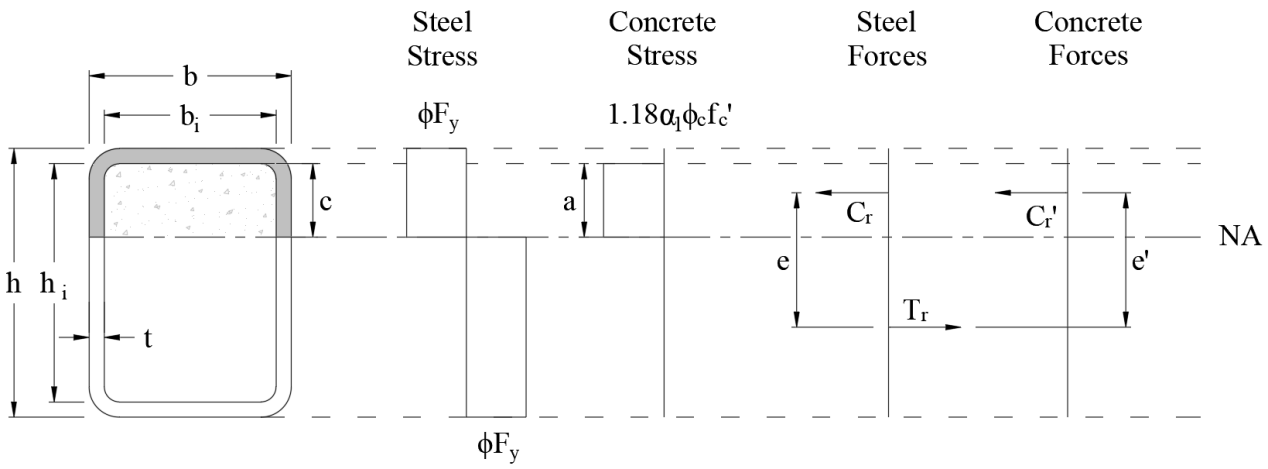

(a)

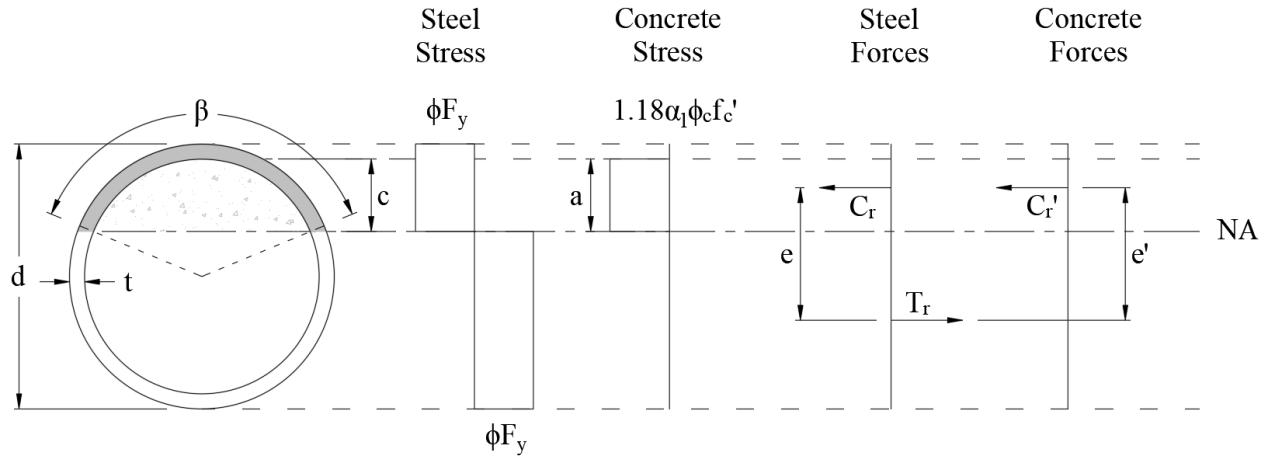

(b)

Figure 2-2. Stress and force diagrams under bending according to CSA S16:19: (a) Concrete-filled RHS; (b) Concrete-filled CHS

2.1.5. AXIAL COMPRESSION PLUS BENDING

In CSA S16:19 Clause 18.2.4, composite concrete-filled hollow structural sections that are required to resist both axial compression and bending moments are proportioned analogously to members conforming to Clause 13.8.2 (for unfilled members) so that:

$$\frac{C_f}{C_{rc}} + \frac{\beta\omega_1 M_f}{M_{rc}\left(1-\frac{C_f}{C_{ec}}\right)} \le 1.0 \quad \text{and} \quad \frac{M_f}{M_{rc}} \le 1.0 \tag{2.18}$$

where C_f = factored compressive force; M_f = factored moment; C_{rc} = compressive resistance; M_{rc} = moment resistance; ω_1 = coefficient to determine the equivalent uniform bending effect (found in CSA S16:19 Clause 13.8.6); C_{ec} = Euler buckling strength; and β = coefficient for bending, taken as:

$$\beta = \frac{C_{rco} - C_{rcm}}{C_{rco}} \tag{2.19}$$

where $C_{rco} = C_{rc}$ calculated with $\lambda = 0$ and $C_{rcm} = 1.18\alpha_1\phi_c A_c f_c'$.

It is important to note that in the 2019 edition of the standard, changes were made to the β values for unfilled HSS beam-columns in Clauses 13.8.3 and 13.8.4. The rationale for the new values chosen was based on designing the members for plastic behaviour (Essa & Kennedy, 2000). It is also important to note that the value or location of ω_1 is not specified in Clause 18.2.4 of CSA S16:19. Another important note about CSA S16:19 provisions for concrete-filled HSS is that the need to check cross-sectional strength, overall member strength and/or lateral torsional buckling (LTB) is not clearly stated. For unfilled HSS, the failure mode of LTB does not apply to CHS and square RHS, and is restricted to just some RHS with high aspect ratios bent about their strong axis. Clause 18.2.3 of CSA S16:19 does not give provisions for LTB of concrete-filled HSS; however, the commentary to CSA S16:19 Clause 18.2.4 states that LTB should be checked "if applicable" for concrete-filled RHS bent about their strong axis.

2.2. Design of Concrete-Filled HSS According to AISC 360

2.2.1. Material Limitations

AISC 360-16 Section I1.3 (AISC, 2016) imposes a maximum yield strength on HSS used for concrete-filled HSS members of 525 MPa. It is important to note that this limit on HSS strength for concrete-filled HSS well-exceeds the specified material strengths available in Canada (F_y = 350 MPa or less). AISC 360-16 Section I1.3 also has a requirement that the HSS cross-sectional area is at least 1% of the total composite cross section.

AISC 360-16 Section I1.3 covers concrete strengths (f_c') between 21 MPa and 69 MPa for all load actions for normal-weight concrete, and 21 MPa $\leq f_c' \leq$ 41 MPa for light-weight concrete. Furthermore, an upper limit of 550 MPa is set on yield strength of steel reinforcing bars (F_{yr}), to be in accord with ACI 318 (2014).

2.2.2. Classification of Cross Sections

In AISC 360-16, concrete-filled HSS cross-sections are classified as "compact", "noncompact" and "slender". "Compact" sections can undergo complete plastification (akin to CSA Class 1 and Class 2 sections), "noncompact" sections will yield but not undergo full plastification (akin to CSA Class 3 sections), and 'slender" sections are expected to locally buckle before reaching yield (akin to CSA Class 4 sections). The maximum width-to-thickness ratio limits are summarized in Table 2-3 and Table 2-4.

Table 2-3. Limits for concrete-filled elements in compression in accordance with AISC 360-16

Shape	Element	Compact/Noncompact	Noncompact/Slender
RHS	Flanges	$1{,}010/\sqrt{F_y}$	$1{,}340/\sqrt{F_y}$
	Webs	$1{,}010/\sqrt{F_y}$	$1{,}340/\sqrt{F_y}$
CHS		$30{,}000/F_y$	$38{,}000/F_y$

Table 2-4. Limits for concrete-filled elements in flexural compression in accordance with AISC 360-16

Shape	Element	Compact/Noncompact	Noncompact/Slender
RHS	Flanges	$1{,}010/\sqrt{F_y}$	$1{,}340/\sqrt{F_y}$
	Webs	$1{,}340/\sqrt{F_y}$	$2{,}550/\sqrt{F_y}$
CHS		$18{,}000/F_y$	$62{,}000/F_y$

It is important to note that unlike CSA S16:19, AISC 360-16 assumes an outside corner radius of $r_0 = 1.5t$ for calculating the width-to-thickness ratios for RHS members (i.e. $b_{el} = b_0 - 3t$ and $h_{el} = h_0 - 3t$).

Comparing Table 2-1 and **Error! Reference source not found.**, a very close relation between AISC's RHS "noncompact" limit ($1340/\sqrt{F_y}$) and CSA's maximum permitted limit ($1350/\sqrt{F_y}$) is observed. Both AISC 360 and CSA S16 intend to avoid local buckling of HSS wall through these limits. AISC 360, however, also includes a "compact" limit on the cross section for the case of axial compression, which relates to the ability of the HSS to provide enhanced concrete confinement (Tousignant & Packer, 2022a). In Table 2-3, for concrete-filled CHS in axial compression, AISC's "noncompact" limits ($38{,}000/F_y$) is much less conservative than CSA's limit ($28{,}000/F_y$).

For flexural compression, comparing **Error! Reference source not found.** and Table 2-4, AISC considers different local buckling scenarios for RHS flange and web in flexural compression while CSA doesn't differentiate between these two cases. On the other hand, AISC's values are less-conservative. CSA's RHS compression flange "compact" (or Class 2) limit (namely $700/\sqrt{F_y}$ per the CSA S16 Clause 18.2.3 Commentary) is greater than its counterpart for unfilled RHS ($525/\sqrt{F_y}$) but is still significantly lower than AISC 360's limit ($1010/\sqrt{F_y}$). The CSA S16 limit merely represents the scope of experimental validation performed by Lu and Kennedy (1994).

2.2.3. Axial Compression

Nearly all manufactured HSS sections, when filled with concrete, fall within the category of "compact" sections based on the definitions and categorizations of CSA S16 and AISC 360. Hence, this section of the thesis relates only to those sections (i.e., those that can undergo complete plasticisation as discussed in the precious section). It is important to note, however, that AISC 360 includes provisions for "non-compact" and "slender" concrete-filled sections, as well as for "compact" sections.

According to AISC 360-16 Clause I2.2b(a), the factored compressive resistance of a "compact" composite concrete-filled hollow structural section (C_{rc}) is taken as:

For $\lambda^2 \leq 2.25$:

$$C_{rc} = \phi_a \left(A_s F_y + C_2 A_c f_c^{'} + C_2 A_{sr} \frac{E_s}{E_c} f_c^{'} \right) . \left(0.658^{\lambda^2} \right) \tag{2.20}$$

For $\lambda^2 > 2.25$:

$$C_{rc} = \phi_a \left(A_s F_y + C_2 A_c f_c^{'} + C_2 A_{sr} \frac{E_s}{E_c} f_c^{'} \right) . \left(\frac{0.877}{\lambda^2} \right) \tag{2.21}$$

where ϕ_a = resistance factor for compression (= 0.75); C_2 = ratio of average concrete stress to f_c' accounting for confinement effects (= 0.85 for RHS and 0.95 for CHS); A_s = HSS's cross sectional area; A_{sr} = total reinforcement cross sectional area (Figure 2-3); and λ is calculated by using Eq. 2.4, where EI_e is given as:

$$EI_e = E_s I_s + E_s I_{sr} + C_1 E_c I_c \tag{2.22}$$

with:

$$C_1 = 0.45 + 3 \left(\frac{A_s + A_{sr}}{A_g} \right) \leq 0.9 \tag{2.23}$$

where A_g = gross cross-sectional area of composite section (= $A_s + A_c + A_{sr}$).

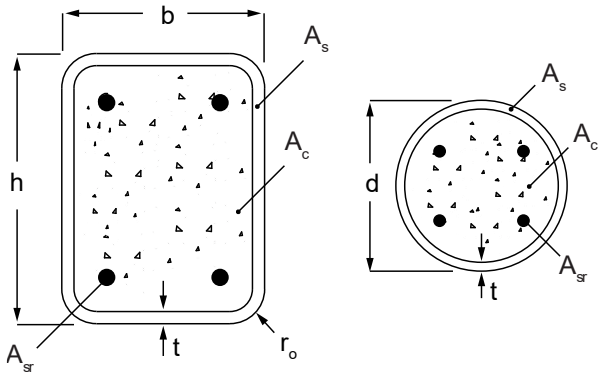

Figure 2-3. Cross-section layout for compressive resistance according to AISC 360-16: (left) Concrete-filled RHS; (right) Concrete-filled CHS

2.2.4. BENDING

According to Clause I4.4 of AISC 360, the available flexural strength of concrete-filled composite members (M_{rc}) is be determined as follows:

$$M_{rc} = \phi_b M_n \tag{2.24}$$

where ϕ_b = resistance factor for bending (=0.90) and M_n = nominal flexural strength (= M_p for "compact" cross sections). M_p is the moment corresponding to plastic stress distribution over the composite cross section which can be calculated in accordance with the AISC Manual (AISC, 2017) Tables 6-4 and 6-5 as follows:

a) For concrete-filled RHS:

$$M_p = \left[\left(F_y Z_s + \frac{0.85 f_c' Z_c}{2}\right) - F_y(2th_n^2) - 0.85 f_c'\left(\frac{b_i h_n^2}{2}\right)\right] \tag{2.25}$$

where:

$$h_n = \frac{0.85 f_c' A_c}{2\left(0.85 f_c' b_i + 4F_y t\right)} \le \frac{h_i}{2} \tag{2.26}$$

$$Z_c = \frac{b_i h_i^2}{4} - 0.429 r_i^2 h_i + 0.192 r_i^3 \tag{2.27}$$

where h_n = the distance from the plastic neutral axis to cross section's centre line; b_i = inner web width of the RHS shell; h_i = inner web height of the RHS shell; Z_s = full plastic section modulus of HSS; and r_i = RHS's inner corner radius (Figure 2-4).

b) For concrete-filled CHS:

$$M_p = \left[\left(F_y \frac{d^3 - d_i^3}{6} \sin\left(\frac{\theta}{2}\right)\right) + 0.95 f_c'\left(\frac{\frac{d_i^3}{6}\sin^3\left(\frac{\theta}{2}\right)}{2}\right)\right] \tag{2.28}$$

where:

$$\theta = \frac{0.0260 k_c - 2k_s}{0.0848 k_c} + \frac{\sqrt{(0.0260 k_c + 2k_s)^2 + 0.857 k_c k_s}}{0.0848 k_c} \tag{2.29}$$

with:

$$k_c = f_c' d_i^2 \quad \text{and} \quad k_s = F_y\left(\frac{d - t}{2}\right)t \tag{2.30}$$

where d = outer diameter of the CHS; d_i = inner diameter of the CHS; θ = angle of the compressive concrete slice measured from the cross-section's centroid; and h_n = distance from the plastic NA to cross section's centre line (Figure 2-4).

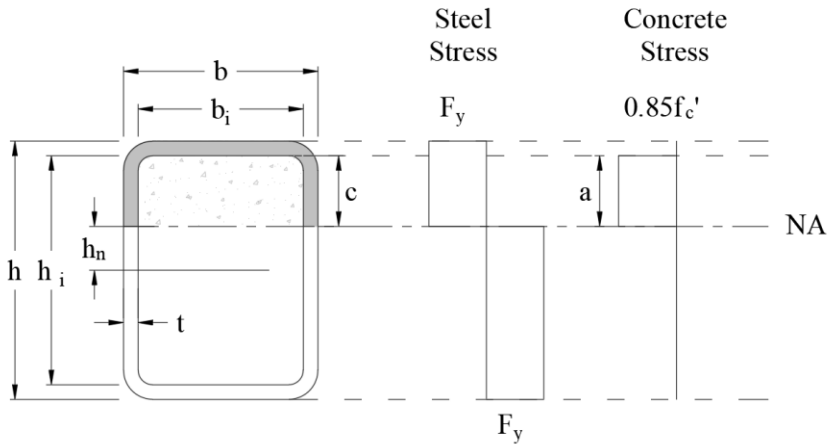

(a)

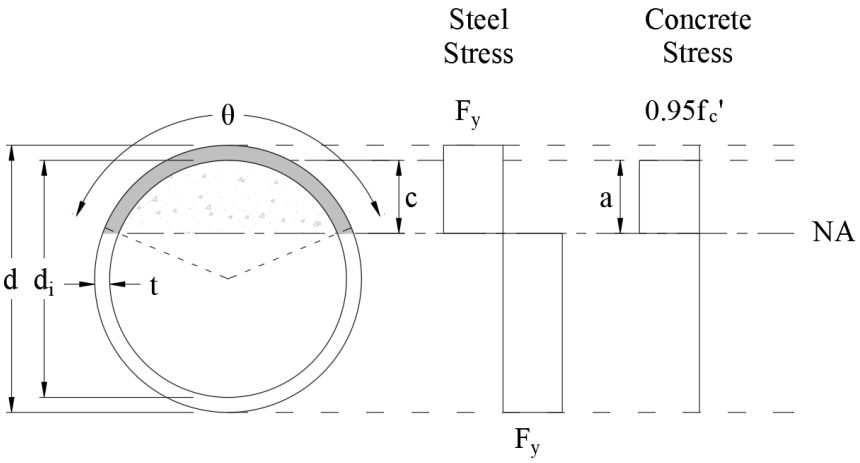

(b)

Figure 2-4. Stress and force diagrams under bending according to AISC 360-16: (a) Concrete-filled RHS; (b) Concrete-filled CHS

2.2.5. AXIAL COMPRESSION PLUS BENDING

According to AISC 360-16 Clause I5(a), axial compression plus bending of "compact" concrete-filled HSS members is covered by using either: (a) the interaction equation of Section H1.1 or (b) one of the methods defined in Section I1.2. Both methods are covered in this section.

a) AISC's first approach according to Section H1.1 (for doubly and singly symmetric members constrained to bend about a geometric axis, *x* and/or *y*) is based on the following interaction equations (which pertain to unfilled HSS beam-columns). Method (a) is akin to CSA S16:19 by treating concrete-filled HSS analogously to unfilled HSS.

1) When $C_f/C_{rc} \geq 0.2$:

$$\frac{C_f}{C_{rc}} + \frac{8}{9}\frac{M_f}{M_{rc}} \leq 1 \tag{2.31}$$

2) When $C_f/C_{rc} < 0.2$:

$$\frac{C_f}{2C_{rc}} + \frac{M_f}{M_{rc}} \leq 1 \tag{2.32}$$

where C_f = required axial strength; C_{rc} = available axial strength; M_f = required flexural strength; and M_{rc} = available flexural strength. (Calculation of available axial and flexural strength were discussed in the previous sections).

b) AISC's second approach according to Section I1.2 (for doubly symmetric compact members) requires computation of several points on the nominal force vs. moment interaction diagram for the cross-section(Figure 2-5). Then the resistance factor for compression ($\phi_a = 0.75$) and the resistance factor for bending ($\phi_b = 0.9$) is applied to the nominal axial and flexural strengths respectively to get the factored resistances. This can be done in a simplified manner (by using a 5-point interaction diagram) according to Tables 6-4 and 6-5 of the AISC Manual (AISC, 2017), for concrete-filled RHS and CHS, respectively, without reinforcing bars.

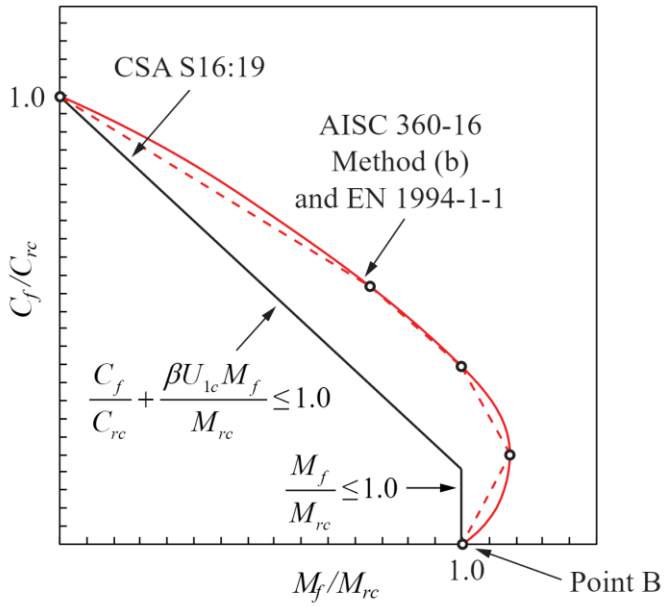

Figure 2-5. Implied beam-column failure envelopes according to CSA S16:19, AISC 360-16, and EN 1994-1-1 (Tousignant & Packer, 2022b)

2.3. Discussion on Design of Concrete-Filled HSS According to Eurocode 4

European design requirements for concrete-filled HSS members are presented in Eurocode 4 (EN 1994-1-1, 2004). Since the Eurocode is not a main part of this research project, it will be discussed generally in this section and only briefly compared with CSA S16 and AISC 360.

EN 1994-1-1 Clause 3.3(2) imposes a 460 MPa yield strength limit on HSS material (CEN, 2004a). Limitations also exist on the permissible range of concrete compressive strengths f_c'. For normal weight concrete, the design methods of EN 1994-1-1 (CEN, 2004a) are applicable to concrete having 20 MPa $\leq f_c' \leq$ 60 MPa.

In terms of reinforcement strength, EN 1994-1-1 (CEN, 2004a) imposes no limits on reinforcement but advises that the elastic modulus of reinforcement may be taken equal to that of structural steel (E_s).

For maximum width-to-thickness ratio for concrete-filled HSS elements under axial compression, EN 1994-1-1 (CEN, 2004a) imposes limits of $800/\sqrt{F_y}$ and $21{,}200/F_y$ for RHS and CHS sections respectively. These EN 1994-1-1 values can be considered excessively conservative as they repeat Class 3 limits for unfilled CHS in axial compression.

For maximum width-to-thickness ratios for elements in concrete-filled HSS elements under flexural compression, like AISC 360-16, EN 1994-1-1 differentiates webs and flanges by proposing different limits for each of them. EN 1994-1-1 proposes limits of $580/\sqrt{F_y}$ and $1270/\sqrt{F_y}$ for flanges and webs of "compact" RHS members respectively and a limit of $16{,}500/F_y$ for "compact" CHS members which are, again, very conservative.

In terms of axial compressive resistance calculations, EN 1994-1-1 is more similar to CSA S16:19 than to AISC 360-16. As shown previously, AISC 360-16 has one resistance factor for composite HSS members, rather than individual ones for separate materials (as in CSA S16:19 and EN 1994-1-1). AISC 360-16 also provides multiple resistance expressions (e.g., for "compact" and "noncompact" cross sections), whereas CSA S16:19 and EN 1994-1-1 do not.

For bending, EN 1994-1-1's design method based on the plastic stress distribution method, where it is assumed that the cross section can undergo complete plasticisation (as discussed in Sections 2.1.2 and 2.2.2). The depth of the concrete compression zone, a, in EN 1994-1-1 depends on the resistance or the partial safety factors applied because, in both cases, equilibrium is established by using factored resistances (like CSA S16:19).

For combined axial compression and bending, the EN 1994-1-1 approach given in Clause 6.7.3.2 (CEN, 2004a) is very similar to AISC 360-16's second method discussed in Section 2.2.5 using a multi-point interaction diagram (Figure 2-5).

2.4. RECENT RESEARCH PERFORMED IN CANADA

The recent study by Tousignant & Packer (2022a,b), mentioned previously, resulted in several proposed changes to CSA S16 Clause 18.2 that cover its scope (i.e., material limitations), the classification of cross sections, and provisions for compressive resistance, bending resistance, and axial compression plus bending.

Tousignant & Packer (2022a) recommended to adopt rounded ranges of 20 MPa $\leq f_c' \leq$ 70 MPa for normal-weight concrete and 20 MPa $\leq f_c' \leq$ 40 MPa for light-weight concrete in CSA S16. Although the former limit is slightly more restrictive than the current limit in CSA S16 for concentrically loaded columns ($f_c' \leq$ 70 MPa versus $f_c' \leq$ 80 MPa), the validated wider range of application for beam-columns is valuable considering that nearly all columns, in practice, are subjected to combined loading.

Tousignant & Packer (2022a) also recommended to replace the current b_{el}/t limit(s) for plastic design in CSA S16 Clause 18.2.1 (see Section 2.1.2) with the proposed limits in Table 2-5. Despite being more restrictive again (in some cases), these limits are met by nearly all RHS in the CISC Handbook (CISC, 2021).

Table 2-5. Proposed limits for concrete-filled HSS members in axial and flexural compression

Shape	Element	Axial compression	Flexural compression
RHS	Flanges	$1{,}350/\sqrt{F_y}$	$1{,}010/\sqrt{F_y}$
	Webs	$1{,}350/\sqrt{F_y}$	$1{,}340/\sqrt{F_y}$
CHS		$38{,}000/F_y$	$18{,}000/F_y$

A modification to the C_{rc} equation was also proposed – to cater to the use of longitudinal steel reinforcing bars; i.e.:

$$C_{rc} = \frac{\tau\phi A_s F_y + \tau'\alpha_1\phi_c A_c f_c' + \phi_r A_r F_{yr}}{(1+\lambda^{2n})^{\frac{1}{n}}} \tag{2.33}$$

where A_r = cross-sectional area of longitudinal reinforcement and ϕ_r = resistance factor for steel reinforcing bars. A new lower limit of 0.75 for α_1 was proposed as a consequence of adopting the upper limit of f_c' = 70 MPa discussed previously.

For consistency, it was also recommended that the expression for EI_e be modified to:

$$EI_e = E_s I_s + \frac{0.6E_c I_c}{1 + C_{fs}/C_f} + EI_r \tag{2.34}$$

where I_r = moment of inertia of the reinforcing bar areas, as computed with respect to the centre of gravity of the cross-section.

Tousignant & Packer (2022b) have shown that omitting the RHS rounded corners (as done in the C_r' equation for RHS in CSA S16:19) is unconservative and, for CHS, questioned the need for recursive function to calculate M_{rc}. The existing expression also does not cater for to the use of longitudinal steel reinforcing bars.

Hence, new formulae based on the integration of fully plastic stress blocks were proposed with a modification to the equation for M_{rc} in CSA S16 (Eq. 2.7) which aimed to make it clearer, as well as to provide for the use of longitudinal steel reinforcing bars. These equations were derived by assuming that the concrete stress block extends the full depth to the NA (i.e., $a = c$), as is now common practice (AISC, 2016)(Figure 2-6). The location of the NA and M_{rc} are determined by finding equilibrium of forces and moments, respectively, that are generated by resistances, for consistency with the approach used in CSA A23.3:19 and elsewhere in CSA S16 (Tousignant & Packer, 2022c).

a) For concrete-filled RHS:

$$M_{rc} = Z\phi F_y - 2t(\frac{h_i}{2} - a)^2 \phi F_y + \frac{Z_c}{2}\phi_c f_c - \frac{b_i}{2}\left(\frac{h_i}{2} - a\right)^2 \phi_c f_c + M_{rr} \tag{2.35}$$

where $f_c = 1.18\alpha_1 f_c'$; Z = plastic modulus of the steel section alone; and $h_i = D - 2t$ (where d = overall depth of hollow section). The depth of the concrete compression zone, a, was also explicitly defined:

$$a = \frac{h_i}{2} - \frac{\left(A_g - A_s\right)\phi_c f_c - 2\phi_r F_{yr}\left(A_{src} + A_{srb} - A_{srt}\left(1 - \phi_c f_c / \phi_r F_{yr}\right)\right)}{8t\phi F_y + 2b_i \phi_c f_c} \tag{2.36}$$

where A_g = gross cross-sectional area of composite section; A_{srt}, A_{src} and A_{srb} = area of reinforcing bars in the top, central, and bottom region, respectively, where only the top region is located above the neutral axis; and Z_c = plastic modulus of the area inside the HSS (concrete plus reinforcing bars), taken as:

$$Z_c = \frac{b_i h_i^2}{4} - 0.429 r_i^2 h_i + 0.192 r_i^3 \tag{2.37}$$

where $b_i = b - 2t$ (b = overall width of hollow section); $r_i = t$; and:

$$M_{rr} = \phi_r F_{yr}\left[A_{srt}\left(a - d_c\right)\left(1 - \phi_c f_c / \phi_r F_{yr}\right) + A_{src}\left(\frac{h_i}{2} - a\right) + A_{srb}\left(h_i - a - d_c\right)\right] \tag{2.38}$$

where A_g = gross cross-sectional area of composite section; A_{srt}, A_{src} and A_{srb} = area of reinforcing bars in the top, central, and bottom region, respectively, where only the top region is located above the neutral axis; and d_c = distance from the inside face of the RHS to the centre of the closest adjacent reinforcing bar (Figure 2-6). The term M_{rr} reflects the incremental contribution to the moment resistance gained by adding steel reinforcing bars.

For concrete-filled RHS members without longitudinal reinforcing, the above approach provides a similar reliability to CSA S16:19 and AISC 360-16 (Tousignant & Packer, 2022b).

b) For concrete-filled CHS:

$$M_{rc} = 4\phi F_y t r_m^{\,2} \cos\gamma_0 + \frac{2}{3}\phi_c f_c r_c^{\,3} \cos^3\gamma_0 + M_{rr} \tag{2.39}$$

where:

$$r_m = \left(\frac{d-t}{2}\right) \quad \text{and} \quad r_c = \left(\frac{d-2t}{2}\right) \tag{2.40}$$

where d = outside diameter of circular hollow section; and:

$$\gamma_0 = \frac{\pi r_c^{\,2}\phi_c f_c + \phi_r F_{yr}\left(A_{src} + A_{srb} - A_{srt}\left(1-\phi_c f_c / \phi_r F_{yr}\right)\right)}{8 t r_m \phi F_y + 3 r_c^{\,2}\phi_c f_c} \tag{2.41}$$

and:

$$M_{rr} = \frac{A_{sr}}{n}\left(\phi_r F_{yr}\sum_{i=1}^{n} e_i - \phi_c f_c \sum_{i=1}^{n_t} e_i\right) \tag{2.42}$$

where γ_0 = angular location of the neutral axis; A_{sr} = total area of steel reinforcing bars; n = number of steel reinforcing bars; and e_i = absolute distance from the i^{th} steel reinforcing bar to the neutral axis. The depth of the neutral axis from the inside face of the CHS can be taken as r_c (1-sinγ_0).

Eq. 2.41 is similar in principle to the one used in the AISC Manual (AISC, 2017) to determine the location of the NA, and the remaining expressions are based on the work by Elchalakani et al. (2001). It was shown that for concrete-filled CHS members without longitudinal reinforcing, the above apporach provides a similar level of reliabilty to CSA S16 while avoiding recurtion (Tousignant & Packer, 2022b).

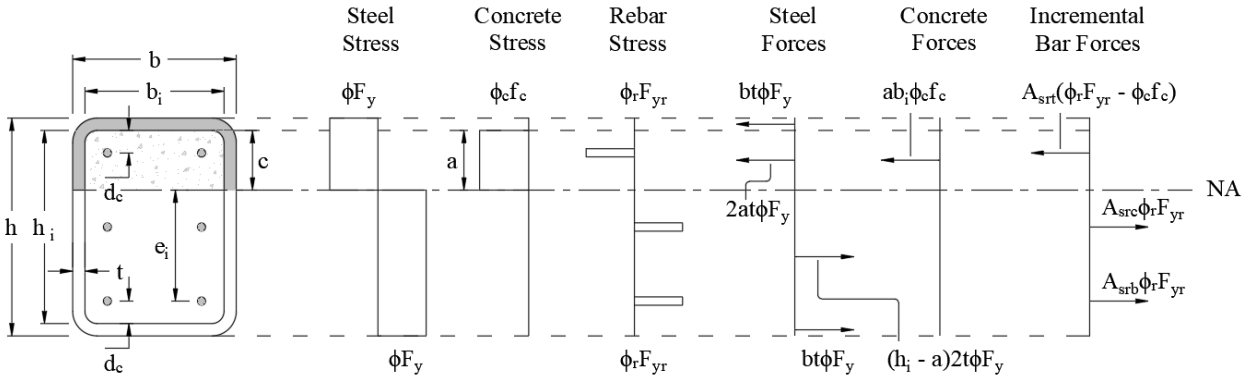

(a)

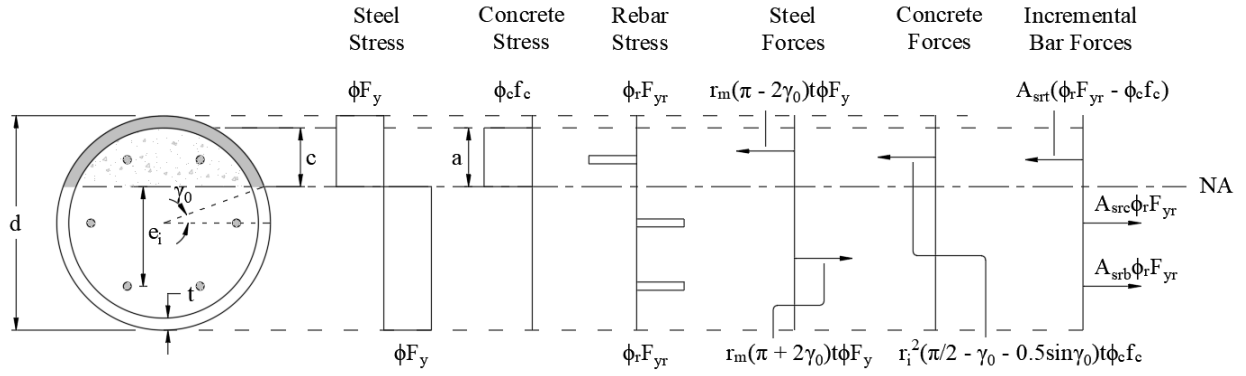

(b)

Figure 2-6. Stress and force diagrams under bending according to Tousignant & Packer (2022b): (a) Concrete-filled RHS; (b) Concrete-filled CHS

With respect to beam-columns, Tousignant & Packer (2022b) made several recommendations for consistency. In addition to using the previously discussed C_{rc} and M_{rc} equations, subject to the proposed f_c' and b_{el}/t limits (20 MPa $\leq f_c' \leq$ 70 MPa for normal-weight concrete, and Table 2-5, respectively), they proposed two possible approaches to determine β:

1. Approach (i): using Eq. 2.18; and
2. Approach (ii): using "β = 0.85 for square and circular hollow structural sections, and 1.0 for all other hollow structural sections".

In Addition, it was also recommended to spell out that the value of ω_1 is defined in clause 13.8.6.

Approach (i) was shown to give similar statistics to the existing CSA S16 method, and Approach (ii) was believed to be more conservative. Approach (ii) is in accord with the previously discussed changes made for unfilled HSS beam-columns in Clauses 13.8.3 and 13.8.4 of CSA S16:19 (CSA, 2019a).

The proposed equations for axial compression and bending were supported by FORM analyses, but for beam-columns, an analysis was left until later (because FORM analyses become difficult to apply to highly

non-linear resistance functions and/or functions with a large number of correlated random variables) (Eamon et al., 2005; Schueller et al., 2004). A suitable alternative technique is to run a Monte Carlo Simulation, as discussed in the following section.

2.5. STRUCTURAL RELIABILITY

The resistance of a structure or a structural component is defined as the maximum force that it can sustain before failure. Since failure is associated with collapse, in the context of structural behaviour, strength can be defined as the force under which a limit state (e.g., plastic failure, buckling, etc.) is attained. Not all limit states cause "collapse", so it is better to define strength as "the limit state which determines the boundary of structural usefulness" (Galambos & Raviranda, 1981). Hence, the structural behaviour of a member or element is suitable only so long as the Resistance (R) ≥ Load Effect (S) (accordingly, having $R < S$ is unacceptable) (Figure 2-7).

2.6. GENERAL

In any design scenario, the variables R and S are random, which makes it theoretically impossible to state with certainty that $S \leq R$ for a given structure or element. Due to their random nature, there is always a probability that $R < S$. Suitable design criteria are those that reduce this probability to within an acceptable target range.

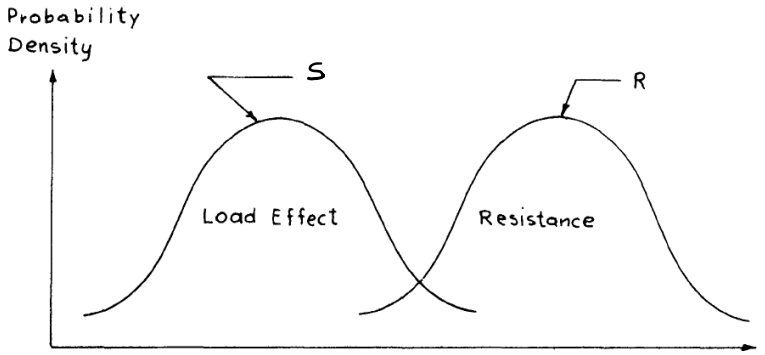

Figure 2-7. Probabilistic distribution of load effect (S) and resistance (R) (Galambos & Raviranda, 1981)

The limit states design (LSD) method [called the load and resistance factor design (LRFD) method, in the United States] is used exclusively in Canada. When checking ultimate limit states (ULS), specified loads are multiplied by load factors (α_i) to become factored loads, and nominal strengths of structural elements are determined from specified material properties and dimensions. In the end, factored resistances are determined as the product of the nominal strength and a resistance factor (ϕ) and compared to the factored loads. The purpose of load and resistance factors (α_i and ϕ) is to account for uncertainties with respect to specified/nominal properties in a systematic way, and to calibrate/achieve a specified probability of failure (i.e., the probability

that $R < S$). The fundamental safety criterion that must be met in the design of steel structures is hence (CSA, 2019a):

$$\phi R \geq \sum \alpha_i S_i \tag{2.43}$$

where ϕR = factored resistance and $\Sigma\alpha_i S_i$ = sum of the factored load effects, in which α_i = load factor (for each load type) and S_i = specified load effect (for each load type).

The structural reliability of a member or element is based on the limit state where the member's resistance (R) and the load effect (S) acting on the member are compared (Melchers & Beck, 2018). A failure event occurs under the following conditions, or any other equivalent criteria, e.g.:

$$R - S < 0 \quad \frac{R}{S} < 0 \quad ln(R) - ln(S) < 0 \tag{2.44}$$

To account for uncertainty, these quantities are necessarily modelled as random variables with their own, inherent probability distributions. Reliability is then understood to be the probability of failure, corresponding to one of the following expressions:

$$p_f = P\left(R - S < 0\right) \quad P\left(\frac{R}{S} < 1\right) \quad P\left(lnR - lnS < 0\right) \tag{2.45}$$

The role of the reliability analyst is then to specify the random variables representing the load and resistance. The probability in Eq. 2.45 is not available analytically unless special distribution assumptions are made, such as the joint normality or log-normality of the load and resistance. In practice, structural design codes specify that basic reliability is performed under these assumptions, for ease of use under a unifying algorithm. CSA S408-11 (CSA, 2011), for example, specifies that the load and resistance are assumed to be independently log-normally distributed variables.

2.7. FOR LOG-NORMAL VARIABLES

If R and S are assumed to be log-normally distributed (Xi & Packer, 2021), the safety margin, G can be expressed as:

$$G = ln(R) - ln(S) = ln(R / S) \tag{2.46}$$

The probability of failure, p_F, is then calculates as:

$$p_F = P\left[G < 0\right] \tag{2.47}$$

However, because the probability distribution of failure is (in a practical sense) unknown (i.e., only the mean and variance can be calculated in a closed-form sense) (Ravindra & Galambos, 1978), a first-order probabilistic method can be used to provide a relative measure of safety.

According to Ellingwood et al. (1980), if R and S are assumed to be statistically independent, then a reliability index (β^+) can be defined as a function of the mean value of G, G_m, and its standard deviation, σ_G:

$$\beta^+ = \frac{G_m}{\sigma_G} \tag{2.48}$$

This equation represents the number of standard deviations between G_m and zero (the failure condition), which can be directly related to the probability of failure of a structural component. When R and S have log-normal distributions, the reliability index, β^+, can be rewritten as:

$$\beta^+ = \frac{\left[\ln\left(\frac{R}{S}\right)\right]_m}{\sigma_{\ln\left(R/S\right)}} \tag{2.49}$$

Figure 2-8 is akin to Figure 2-7, but with ln(R/S) as the horizontal axis. The shaded area shows the event of exceeding the limit state (ln(R/S) < 1) and is equal to the probability of failure. When β^+ increases, the probability of exceeding the limit state decreases. The above equation can also be written as:

$$\beta^+ \simeq \frac{\ln\left(\frac{R_m}{S_m}\right)}{\sqrt{V_R^2 + V_S^2}} \tag{2.50}$$

where R_m and S_m = mean values of the resistance and load effect, respectively; and V_R and V_S = coefficients of variation (COVs) of the resistance and load effect, respectively. Eq. 2.50 includes a small-variance approximation (i.e., substitutions for $\ln(R/S)_m$ and $\sigma_{\ln(R/S)}$) that is valid when V_R and V_S are both less than about 0.30 (Ellingwood et al., 1980).

It is important to note that the COV is a relative measure of variability that indicates the size of standard deviation in relation to mean value of the population. The COV is a standardized, unitless measure that allows comparing variability between disparate groups and characteristics and may, in some references, be called the relative standard deviation (RSV). Higher values of the COV indicate that the standard deviation is relatively large compared to the mean value of a distribution. The COV (denoted as V, in general) can be formulated as:

$$V = \frac{\sigma \text{ (mean value)}}{\mu \text{ (standard deviation)}} \tag{2.51}$$

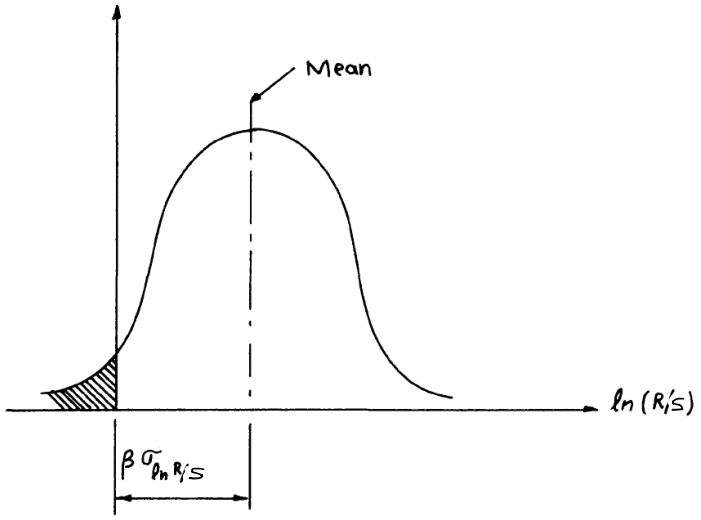

Figure 2-8. Definition of the reliability index (Galambos & Raviranda, 1981)

The mean resistance (R_m) is often considered to be the product of the nominal resistance multiplied by a material, geometric, and professional factor. Hence, R_m can be written as (Ravindra & Galambos, 1978):

$$R_m = \delta_M \delta_G \delta_P R_n \tag{2.52}$$

where δ_M = "material" ratio (for example, it can be the ratio of mean yield strength over the nominal yield strength), δ_G = "geometric" or fabrication ratio (for example, it can be the ratio of mean cross-sectional area over nominal cross-sectional area); and δ_P = "professional" ratio (for example, it can be the ratio of the tests capacity results over the calculated capacity results) (Kennedy et al., 1980). If the abovementioned factors are assumed linear and independent, then the following equation governs the relationship between the COVs of the parameters and the COV of the resistance:

$$V_R^2 = V_M^2 + V_G^2 + V_P^2 \tag{2.53}$$

where V_M, V_G, and V_P = COVs for δ_M, δ_G, and δ_P respectively.

Similarly, the load effect of a steel member is represented by the sum of the actual-to-nominal ratios for the applied loads $\delta_{S,i}$ and their corresponding nominal value. The mean load effect (S_m) can be written as:

$$S_m = \Sigma \delta_{S,i} S_{n,i} \tag{2.54}$$

where $\delta_{S,i}$ = the actual-to-nominal ratio of load effect and $S_{n,i}$ = the nominal load effect corresponding to $\delta_{S,i}$. The subscript i refers to the load effect under consideration (dead, live, etc.).

2.7.1. CLOSED FORM SOLUTIONS

The limit state design equation (Eq. 2.43) can be re-arranged to find a closed form expression for the acceptable value of ϕ to satisfy a target reliability index (β^+) for a specific structural component. For simplicity,

it is often desirable to determine this value regardless of the factored load effect; however, in reality, the load and resistance and hence, the probability of failure, are coupled. Several approaches have been developed to overcome this challenge.

2.7.2. SEPARATION FACTOR APPROACH

Ravindra & Galambos (1978) developed a "Separation Factor Approach" whereby a linear approximation [originally proposed by Lind (1971)] is used to uncouple the load and resistance sides of the limit states equation. This approach incorporates a so-called efficient of separation, α; i.e.:

$$\phi = \frac{R_m}{R_n} e^{\left(-\alpha\beta^+ V_R\right)} = \delta_M \delta_G \delta_P e^{\left(-\alpha\beta^+ V_R\right)} = \delta_R e^{\left(-\alpha\beta^+ V_R\right)} \tag{2.55}$$

where δ_R = bias factor for the resistance.

This linear approximation gives an average error and standard deviation of nearly zero and 3% respectively compared to more rigorous approaches if α is set to 0.55 (Ravindra & Galambos, 1978). A value of $\alpha = 0.75$ was initially proposed by (Lind, 1971) and has also been used, historically, with (ASCE, 2016) currently advocating for a value of $\alpha \approx 0.70$.

In this method, a formula or an algorithm for nominal resistance is selected. Then the mean value and COV are calculated for the element using the formula of the previous step and the information available for the mechanical properties of the material or test results of the element. The resistance factor, ϕ, is then calculated using the abovementioned equation. It is important to mention that, in most cases, the resistance of the structural component being studied must be expressed as a function of a characteristic variable, e.g., the slenderness for columns (Ravindra & Galambos, 1978).

This approach applies to members in which the resistance is a direct product of a geometric and material property. For non-linear resistance functions, the contribution from each property must be determined over the range of the independent variable. The relative contribution of each of the distinct property to the bias factors and corresponding COVs can be approximated by mathematical manipulation of the resistance equation, using a partial derivative approach (Kennedy & Gad Aly, 1980). Depending on how the equation describing the property was determined, either on a solely mathematical basis or a semi-empirical or curve-fitting basis, different participation factors for the various properties involved will be determined (Kennedy & Gad Aly, 1980).

2.7.3. APPROXIMATE FORM ANALYSIS

The Canadian Standard Association provides a standard, CSA S408-11 (CSA, 2011), with guidelines for the development of limit state design standards. Annex B.2.5 of CSA S408-11 describes a so-called Approximate Method (an approximate FORM method) for calculating the resistance factor (using Eq. 2.56) to achieve target β^+ for arbitrary limit states:

$$\phi = \delta_R \frac{\sum_i \alpha_i S_i}{S_m} e^{\left(-\beta^+ \sqrt{V_R^2 + V_S^2}\right)} \tag{2.56}$$

All variables have been previously defined.

Eq. 2.56 is derived from Eq. 2.50 for the reliability index, β^+, where the resistance factor and load effect are represented by independent lognormal distributions. This equation, also rather dated, has been used extensively for code calibration in Canada and the United States and gives results that are consistent with these past calibrations.

2.7.4. MONTE CARLO SIMULATIONS

As yet another alternative for reliability analysis, Monte Carlo techniques can be used to randomly sample from the various resistance and load effect parameter distributions to determine a possible resistance and load effect scenario for a member or connection. This process closely approximates the probabilistic behaviour of the resistance and load effect for the desired design scenario with a large number of samples. Kennedy & Baker (1984) and Lundberg & Galambos (1996), along with countless others, provide examples of MCS, and it is also advocated in several key codes and standards (e.g. CSA S408- 11). MCS are particularly useful for non-linear resistance equations, where the participation of variables is difficult to ascertain mathematically.

2.8. TARGET RELIABILITY INDEX

As previously discussed, the target reliability index (β^+) is an approximate measure of the acceptable probability of failure that accounts for the mean values, uncertainties, and form of the probability distribution of the loads and resistances. These parameters should be determined using large, unbiased databases, because the calculated reliability index can be very sensitive to lower tail of the resistance distribution and the upper tail of the load effect distribution (CSA, 2011).

The recommended target reliability indices for steel and concrete buildings specified in the 1981 edition of the NBCC (CSA, 2011) are shown in Table 2-6 below.

Table 2-6. Target reliability indices for steel and concrete buildings – Ultimate limit states (based on 30-year life) (CSA, 2011)

Safety Class	Type of Failure	
	Gradual (Ductile)	Sudden (Brittle)
Not serious	2.5	3.0
Serious (normal buildings)	3.5	4.0
Very serious	4.0	4.5

As Clause B.3 in CSA S16:19 states, LSD was first introduced in the NBCC (1975), where the reliability index for steel buildings as a whole was taken as 3.0. A greater reliability index was used for connectors so that the probability of the connector failing before the member as a whole was reduced and the more ductile mode of failure of the member was favoured. This was done to make the connection stronger than the member they joined. In the current NBCC and current edition of CSA S16:19, the reliability index for steel buildings as a whole remains at 3.0, and indices greater than this value are used for connections (CSA, 2019a). AISC 360-16 proposes the same reliability index of 3.0 in the Commentary of Section B3.1 (AISC, 2016); however, values as low as 2.6 are not uncommon for some elements or design scenarios (e.g., steel columns).

2.9. SUMMARY OF CHOSEN APPROACH AND LIMITATIONS

In this research, the two approaches proposed by Tousignant & Packer (2022b) for the design of concrete-filled HSS beam-columns (Approaches (i) and (ii) described in Section 2.4) along with the current CSA S16:19 and AISC 360-16 methods are evaluated by using MCS to simulate various design scenarios for characteristic members, without reinforcement, over a range of live-to-dead load ratios. Reliability indices are then obtained and compared to the target value of $\beta^+ = 3.0$ spelled out in Annex B of CSA S16:19 (CSA, 2019a).

The reliability indices determined herein are based on comparison of the member resistance (R) and load effect (S) distributions, assuming perfect design (which will be discussed later in Section 3.4), whereby the safety margin (G) is given by Eq. 2.46 in which the failure event occurs when $G < 0$. As discussed earlier in Section 2.5, the probabilistic methods used by the authors relates the probability of failure (i.e., the probability that $G < 0$) to the mean and standard deviation of G (G_m and σ_G, respectively) using a safety/reliability index (β^+) defined in Eq. 2.48. β^+ can be viewed simply as the number of standard deviations between G_m and the failure condition, for which targets are given in design codes (e.g., CSA, 2019a and AISC, 2016).

Chapter 3: MONTE CARLO SIMULATIONS

3.1. OVERVIEW

The two proposed approaches by Tousignant & Packer (2022b) for the design of concrete-filled HSS beam-columns are evaluated herein and compared to those of current CSA S16:19 and AISC 360-16 by using MCS to simulate various design scenarios for characteristic members. A representative set of 12 concrete-filled RHS and 12 concrete-filled CHS members, without reinforcement, are analyzed with variation in concrete strength, wall slenderness, effective length and loading eccentricity. Using MCS, reliability indices (β^+) are determined over a range of live-to-dead load ratios and the resulting β^+ values are compared to the code specified targets.

3.2. MONTE CARLO SIMULATION INPUTS

As discussed earlier, in Section 2.9, β^+ can be viewed simply as the number of standard deviations between mean of safety margin (G_m) and the failure condition, for which target values are given in design codes (e.g. CSA 2019a, AISC 2016). The participating random variables for determining the reliability index here are the professional factors, yield strength of steel (F_y), concrete cylinder strength (f_c'), modulus of elasticity (E), wall slenderness (b_{el}/t and d/t), effective length (KL/r) and eccentricity (e).

Herein, random samples are drawn from the participating random variable distributions to determine a possible resistance and load effect scenario for a member. For each design scenario, a possible resistance and load effect are determined, and this process is repeated 1×10^6 times to approximate the distribution of R and S (from which G, G_m, σ_m and β^+ can be determined).

3.2.1. RESISTANCE PARAMETERS

The basic random variable distributions for the resistance are shown in Table 3-1. The distributions of these variables are taken from the literature and are assumed to be log-normally distributed in general accordance with CSA S408-11 (CSA, 2011). The bias coefficient (δ) and the corresponding coefficient of variation (V) for F_y in Table 3-1 were taken from (Xi & Packer, 2021) which, in turn, came from the database of Liu (2016). The values for f_c' are in accord with those used in Bartlett (2007) which, in turn, are based on Bartlett & Macgregor (1996). Since both F_y and f_c' reflect minimum specified strength in CSA standards, their distribution were truncated to limit the selection of bias coefficients to a minimum of 1.0. The modulus of elasticity, depth and width statistical parameters were obtained from Kennedy & Gad Aly (1980).

In addition to the above, the probability distribution of R is a function of the so-called professional factor, as discussed earlier, which accounts for imperfect nominal resistance design equations. The professional factor variations were determined from the database extracted from Thai et al. (2019), which is further discussed in Section 3.2.3.

Table 3-1. Bias coefficients and COVs for resistance parameters (excluding the professional factors)

parameter	δ	V	Reference
F_y	1.178	0.086	Xi & Packer (2021)
f_c'	1.270	0.122	Bartlett (2007)
E	1.00	0.019	Kennedy & Gad Aly (1980)
b, h or d	1.00	0.002	Kennedy & Gad Aly (1980)
t	0.975	0.025	Kennedy & Gad Aly (1980)

3.2.2. Load Effect Parameters

The participating random variables for the load effect are dead and live load. The load effect parameter distributions were obtained from Schmidt & Bartlett (2002), and are summarized in Table 3-2. Again, these random variables are assumed to be log-normally distributed in general accordance with CSA S408-11 (CSA, 2011).

Table 3-2. Bias coefficients and COVs for load effect parameters

parameter	δ	V	Reference
Live load	0.78	0.32	Schmidt & Bartlett (2002)
Dead load	1.05	0.10	Schmidt & Bartlett (2002)

3.2.3. Database of Tests

3.2.3.1. Description of Test Database

The database of tests used to determine the professional factor statistics was extracted from a large database of test on concentrically and eccentrically loaded concrete-filled HSS members compiled by Thai et al. (2019). The database was screened to include only specimens that met the proposed new limits of validity (for f_c', b_{el}/t and h_{el}/t for RHS members and d/t for CHS members) discussed in Section 2.4. Further screening was performed to remove experiments with $F_y < 300$ MPa and $F_y > 450$ to reflect the range of typical measured HSS yield strength available in Canada.

For the remaining experiments with loading eccentricity (e) > 0, the nominal predicted compressive strength in the presence of bending (C_n) was calculated for all approaches by rearranging the interaction equation (e.g. Eq. 2.18) with instances of C_f and M_f replaced by C_n and $C_n \times e$, respectively. It was necessary

in calculating C_n to assume that $r = 2t$ and $\rho_c = 2400$ kg/m^2 in accord with above. The test to predicted ratios (or bias coefficients, δ) and corresponding coefficient of variations, V, for each method was taken as the average of the actual (experimental) strength (C_a) divided by C_n over all tests.

A similar re-analysis was performed of the Thai et al. (2019) database to determine the resulting professional factor statistics for concentrically loaded RHS and CHS members with $e = 0$, which are designed according to only compressive resistance equations (e.g. Eq. 2.1).

3.2.3.2. CALCULATION OF PROFESSIONAL FACTORS

For CSA S16:19, C_n was calculated by rearranging the interaction equation (e.g. Eq. 2.18) with instances of C_f and M_f replaced by C_n and $C_n \times e$, respectively. Then the bias coefficient, δ_P and the corresponding COV (V_P) was determined by taking the average of the C_a/C_n values. A similar re-analysis was also performed to determine the professional factors for concentrically loaded HSS members when there is no eccentricity, as discussed in Section 3.2.3.1. The results (δ_P and V_P values) are presented in Table 3-3. All calculations assumed an outside corner radius for RHS of $2t$, concrete density of $\rho_c = 2400$ kg/m^3 and when necessary, $C_{fs}/C_f = 0$. Figure 3-1 and Figure 3-2 demonstrate the distribution of actual/predicted strength for Concrete-filled RHS and CHS beam-columns, respectively. Database of tests for concentrically and eccentrically loaded members are tabulated in Appendix C: and Appendix D:, respectively.

Table 3-3. Bias coefficients and COVs for the professional factors in accordance with CSA S16:19

	Shape	Number of tests	δ_P	V_P
Beam-columns ($e > 0$)	RHS	14	1.21	0.05
Columns ($e = 0$)		189	1.24	0.16
Beam-columns ($e > 0$)	CHS	22	0.98	0.11
Columns ($e = 0$)		263	1.10	0.17

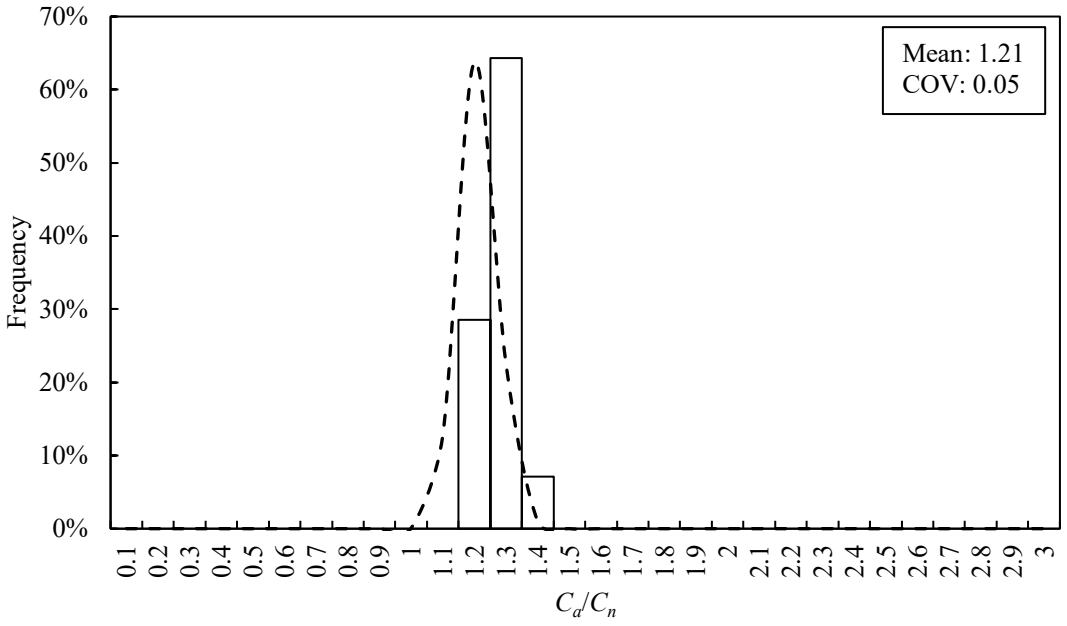

Figure 3-1. Histogram of professional factor distribution for concrete-filled RHS beam-columns in accordance with CSA S16:19

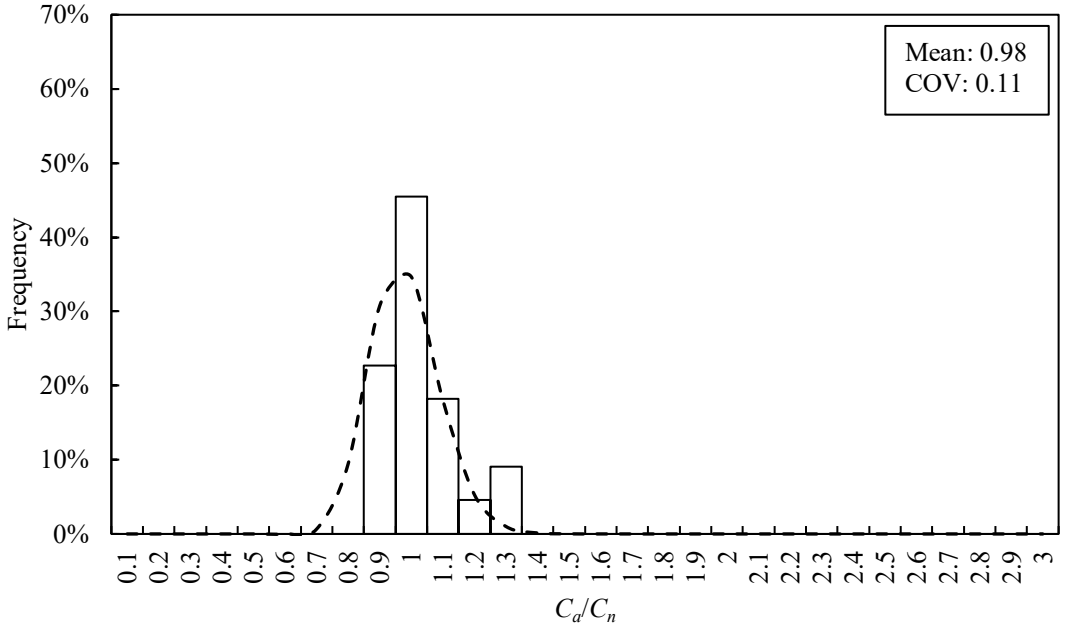

Figure 3-2. Histogram of professional factor distribution for concrete-filled CHS beam-columns in accordance with CSA S16:19

For AISC 360, the same approach was used to calculate the professional factors. The results (δ_P and V_P values) are summarized in Table 3-4. It is important to again note that all calculations assumed an outside corner radius for RHS of $2t$, concrete density of ρ_c = 2400 kg/m^3 and when necessary, C_{fs}/C_f = 0. Figure 3-3 and Figure 3-4 show the distribution of actual/predicted strength for concrete-filled RHS and CHS beam-

columns, respectively. Database of tests for concentrically and eccentrically loaded members are tabulated in Appendix C: and Appendix D:, respectively.

Table 3-4. Bias coefficients and COVs for the professional factors in accordance with AISC 360-16

	Shape	Number of tests	δ_P	V_P
Beam-columns ($e > 0$)	RHS	48	1.24	0.28
Columns ($e = 0$)		149	1.24	0.15
Beam-columns ($e > 0$)	CHS	12	0.94	0.09
Columns ($e = 0$)		238	1.22	0.13

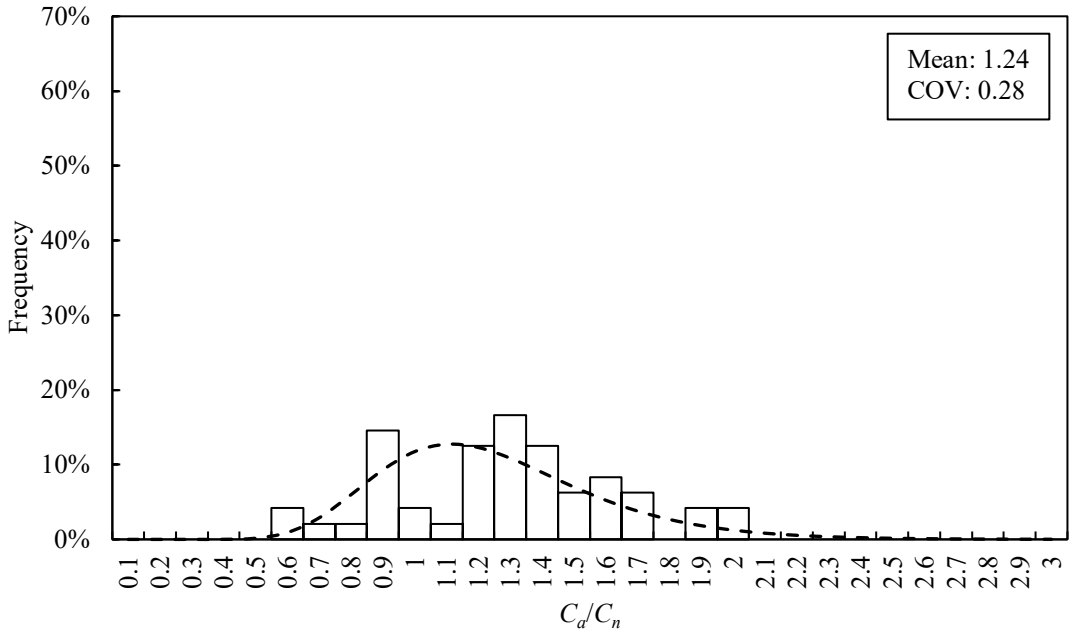

Figure 3-3. Histogram of professional factor distribution for concrete-filled RHS beam-columns in accordance with AISC 360-16

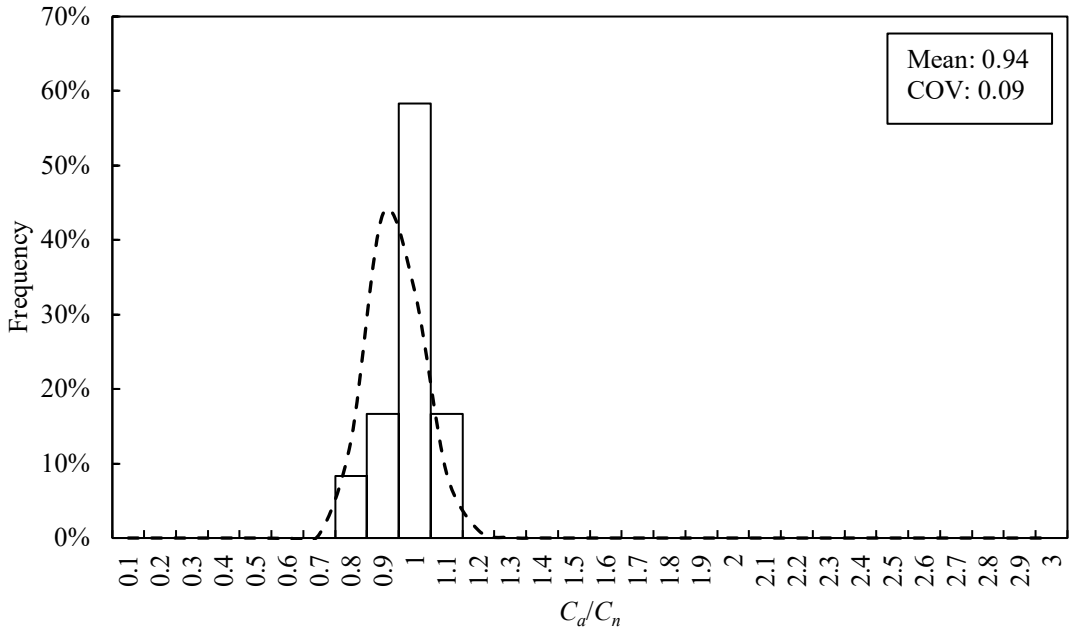

Figure 3-4. Histogram of professional factor distribution for concrete-filled CHS beam-columns in accordance with AISC 360-16

For the Tousignant & Packer (2022a,b) proposal, the same approach was used to determine C_n by rearranging the interaction equation (Eq. 2.18) with instances of C_f and M_f replaced by C_n and $C_n \times e$, respectively. Then the bias coefficient, δ_P and the corresponding COV was determined by taking the average of the C_a/C_n values. A similar re-analysis was also performed to determine the professional factors for concentrically loaded HSS members when there is no eccentricity, as discussed in Section 3.2.3.1. Database of tests for concentrically and eccentrically loaded members are tabulated in Appendix C: and Appendix D:, respectively.

The results (δ_P and V_P values) are summarized in Table 3-5, which shows that for RHS concrete-filled beam-columns, Approach (ii) produces higher C_a/C_n values, on average, but is less precise than Approach (i). Comparing the results to those of CSA S16:19 (Table 3-3), it can be seen that CSA S16:19 produces higher C_a/C_n values than Approach (i) and lower C_a/C_n values than Approach (ii) but has the lowest COV. Comparing the results to those of AISC 360-16 (Table 3-4), it can also be deduced that AISC 360-16 produces C_a/C_n values between Approach (i) and Approach (ii) but is the least precise. It can also be deduced that for CHS concrete-filled beam-columns, Approach (ii) produces higher C_a/C_n values but has the same level of accuracy as Approach (i). Comparing the results to those of CSA S16:19 (Table 3-4), one can infer that the statistics are similar – for both approaches. Compared to AISC 360-16 (Table 3-4), Tousignant & Packer's approaches produce higher mean and COV values. Figure 3-5 and Figure 3-6 show the distributions of actual/predicted strength for concrete-filled RHS beam-columns according to Tousignant & Packer's (2022b) approaches, and Figure 3-7 and Figure 3-8 illustrate the same for concrete-filled CHS beam-columns.

Table 3-5. Bias coefficients and COVs for the professional factors in accordance with Tousignant & Packer' s (2022a,b) Proposal

	Shape	Number of tests	Approach (i)		Approach (ii)	
			δ_P	V_P	δ_P	V_P
Beam-columns ($e > 0$)	RHS	48	1.17	0.19	1.44	0.24
Columns ($e = 0$)		181	1.27	0.16	1.27	0.16
Beam-columns ($e > 0$)	CHS	12	1.05	0.13	1.16	0.13
Columns ($e = 0$)		238	1.09	0.17	1.09	0.17

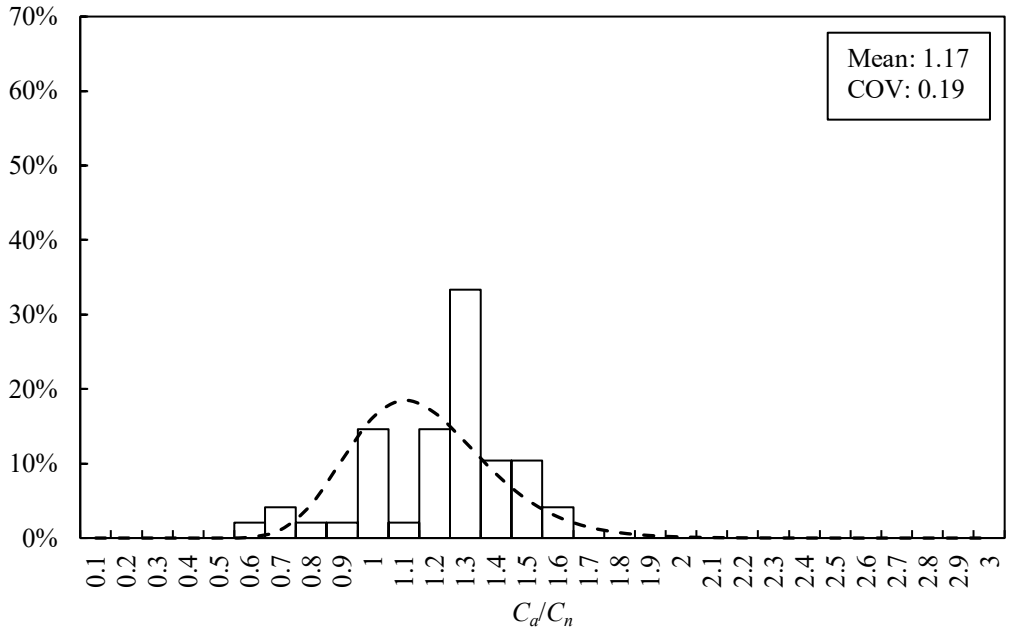

Figure 3-5. Histogram of professional factor distribution for concrete-filled RHS beam-columns in accordance with Proposed Approach (i)

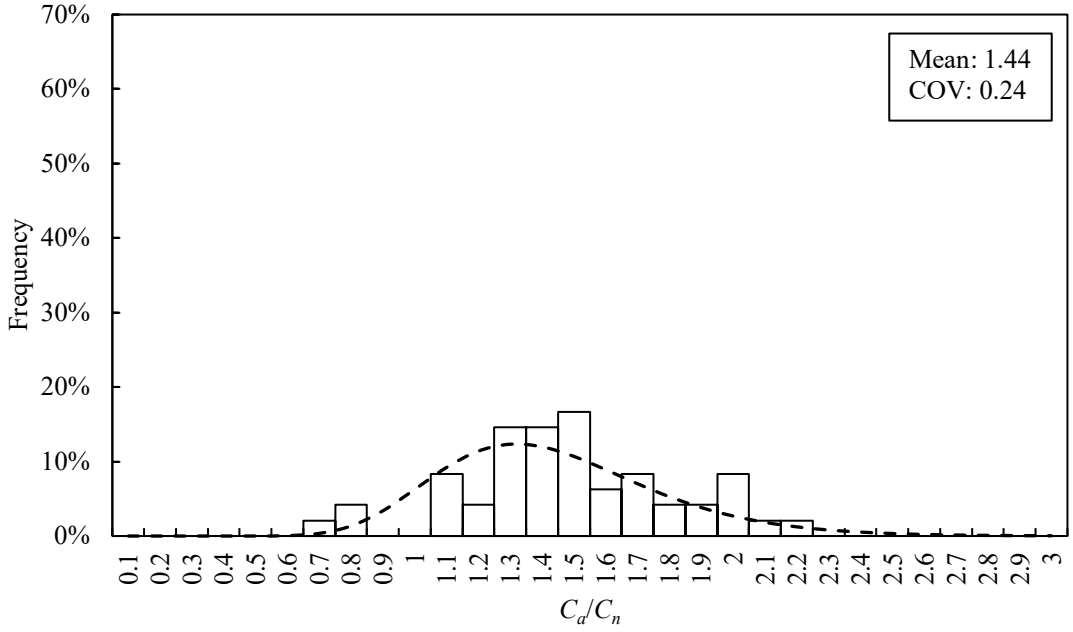

Figure 3-6. Histogram of professional factor distribution for concrete-filled RHS beam-columns in accordance with Proposed Approach (ii)

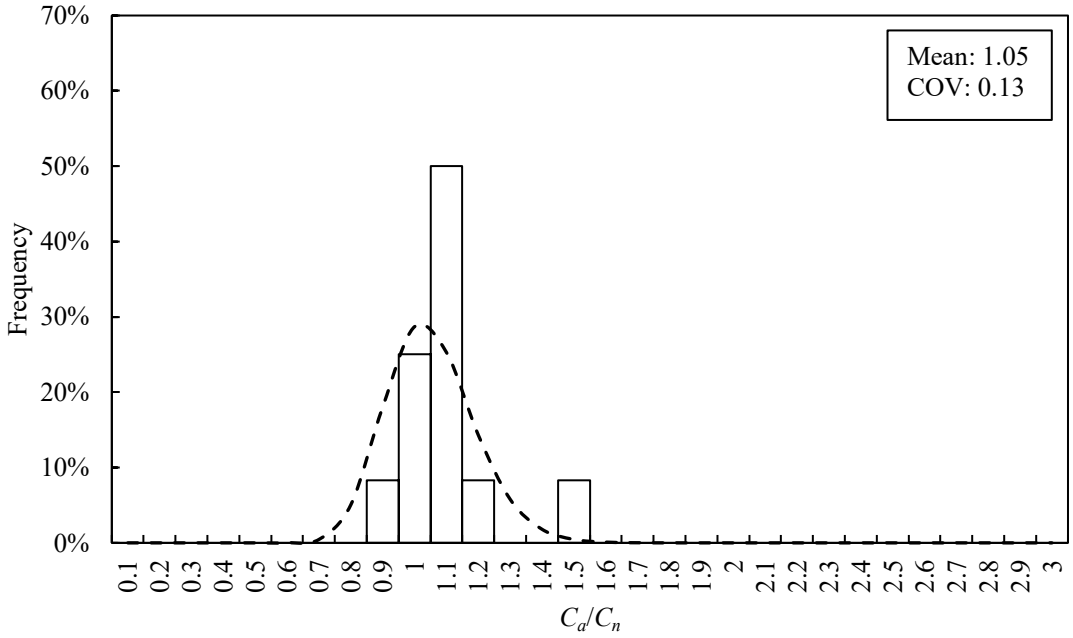

Figure 3-7. Histogram of professional factor distribution for concrete-filled CHS beam-columns in accordance with Proposed Approach (i)

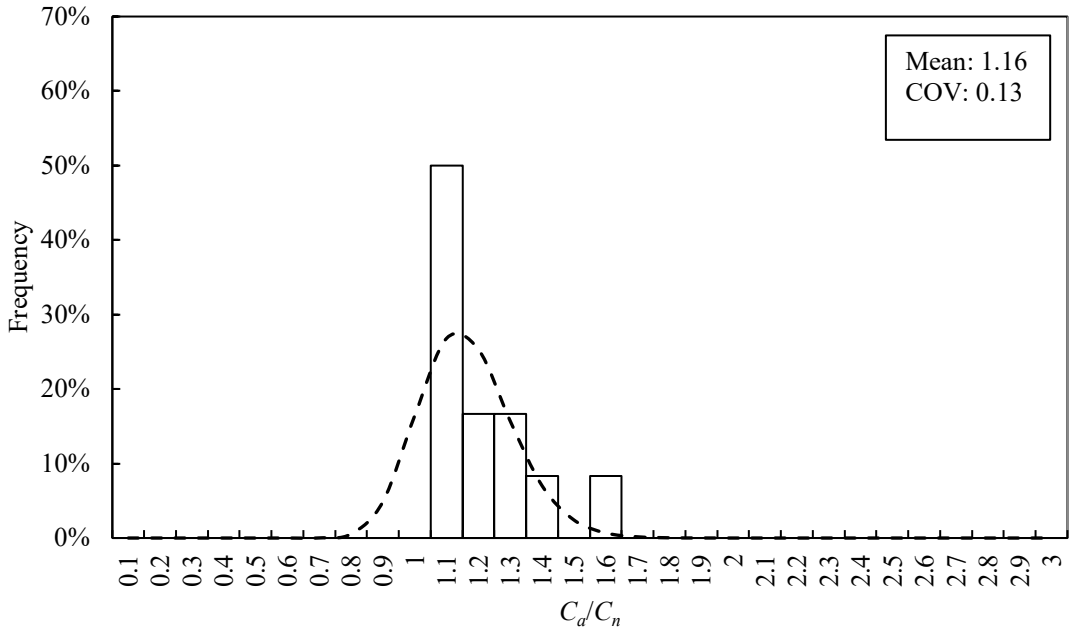

Figure 3-8. Histogram of professional factor distribution for concrete-filled CHS beam-columns in accordance with Proposed Approach (ii)

Figures 3-9 to 3-14 compare the ratio of C_a/C_n for beam-column tests of the database with values of e, KL and f_c' from the corresponding experiments. Looking at Figure 3-9 and Figure 3-12, it can be demonstrated that C_a/C_n remains somewhat constant as e goes up for all of the design methods considered. It can be deduced from the plots (Figure 3-10 and Figure 3-13) that the ratio of C_a/C_n decreases somewhat for all the approaches as KL goes up for both RHS and CHS beam-columns. Moreover, by looking at Figure 3-11 and Figure 3-14, it can be seen that the ratio of C_a/C_n increases for all the approaches as f_c' goes up. Nonetheless, all approaches maintain a reasonable level of accuracy over the full ranges of each variable.

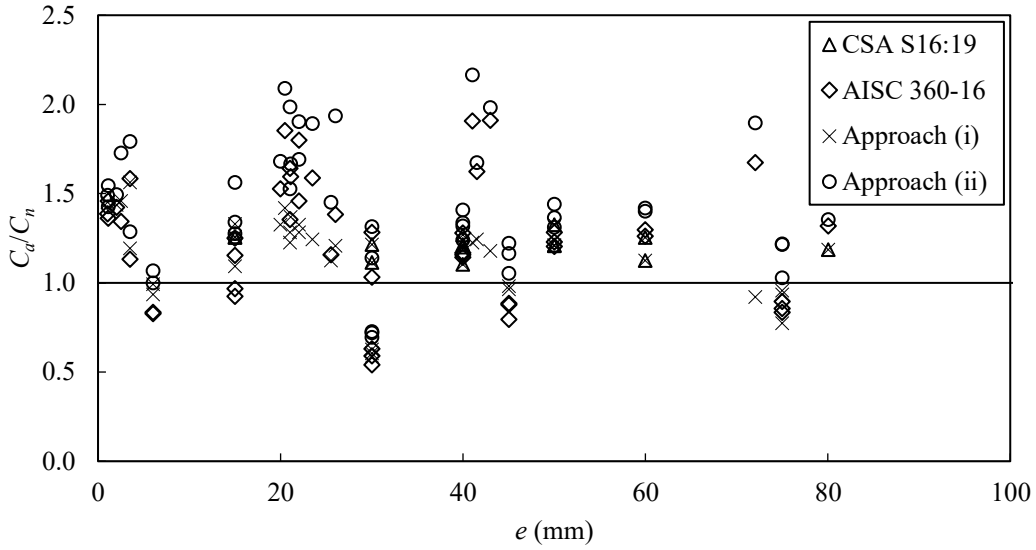

Figure 3-9. Comparison of concrete-filled RHS beam-column tests to predictions for eccentricity

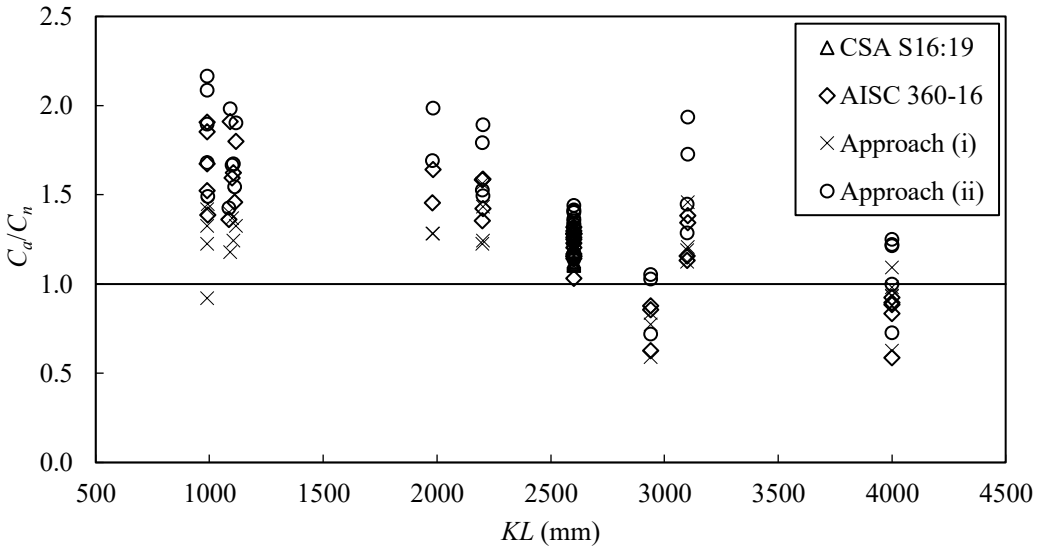

Figure 3-10. Comparison of concrete-filled RHS beam-column tests to predictions for effective length

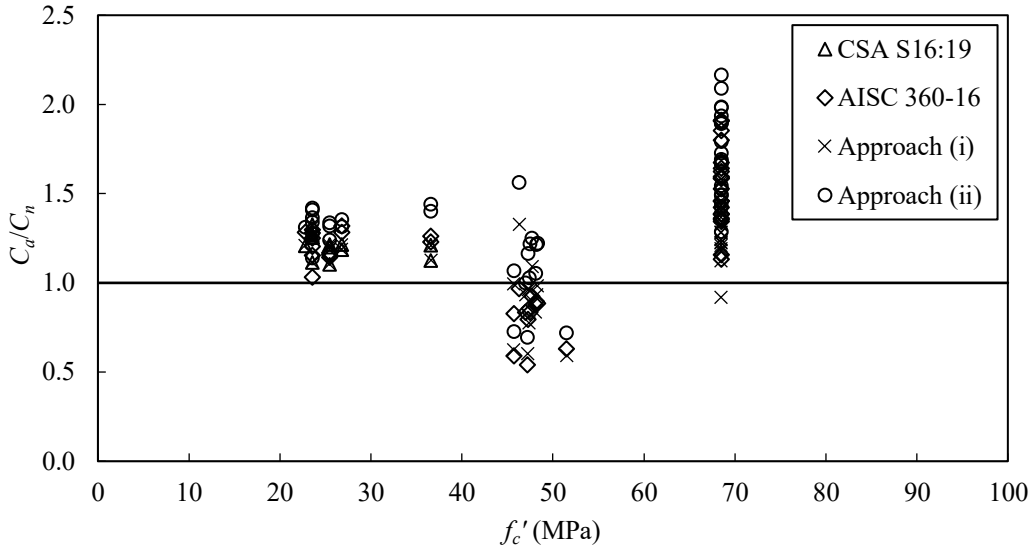

Figure 3-11. Comparison of concrete-filled RHS beam-column tests to predictions for concrete strength

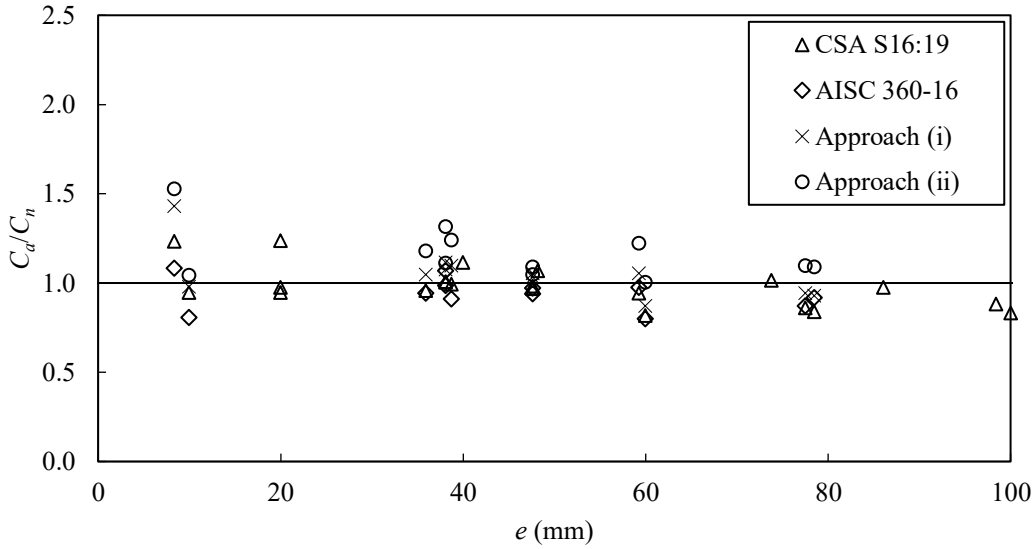

Figure 3-12. Comparison of concrete-filled CHS beam-column tests to predictions for eccentricity

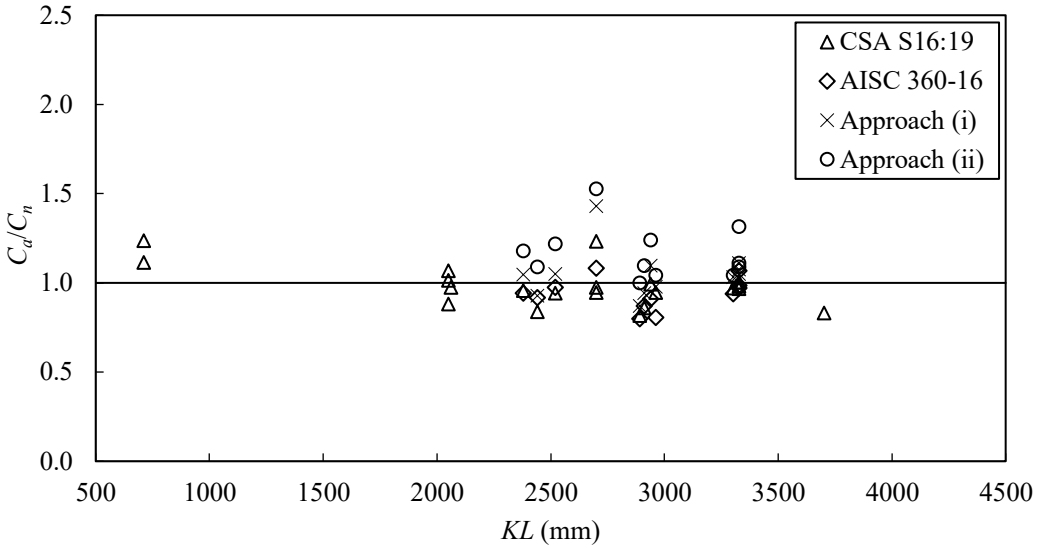

Figure 3-13. Comparison of concrete-filled CHS beam-column tests to predictions for effective length

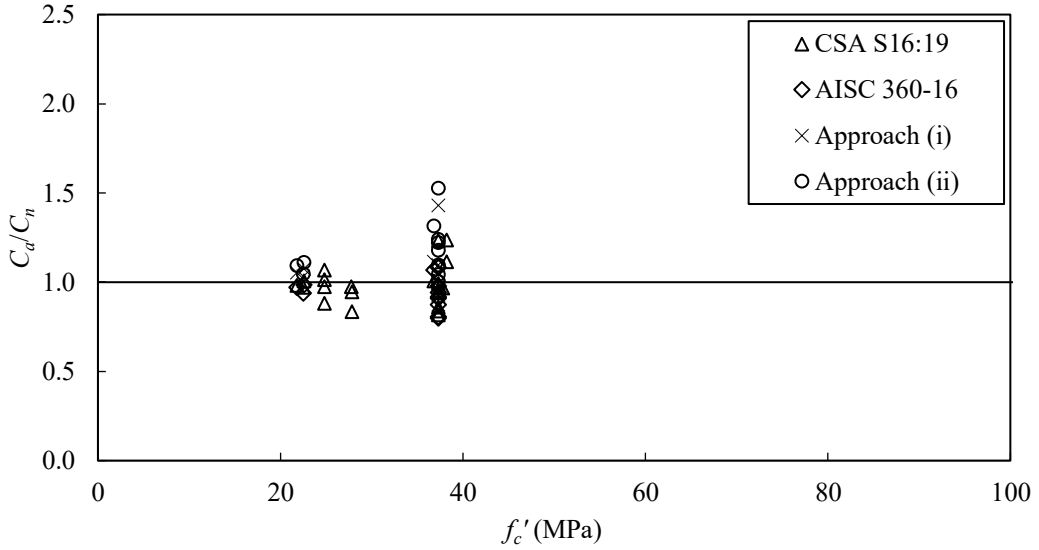

Figure 3-14. Comparison of concrete-filled CHS beam-column tests to predictions for concrete strength

3.3. REPRESENTATIVE MEMBERS FOR MONTE CARLO SIMULATION

A representative set of 12 concrete-filled RHS and 12 concrete-filled CHS members were analyzed with variation in concrete strength, wall slenderness, effective length and loading eccentricity. The representative members were formulated to cover a range of KL/r (= 20, 50, 100, 150, 200, 250, 300) and b_{el}/t or d/t (The maximum limit was selected to be within the proposed limits of validities. Each member was further analyzed under axial load applied at five different values of eccentricity (e = 0, 100, 200, 300, 500) to produce the corresponding ratios of M_f/C_f, as well as for a range of L/D ratios from 0 to 3. The concrete strength, f_c' was varied between 20 and 90 (= 20, 50, 70, 90). In all analyses performed, the nominal strength of steel was taken

as F_y = 350 MPa (representative of CSA G40 HSS in Canada) (CSA, 2018). Nominal properties of the representative members are summarized in Table 3-6 and Table 3-7. It is important to mention that Tousignant & Packer's proposal (2022) puts a cap limit of 200 for *KL/r* and 70 MPa for the concrete strength, f_c' and the purpose of passing these limits in this research project is to investigate the probable potentials of this approach for higher strength and/or higher effective length scenarios.

Table 3-6. Representative RHS members for Monte Carlo Simulation

Member	*h* (mm)	*b* (mm)	*t* (mm)	B_{el}/t
356x356x13	355.6	355.6	12.70	24.0
356x356x6.4	355.6	355.6	6.35	52.0
305x305x13	304.8	304.8	12.70	20.0
305x305x6.4	304.8	304.8	6.35	44.0
254x254x13	254.0	254.0	12.70	16.0
254x254x6.4	254.0	254.0	6.35	36.0
203x203x13	203.2	203.2	12.70	12.0
203x203x6.4	203.2	203.2	6.35	28.0
178x178x13	177.8	177.8	12.70	10.0
178x178x6.4	177.8	177.8	6.35	24.0
152x152x13	152.4	152.4	12.70	8.0
152x152x6.4	152.4	152.4	6.35	20.0

Table 3-7. Representative CHS members for Monte Carlo Simulation

Member	*d* (mm)	*t* (mm)	*d*/*t*
508x6.4	508.0	6.35	80.0
457x6.4	457.2	6.35	72.0
356x9.5	355.6	9.53	37.3
356x6.4	355.6	6.35	56.0
324x9.5	323.9	9.53	34.0
324x6.4	323.9	6.35	51.0
245x9.5	244.5	9.53	25.7
245x6.4	244.5	6.35	38.5
219x9.5	219.1	9.53	23.0
219x6.4	219.1	6.35	34.5
168x9.5	168.3	9.53	17.7
168x6.4	168.3	6.35	26.5

3.4. MONTE CARLO SIMULATION PROCEDURE

In order to determine the reliability index for one of the representative connections, the following steps were taken:

1. The factored resistance of the member was determined using nominal values of material and geometrical properties discussed in Section 3.3.
2. Random samples were drawn from the probability distributions for resistance parameters in Table 3-1.
3. The sampled values were multiplied by their nominal counterparts.
4. The nominal member resistance was computed using the corresponding parameter values. The nominal resistance is determined by rearranging the interaction equation for beam-columns (See Appendix B: for the derivation of C_f).
5. A random sample was drawn from the probability distribution(s) for the professional factor(s) in Table 3-3 for CSA S16, Table 3-4 for AISC, and Table 3-5 for proposed methods by Tousignant & Packer (2022a,b).
6. The nominal member resistance (Step 4) was multiplied by the professional factor to obtain the final (unfactored) resistance.
7. The nominal dead and live load required for perfect design (when utilization ratio = 1.0) were determined for the governing load case.
8. Random samples were drawn from the probability distribution for load effect parameters in Table 3-2.
9. The sampled values were multiplied by their nominal counterparts, and the results were summed together, if necessary, to obtain the final (unfactored) load effect.

Steps 1-9 were repeated 1×10^6 times for each design scenario and the resulting distribution(s) of R and S, for each scenario, was used to determine G, G_m, σ_G and β^+. Figure 3-15 and Figure 3-16 show typical plots of R and S distributions obtained by completing 1×10^6 iterations of Step 1-9 for member 254x254x13, with f_c' = 50 MPa, e = 100 mm, KL/r = 100, and L/D = 1.0 for CSA S16:19 and Approach (i), respectively. It can be seen, therein, that both distributions are approximately log-normal. As can be seen in these figures, samples resistance distribution is more scattered and less concentrated around the mean value for the Approach (i) compared to CSA S16:19. That is due to lower coefficient of variation of CSA S16:19 derived from database of tests (see Section 3.2.3). A sample of the MCS code done by MATLAB software for concrete-filled RHS members in accordance with Approach (i) is explained in Appendix E:.

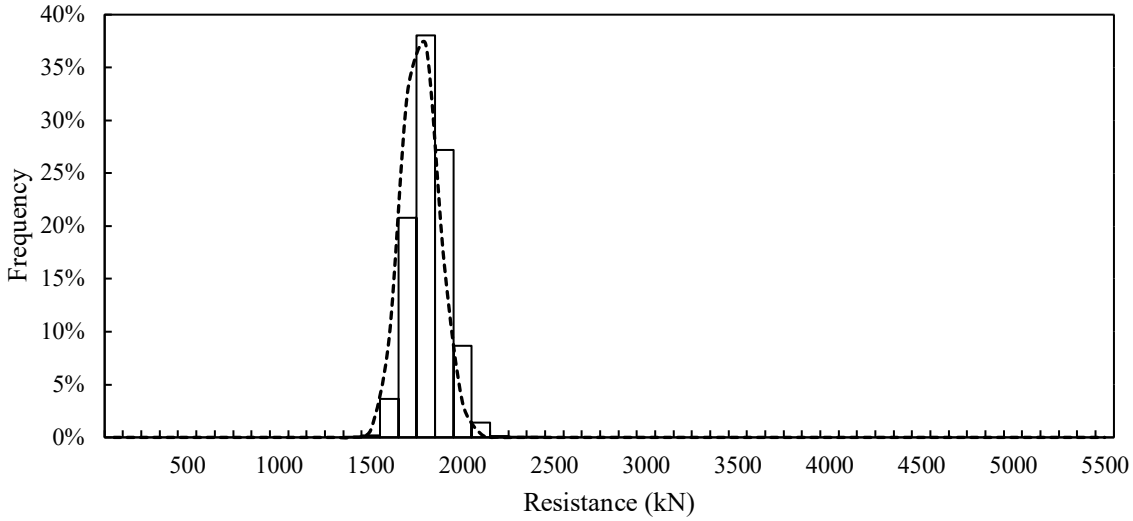

(a) Resistance

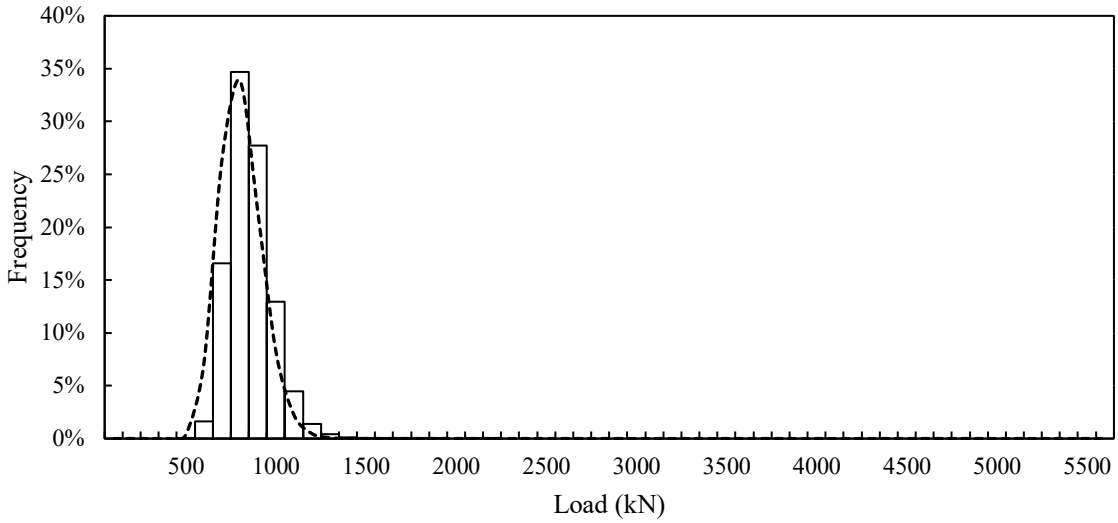

(b) Load effect

Figure 3-15. Resistance and load effect distributions for member 254x254x13, using CSA S16:19 with f_c' = 50 MPa, e = 100 mm, KL/r = 100, and L/D = 1.0

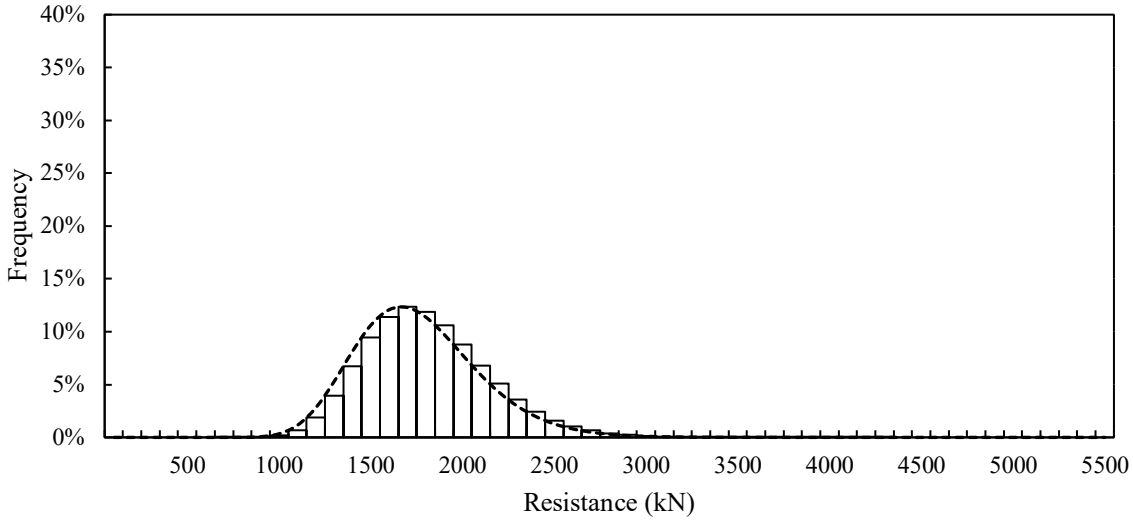

(a) Resistance

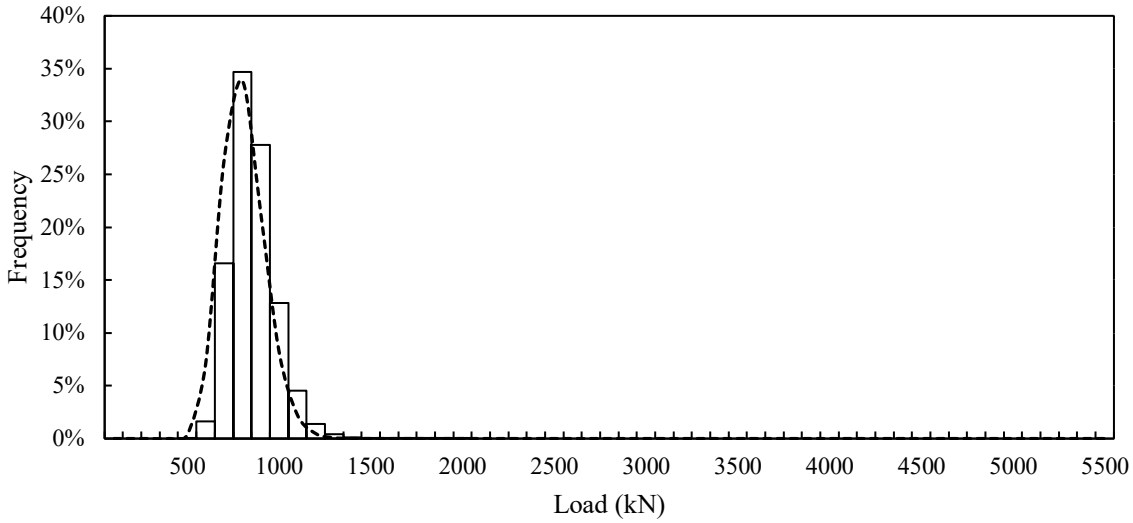

(b) Load effect

Figure 3-16. Resistance and load effect distributions for member 254x254x13, using Approach (i) with f_c' = 50 MPa, e = 100 mm, KL/r = 100, and L/D = 1.0

Chapter 4: RESULTS

4.1. OVERVIEW

The results of the MCS analysis (i.e. plots of β^+ vs. L/D) on CSA S16:19, AISC 360-16 and the two proposed approaches by Tousignant & Packer (2022a,b) design provisions are described in this chapter. Section 4.2 illustrates the effect of effective length (KL/r) on β^+, Section 4.3 shows the effect of eccentricity on β^+ and Section 4.4 illustrates the effect of concrete strength (f_c') on β^+. Each of the curves has been calculated by taking the average β^+ value over all 12 connections for RHS and CHS members at a given L/D ratio. Section 4.5 compares the overall β^+ for all of the approaches computed at each L/D ratio by taking the average β^+ value obtained across all members, eccentricities, and effective lengths.

The dip at a live-to-dead load ratio of about 0.15 in all of the figures is due to the intersection of the two factored load combinations of: 1.4D (dead load only) and 1.2D + 1.6L (for AISC) or (1.25D + 1.5L) for CSA S16. By equating these two loading situations with mean loads one obtains (L/D) = 0.168 and 0.135 respectively.

4.2. EFFECT OF EFFECTIVE LENGTH ON RELIABILITY INDEX

As discussed earlier, when e = 0, the professional factor statistics for concentrically loaded columns were used and Approach (i) and Approach (ii) will have the same results [since the only difference between these two approaches is the method for calculating the coefficient of bending (β) which is not required for concentrically loaded columns].

When e = 0 mm and f_c' = 70 MPa, by looking at Figure 4-1 (a-d), it can be seen that for concrete-filled RHS members, for all approaches, β^+ is above the target value of β^+ = 3.0 per Annex B of CSA S16:19. It can also be seen that β^+ decreases somewhat as KL/r increases, in accord with the general trend found previously in Figure 3-10. When e = 0 mm and f_c' = 70 MPa, AISC 360-16 provides the highest level of reliability, and CSA 16:19 provides the lowest. The two approaches by Tousignant & Packer (2022a,b) [Approaches (i) and (ii)] fall in between.

Figure 4-2 (a-d) shows a similar trend, i.e., that β^+ generally decreases as KL/r goes up for beam-columns with e = 200 mm and f_c' = 70 MPa. However, AISC 360-16 has the lowest reliability, in this case, and compared to the other approaches, shows an inverse trend (i.e., as KL/r goes up β^+ decreases). For Approach (i), the ranges of β^+ are slightly higher than Approach (ii) because the higher bias coefficient (δ_P, in Table 3-5) is coupled with

a lower precision (i.e., higher V_P). The CSA S16:19 approach is generally more reliable than the other methods because, while δ_P is similar to the other methods, V_P is much lower.

For some low L/D ratios, CSA S16:19, Approach (i), and Approach (ii), produce β^+ values that fall below the target reliability of 3.0. However, in all these cases, β^+ still exceeds 2.6, on average. The value 2.6 is the minimum reliability index currently expected in North American codes (AISC, 2016). Over the practical range of $1 \leq L/D \leq 3$ for steel members (Schmidt & Bartlett, 2002), β^+ always exceeds 3.0, except for the AISC 360-16 approach, in which β^+ is below 3.0 but above 2.6.

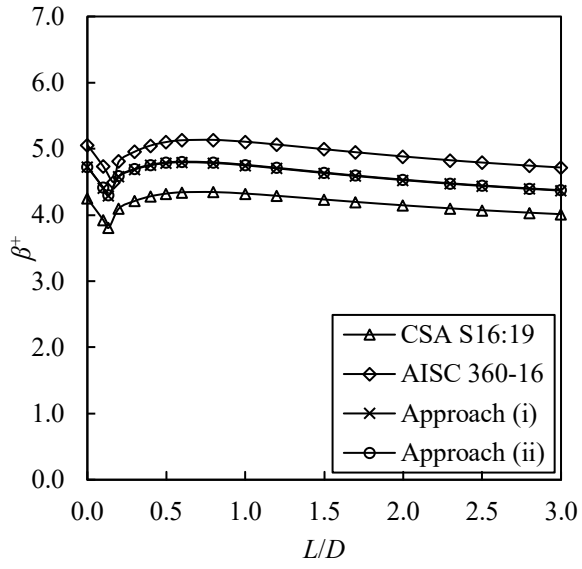

(a) $KL/r = 20$

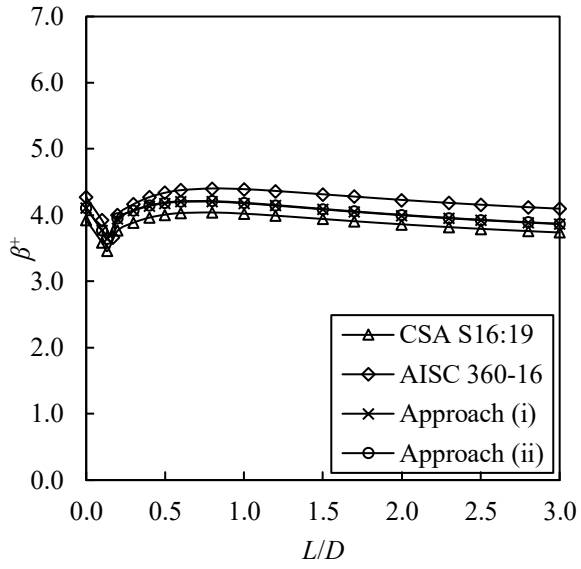

(b) $KL/r = 100$

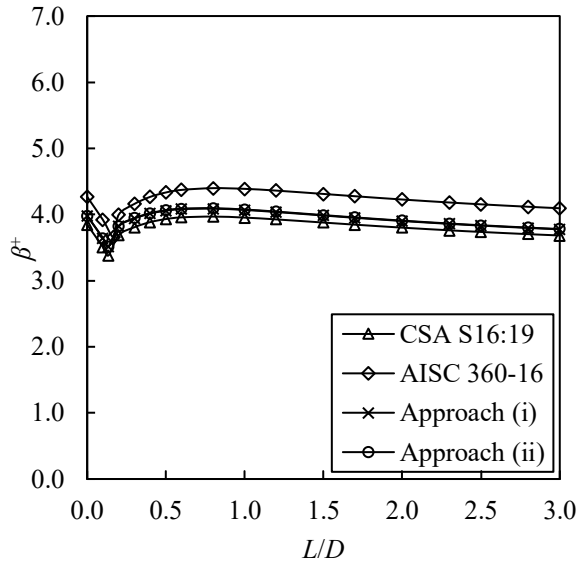

(c) $KL/r = 200$

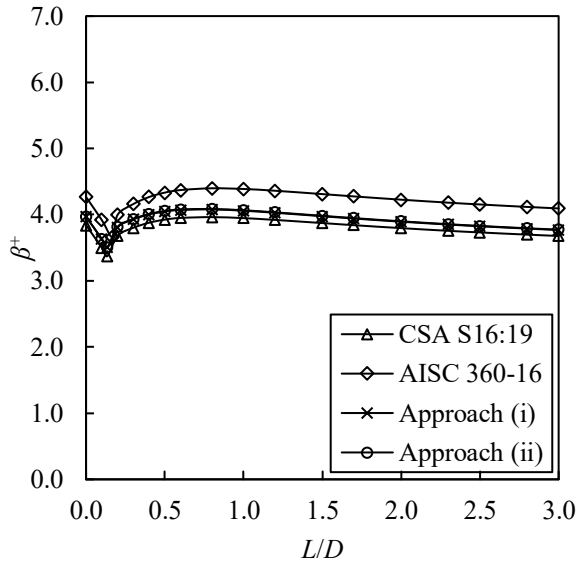

(d) $KL/r = 300$

Figure 4-1. Effect of variation in KL/r on reliability index when $f_c' = 70$ (MPa) and $e = 0$ (mm) for concrete-filled RHS beam-columns

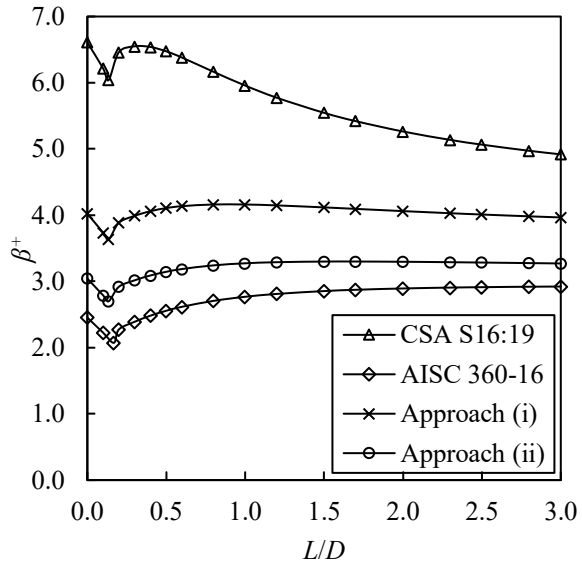

(a) $KL/r = 20$

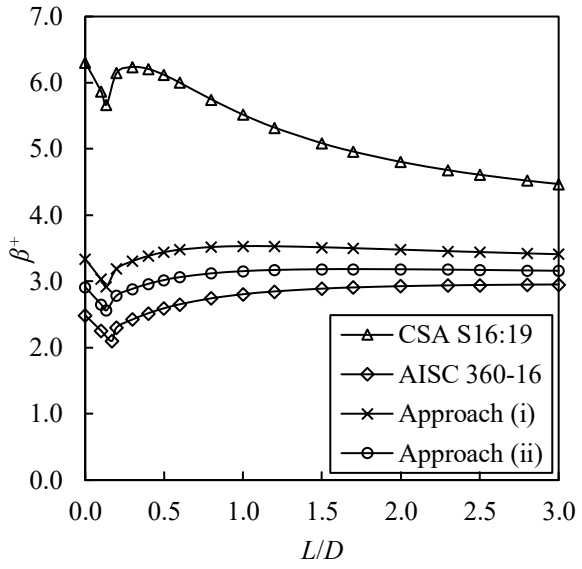

(b) $KL/r = 100$

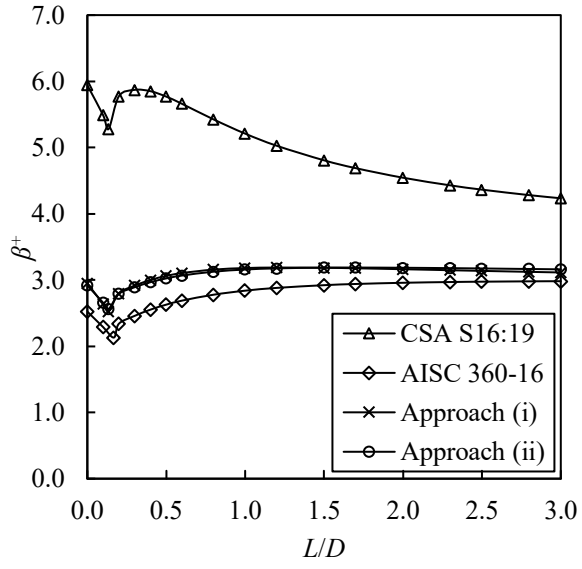

(c) $KL/r = 200$

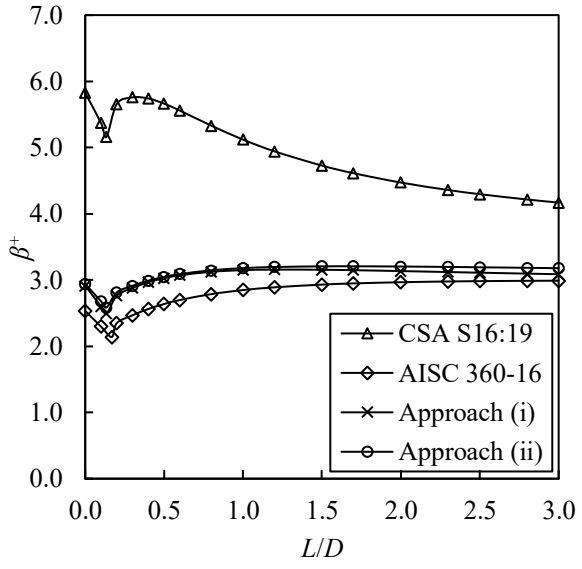

(d) $KL/r = 300$

Figure 4-2. Effect of variation in KL/r on reliability index when $f_c' = 70$ (MPa) and $e = 200$ (mm) for concrete-filled RHS beam-columns

By looking at Figure 4-3 (a-d) it can be seen that, when $e = 0$ mm, the resulting ranges of β^+ for CHS beam-columns are similar to those for RHS beam-columns (and as β^+ decreases as KL/r goes up); however, Tousignant and Packer's (2022a,b) Approaches (i) and (ii) in this case yield β^+ values that are closer to those of CSA S16:19.

Figure 4-4 (a-d) show the results of CHS beam- columns for when e = 200 mm and f_c' = 70 MPa. When e > 0 mm, the resulting ranges of β^+ for CHS beam-columns are, again, similar to those for RHS beam-columns (i.e., β^+ decreases as KL/r goes up, except for AISC in which β^+ increases as KL/r goes up). Over the practical range of $1 \leq L/D \leq 3$ for steel members (Schmidt & Bartlett, 2002), all β^+ values, for all of the approaches, exceed 3.0.

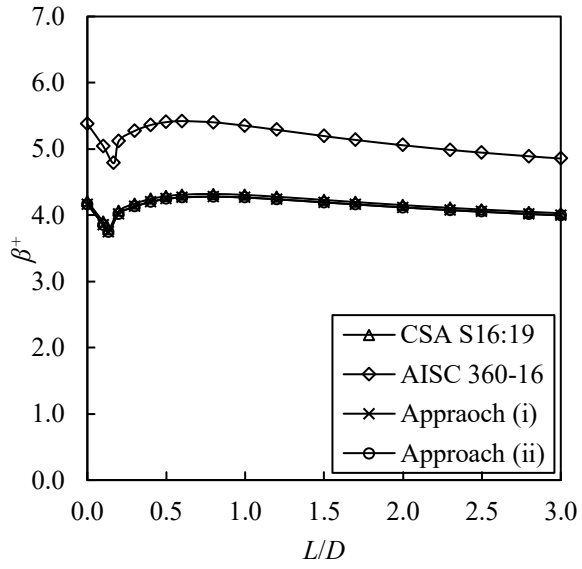

(a) KL/r = 20

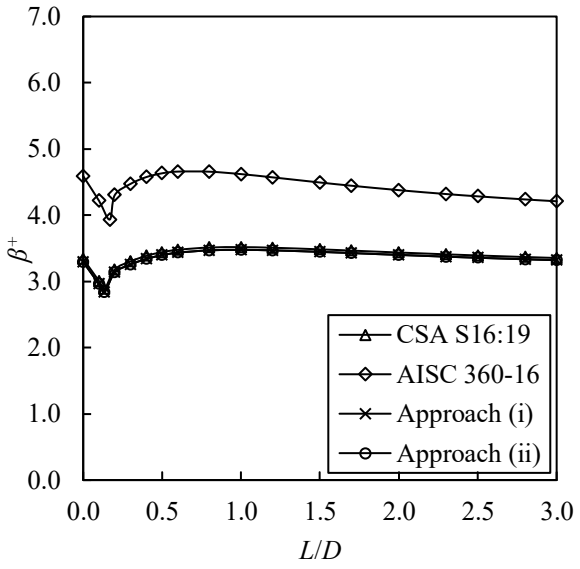

(b) KL/r = 100

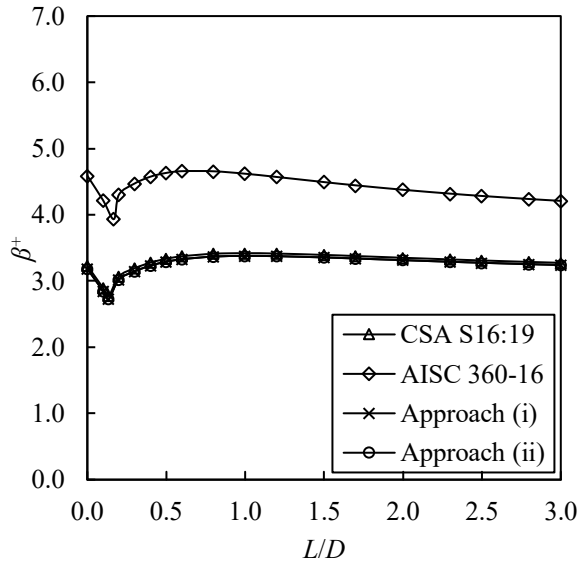

(c) KL/r = 200

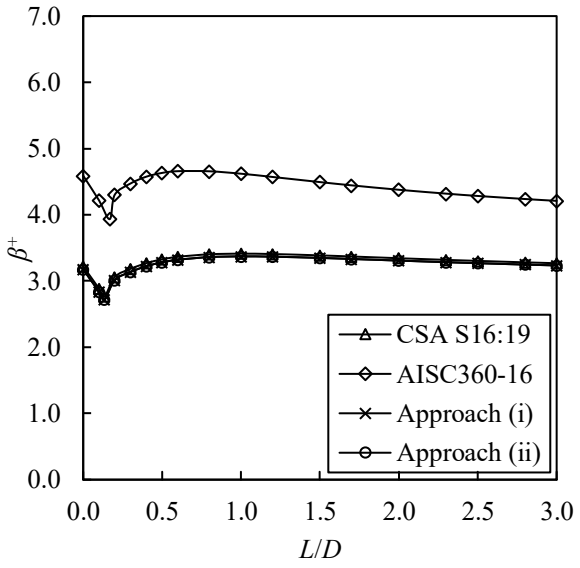

(d) KL/r = 300

Figure 4-3. Effect of variation in KL/r on reliability index when f_c' = 70 (MPa) and e = 0 (mm) for concrete-filled CHS beam-columns

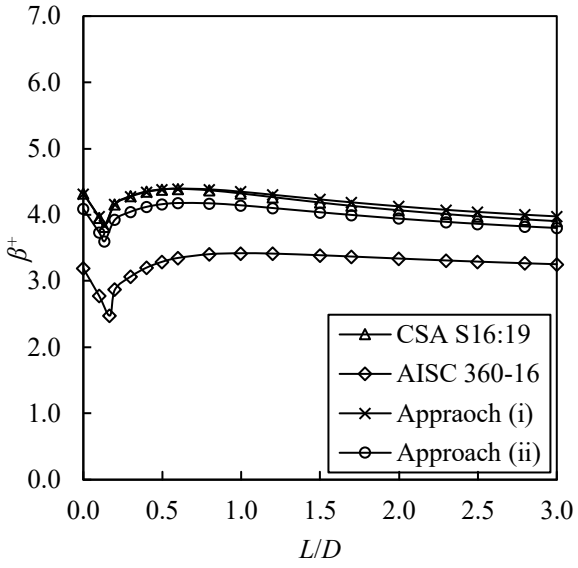

(a) $KL/r = 20$

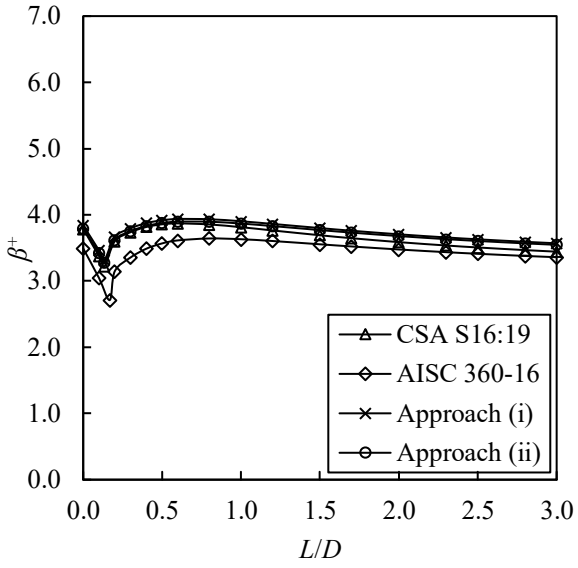

(b) $KL/r = 100$

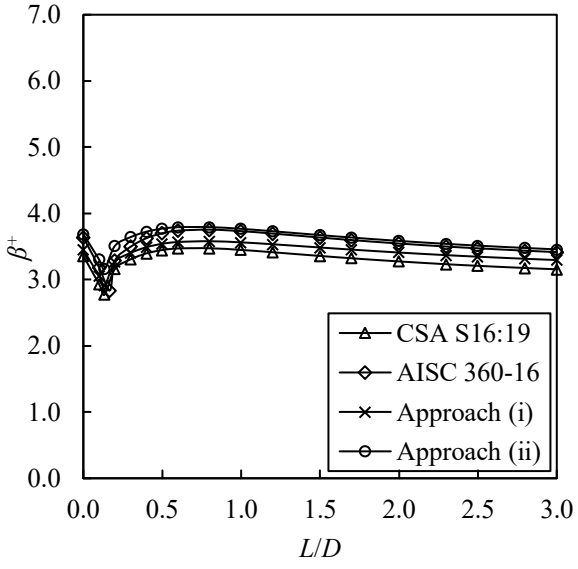

(c) $KL/r = 200$

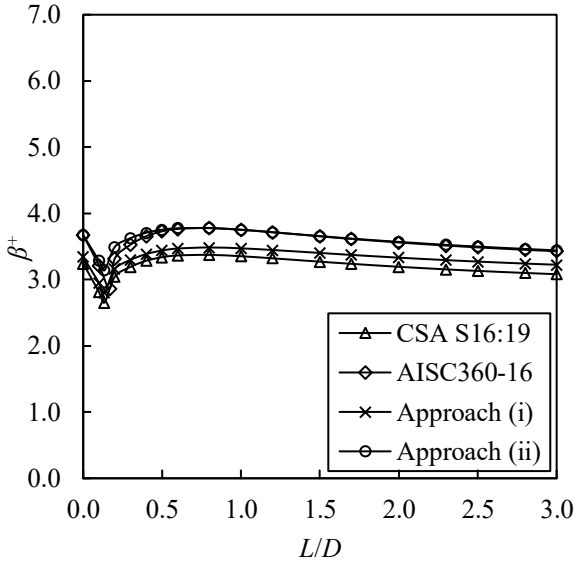

(d) $KL/r = 300$

Figure 4-4. Effect of variation in KL/r on reliability index when $f_c' = 70$ (MPa) and $e = 200$ (mm) for concrete-filled CHS beam-columns

Figure 4-1 to Figure 4-4 (c and d) also demonstrate that β^+ is not particularly sensitive to variations in KL/r when $KL/r \geq 200$ (which is the limit for unfilled HSS compression members). This is most likely because KL/r is determined by using r of the steel section, alone, without considering the concrete infill. It may be possible to relax this requirement for concrete-filled HSS covered by CSA S16; however, it should be noted that the database of tests used in this study did not include members with $KL/r > 173$.

4.3. EFFECT OF ECCENTRICITY ON RELIABILITY INDEX

Figure 4-5 (a-d) and Figure 4-6 (a-d) demonstrate the effect of eccentricity on reliability index for RHS members with KL/r = 100 and f_c' = 50 and 70 MPa, respectively. It is important to note that when e = 0 mm, the professional factor statistics for concentrically loaded members were used. Again, the values of β^+ for CSA S16:19 are higher than those of the other methods because, while δ_P is similar, V_P is much lower. Furthermore, it can be seen that as e increases, the resulting ranges of β^+ increase. For some low L/D ratios, CSA S16:19, Approach (i), and Approach (ii), produce β^+ values that fall below the target reliability of 3.0. However, in these cases, β^+ still exceeds 2.6, on average, and over the practical range of $1 \leq L/D \leq 3$ for steel members (Schmidt & Bartlett, 2002), β^+ always exceeds 3.0.

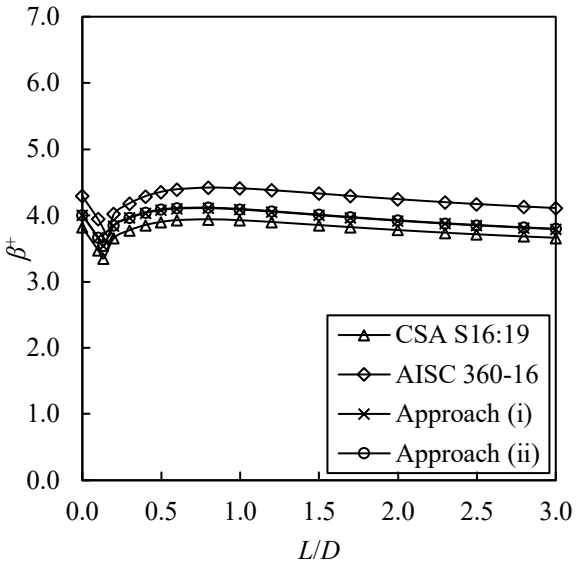

(a) e = 0 (mm)

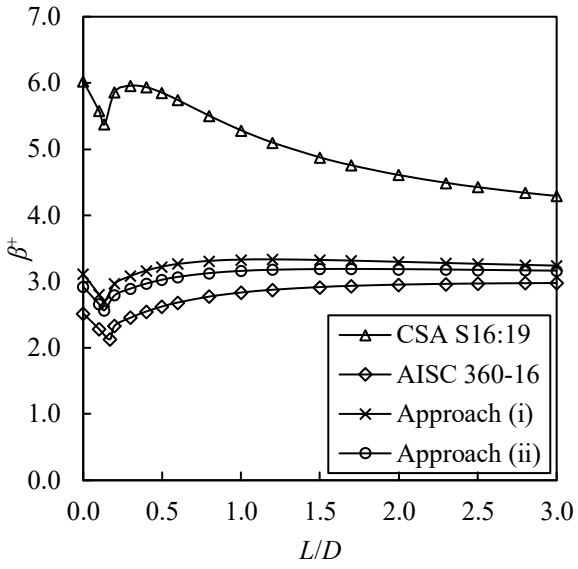

(b) e = 100 (mm)

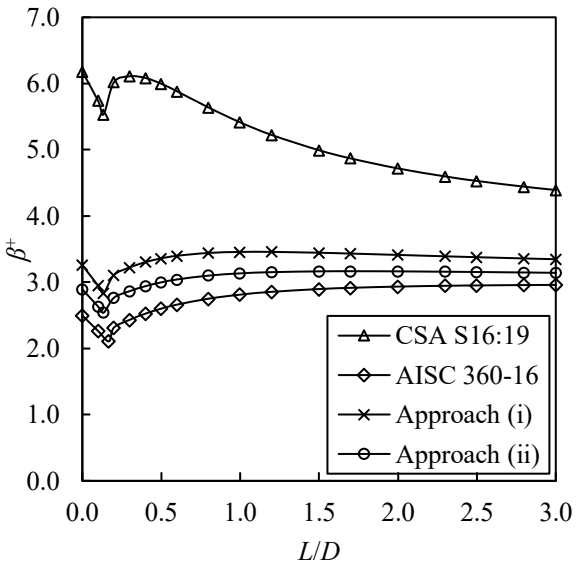

(c) e = 200 (mm)

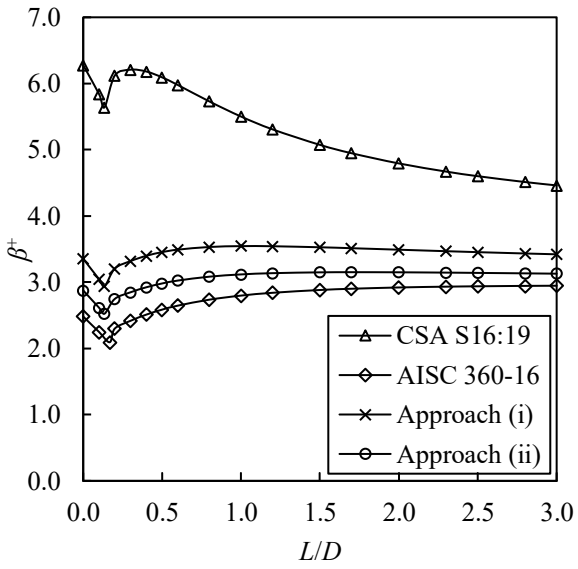

(d) e = 300 (mm)

Figure 4-5. Effect of variation in e on reliability index when f_c' = 50 (MPa) and KL/r = 100 for concrete-filled RHS beam-columns

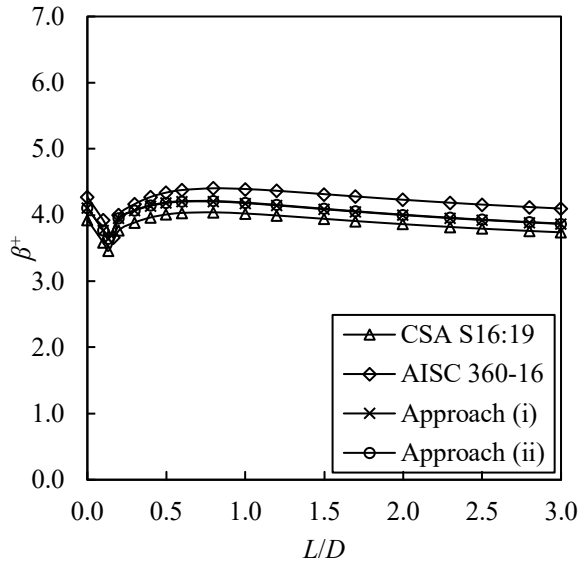

(a) e = 0 (mm)

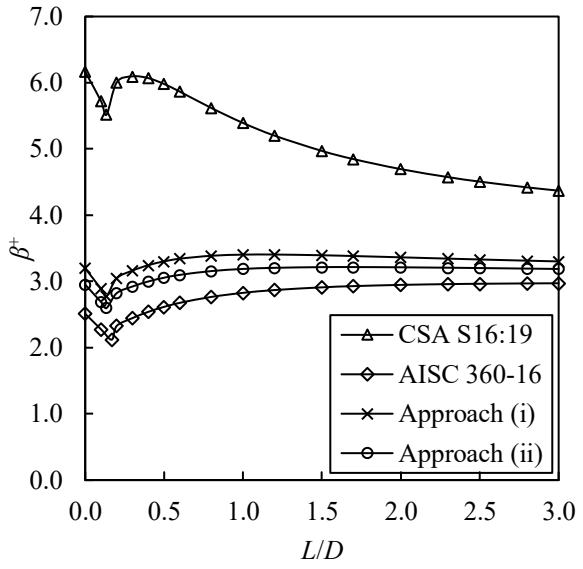

(b) e = 100 (mm)

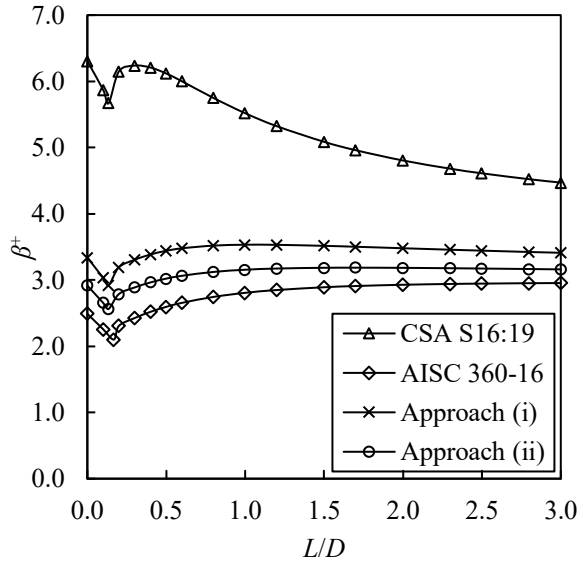

(c) e = 200 (mm)

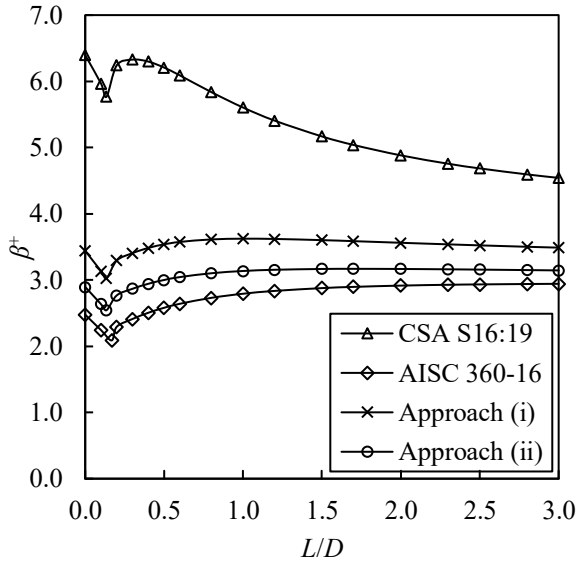

(d) e = 300 (mm)

Figure 4-6. Effect of variation in e on reliability index when f_c' = 70 (MPa) and KL/r = 100 for concrete-filled RHS beam-columns

Figure 4-7 (a-d) and Figure 4-8 (a-d) demonstrate the effect of eccentricity on reliability index for CHS members with KL/r = 100, and f_c' = 50 and 70 MPa, respectively. The resulting ranges of β^+ are similar to those for RHS beam-columns over the same parameter range, and β^+ always remains above 2.6 (and above 3.0 for 1 $\leq L/D \leq$ 3).

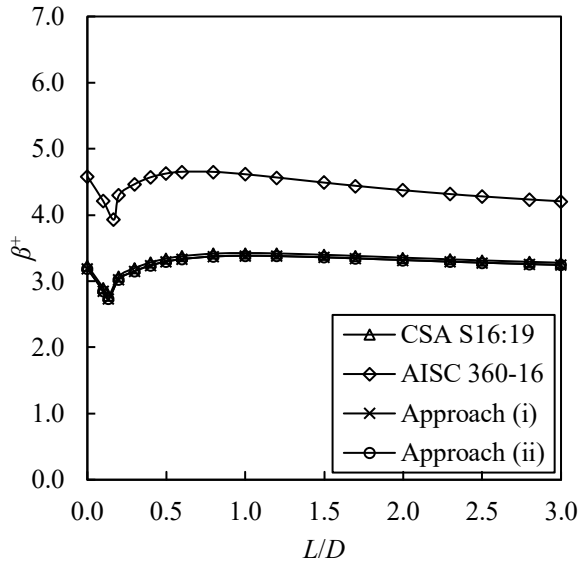

(a) e = 0 (mm)

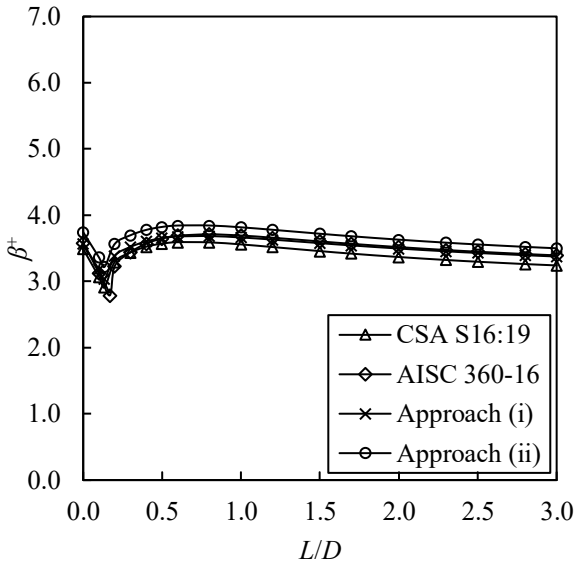

(b) e = 100 (mm)

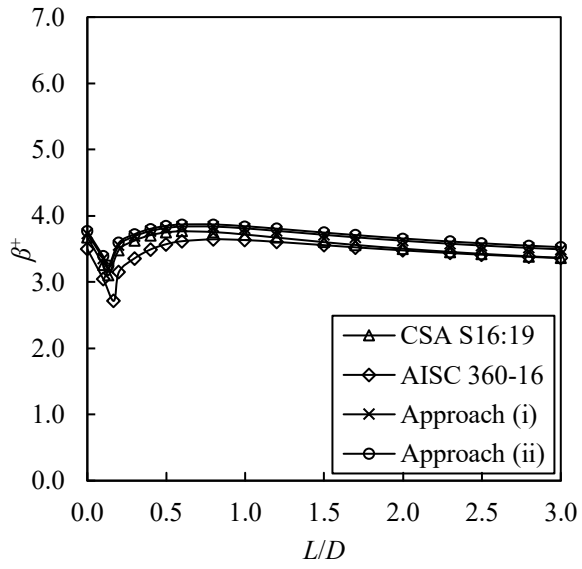

(c) e = 200 (mm)

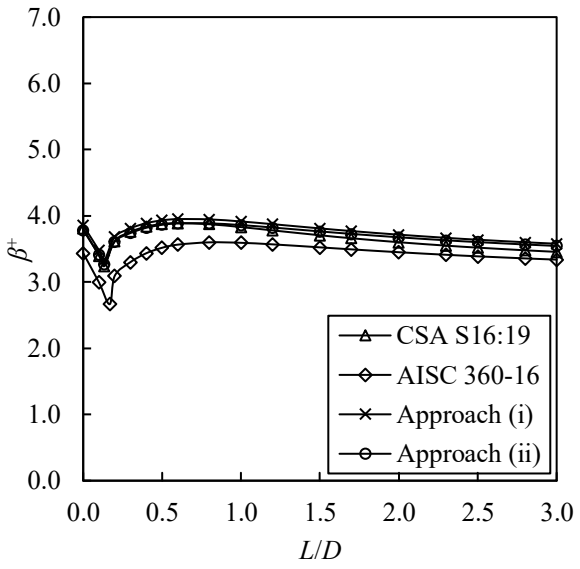

(d) e = 300 (mm)

Figure 4-7. Effect of variation in e on reliability index when f_c' = 50 (MPa) and KL/r = 100 for concrete-filled CHS beam-columns

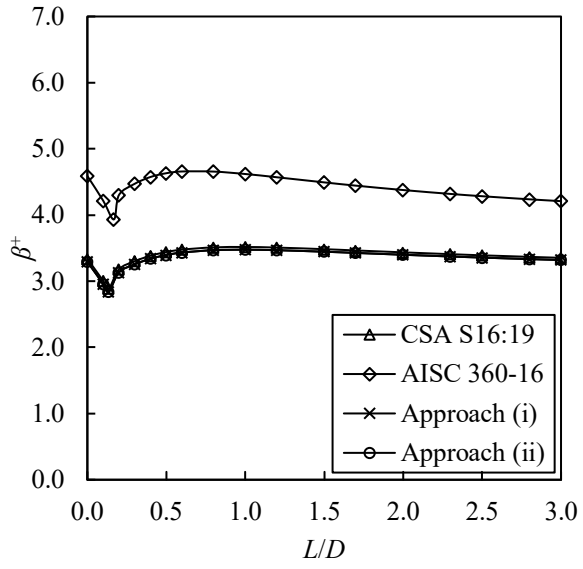

(a) e = 0 (mm)

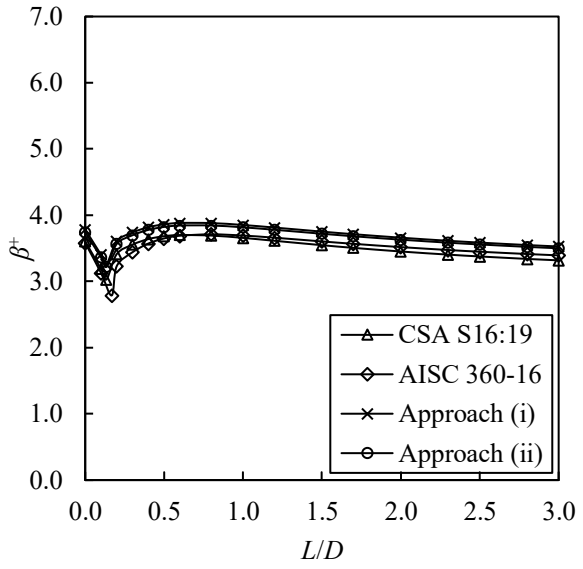

(b) e = 100 (mm)

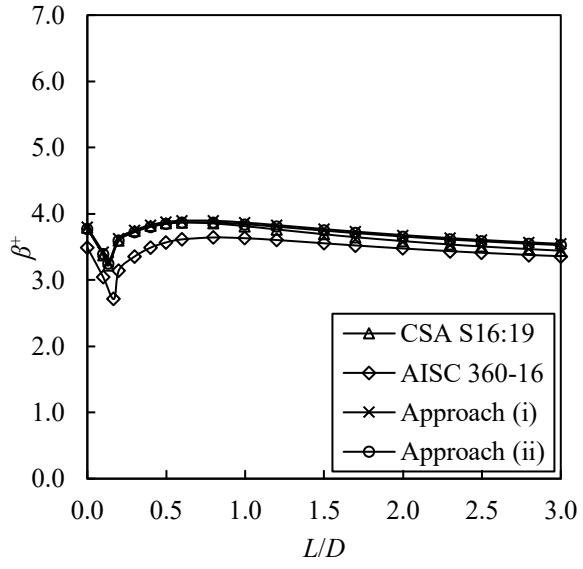

(c) e = 200 (mm)

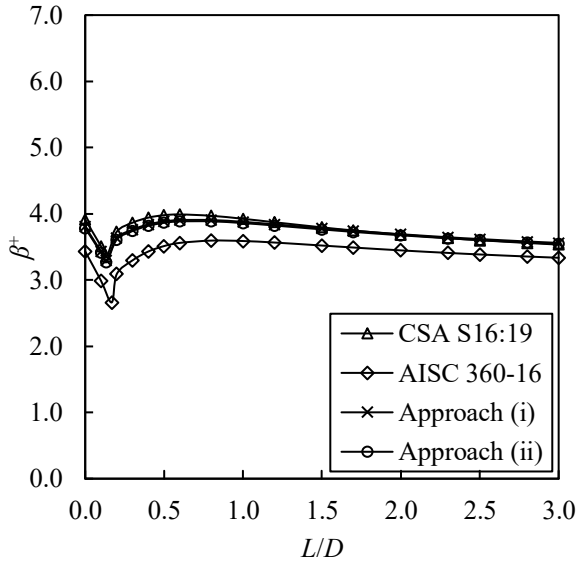

(d) e = 300 (mm)

Figure 4-8. Effect of variation in e on reliability index when f_c' = 70 (MPa) and KL/r = 100 for concrete-filled CHS beam-columns

4.4. EFFECT OF CONCRETE STRENGTH ON RELIABILITY INDEX

Figure 4-9 (a-d) and Figure 4-10 (a-d) show the effect of concrete strength on reliability indices for RHS beam-columns with KL/r = 100 and e = 0 and 200 mm, respectively. It can be seen that as f_c' increases, β^+ increases (in accord with the general trend illustrated in Figure 3-11). Figure 4-11(a-d) and Figure 4-12 (a-d)

show a similar trend for CHS beam-columns. Figure 4-9 to Figure 4-12 might appear to indicate that values of $f_c' > 70$ MPa [the maximum limit recommended by Tousignant & Packer (2022a)] still provide an acceptable level of reliability; however, it is important to note that the professional factors used in this exercise were determined only after screening the database of tests to include those with 20 MPa $\leq f_c' \leq 70$ MPa.

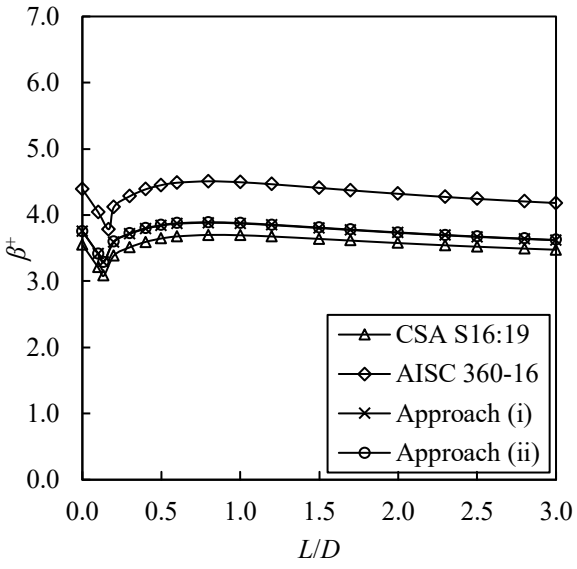

(a) $f_c' = 20$ (MPa)

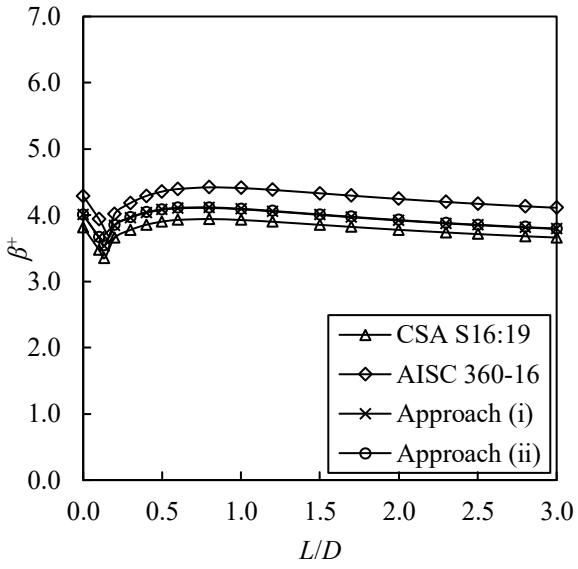

(b) $f_c' = 50$ (MPa)

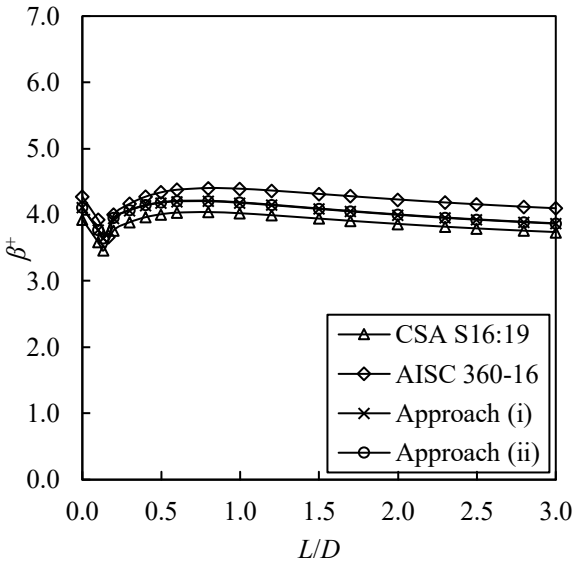

(c) $f_c' = 70$ (MPa)

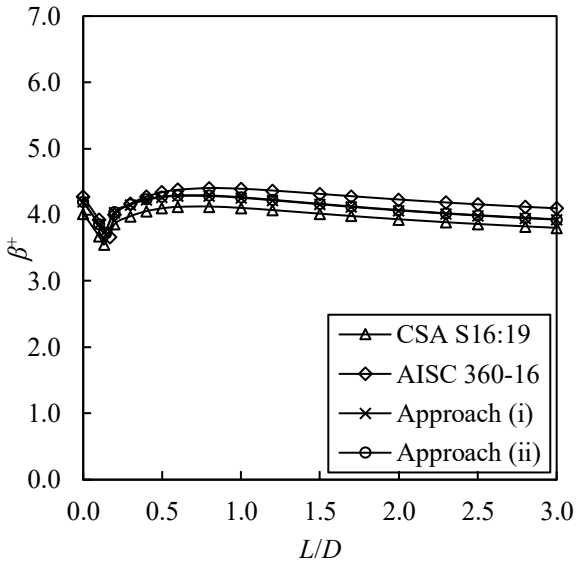

(d) $f_c' = 90$ (MPa)

Figure 4-9. Effect of variation in f_c' on reliability index when $e = 0$ (mm) and $KL/r = 100$ for concrete-filled RHS beam-columns

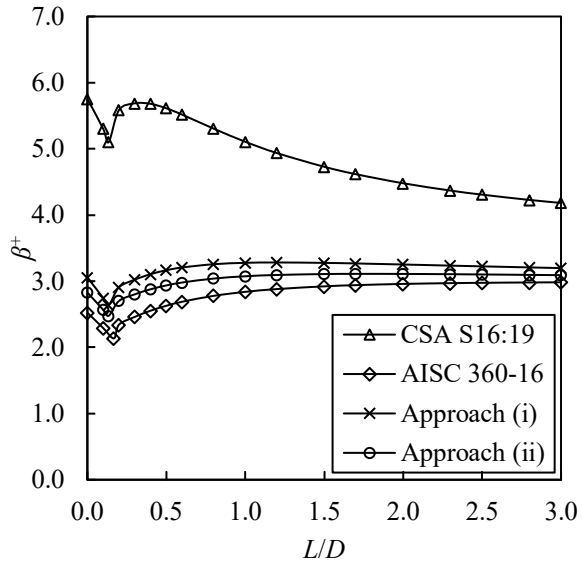

(a) f_c' = 20 (MPa)

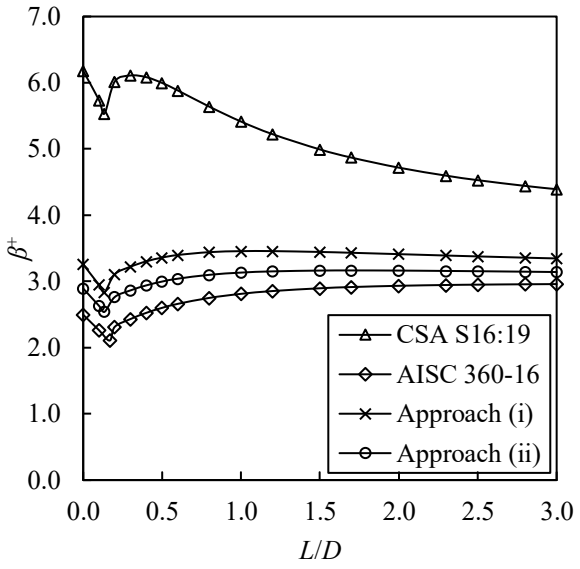

(b) f_c' = 50 (MPa)

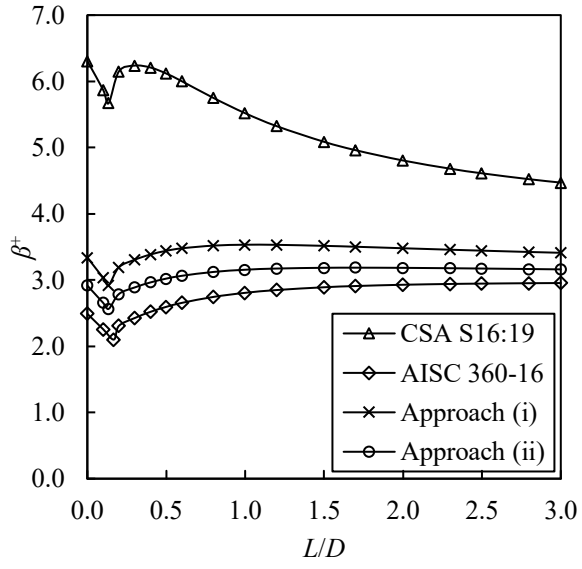

(c) f_c' = 70 (MPa)

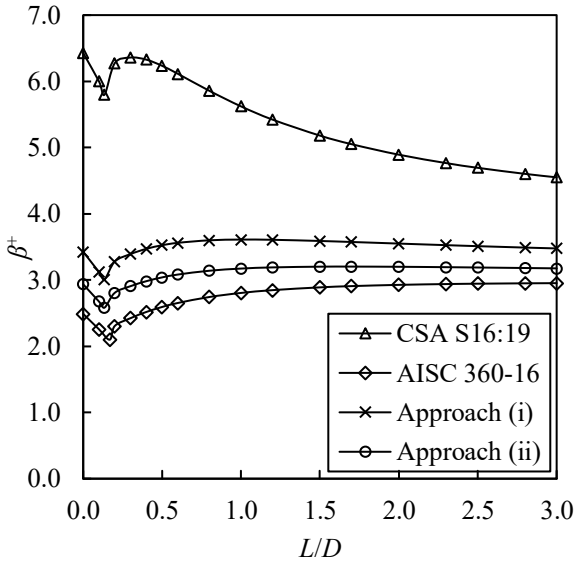

(d) f_c' = 90 (MPa)

Figure 4-10. Effect of variation in f_c' on reliability index when e = 200 (mm) and KL/r = 100 for concrete-filled RHS beam-columns

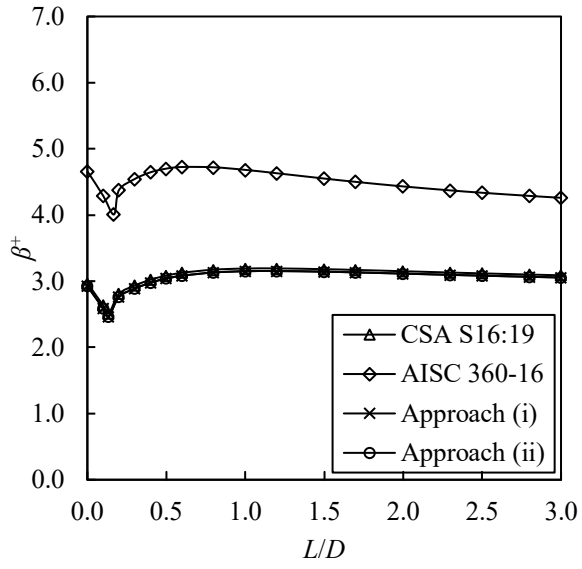

(a) f_c' = 20 (MPa)

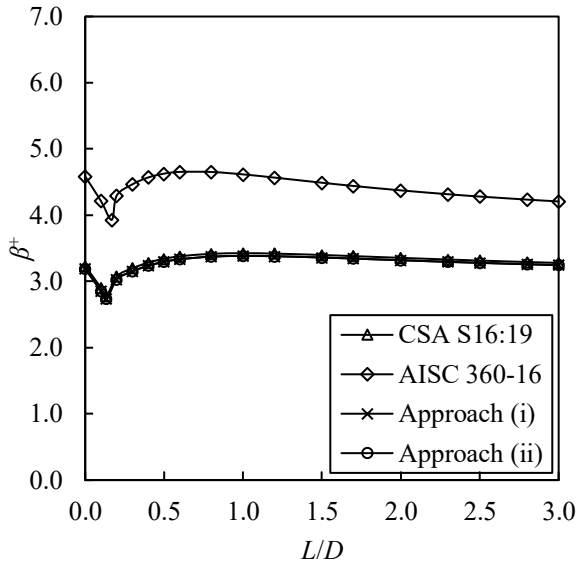

(b) f_c' = 50 (MPa)

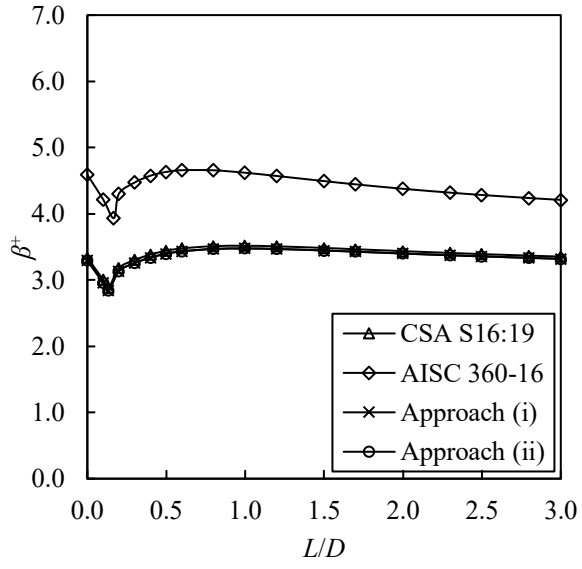

(c) f_c' = 70 (MPa)

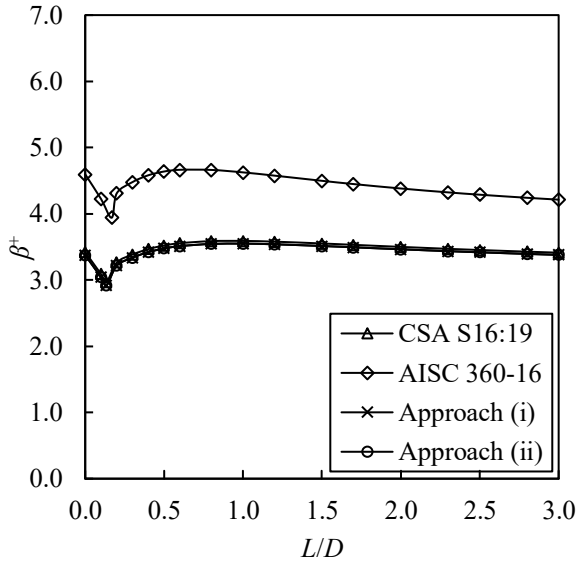

(d) f_c' = 90 (MPa)

Figure 4-11. Effect of variation in f_c' on reliability index when e = 0 (mm) and KL/r = 100 for concrete-filled CHS beam-columns

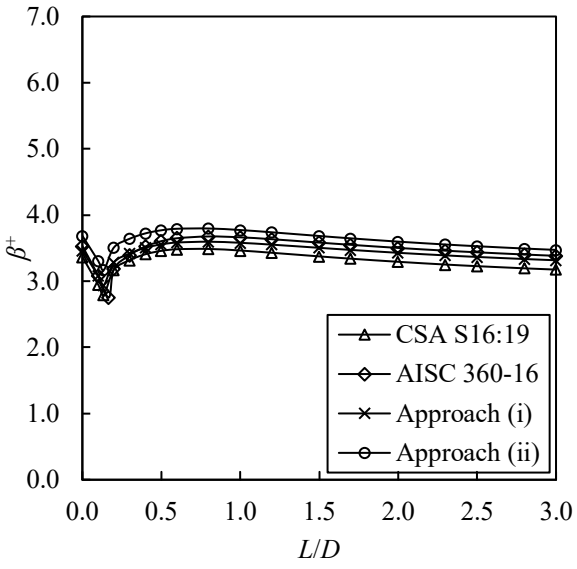

(a) f_c' = 20 (MPa)

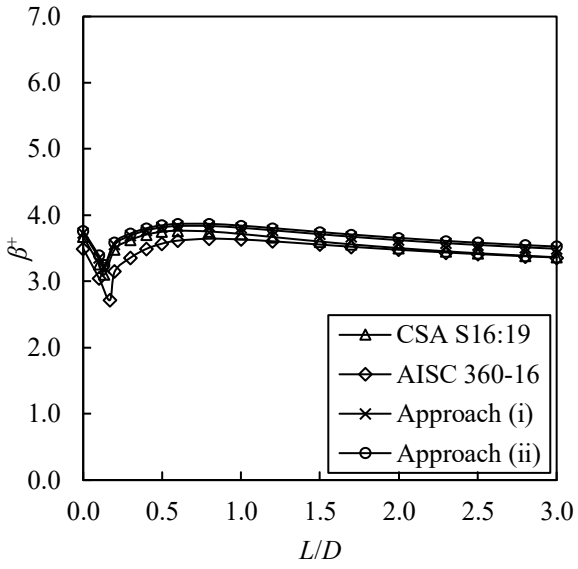

(b) f_c' = 50 (MPa)

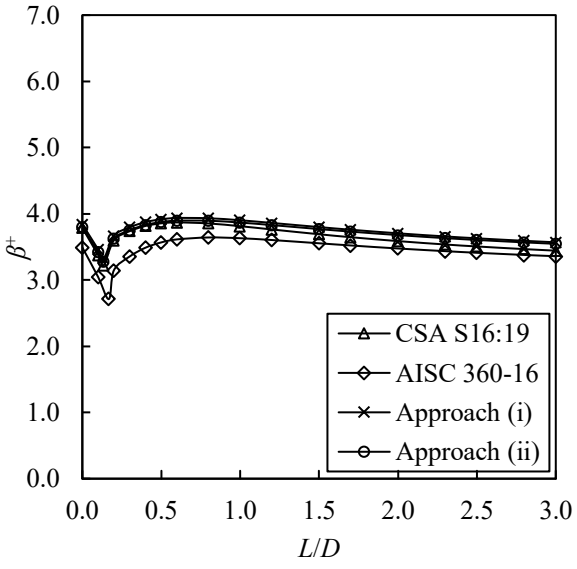

(c) f_c' = 70 (MPa)

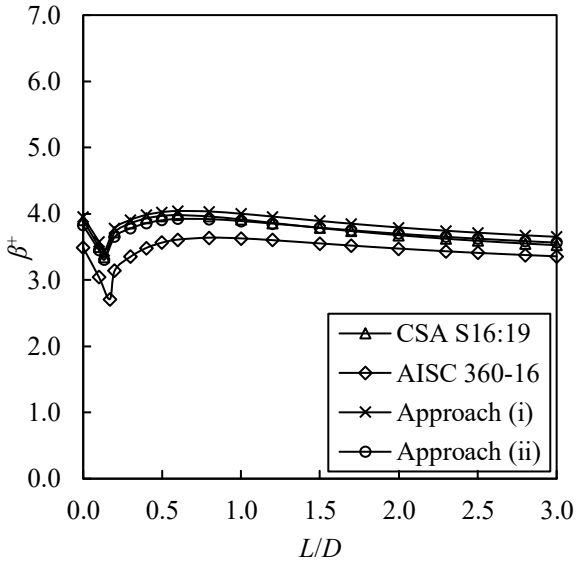

(d) f_c' = 90 (MPa)

Figure 4-12. Effect of variation in f_c' on reliability index when e = 200 (mm) and KL/r = 100 for concrete-filled CHS beam-columns

4.5. OVERALL RELIABILITY INDICES

Figure 4-13 and Figure 4-14 show the overall β^+ computed at each L/D ratio by taking the average β^+ value obtained across all members, effective lengths, eccentricities, and concrete strengths for RHS and CHS beam-columns, respectively. By looking at Figure 4-13, for RHS members, it can be demonstrated that for all of the approaches (CSA S16:19, AISC 360-16, and Approaches (i) and (ii)] β^+ remains above the target value of 3.0 within the practical range of $1 \leq L/D \leq 3$. In some cases (i.e., for low values of L/D), β^+ falls below 3.0 but remains above 2.6. Moreover, the level of safety provided by Tousignant & Packer's (2022a,b) approach(es) is always similar to that of AISC 360-16. From Figure 4-14 it can be illustrated that for CHS members, β^+ is always greater than 3.0.

Based on the above, it can be concluded that both approaches proposed by Tousignant & Packer (2022a,b) for the design of concrete filled HSS beam-columns obtain a level of safety commensurate with CSA S16 (CSA, 2019a).

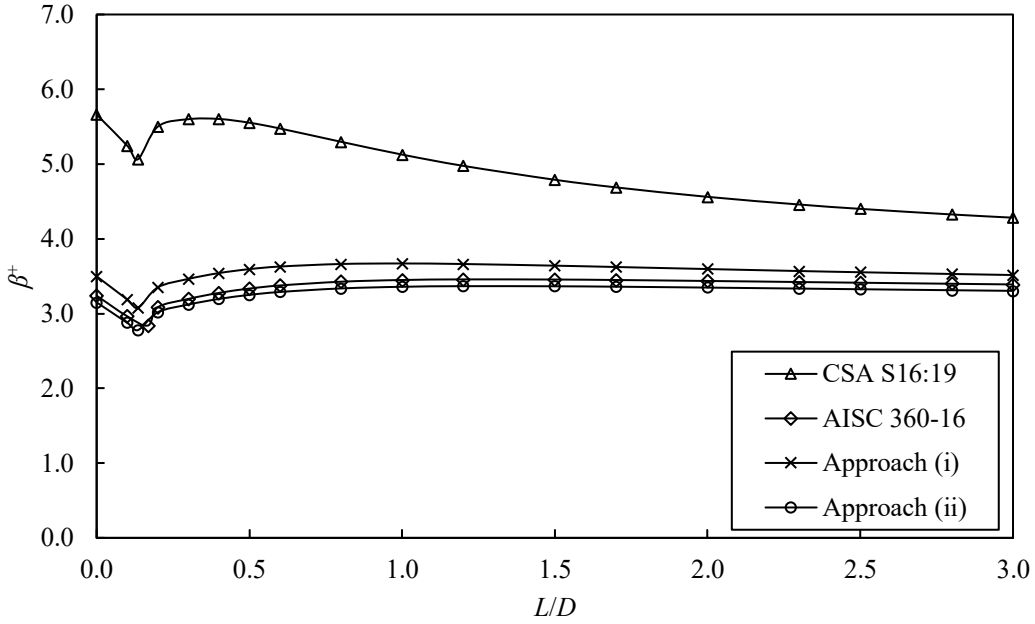

Figure 4-13. Overall reliability index vs. L/D for concrete-filled RHS beam-columns

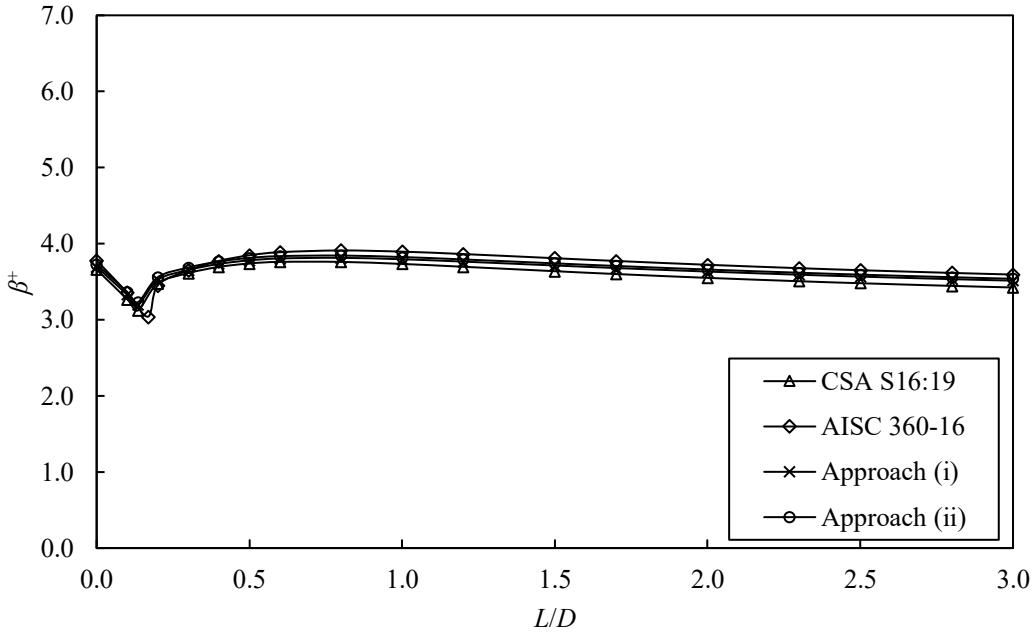

Figure 4-14. Overall reliability index vs. L/D for concrete-filled CHS beam-columns

Chapter 5: SUMMARY, CONCLUSIONS AND RECOMMENDATIONS

5.1. SUMMARY

Reliability indices were determined for 12 concrete-filled RHS and 12 concrete-filled CHS beam-column members. Simulations (using MCS) were performed for each member over a range of concrete strengths (f_c' = 20, 50, 70, and 90 MPa), slenderness values (KL/r = 20, 50, 100, 150, 200, 250, and 300), loading eccentricities (e = 0, 100, 200, 300 and 500 mm) and for 18 live-to-dead load ratios ($0 \leq L/D \leq 3$) – for design approaches in accordance with CSA S16:19, AISC 360-16 and the two approaches proposed by Tousignant & Packer (2022a,b). In total 30,240 design scenarios for RHS and 30,240 design scenarios for CHS members were covered, and 30,240 × 10^6 simulations were performed for each method.

It is important to note that all calculations assumed a yield strength of 350 MPa for steel, a concrete density of ρ_c = 2400 kg/m^3 and an outside corner radius for RHS of 2t. In addition, for the CSA existing and the two proposed approaches equations, C_{fs}/C_f was taken as 0 in calculating EI_e for all members, ω_1 was taken as 1.0, and the modulus of elasticity of steel was set to 200 GPa.

5.2. CONCLUSIONS

The following conclusions can be made from the results:

For both concrete-filled RHS and CHS beam-columns (in general):

- For CSA S16:19, Approach (i) and Approach (ii), the resulting β^+ decreases as KL/r goes up, and for AISC 360-16, β^+ increases with the increase in KL/r.
- All the approaches yield higher β^+ as e increases.
- All the approaches yield higher β^+ as f_c' increases.

With respect to the reliability indices obtained for concrete-filled RHS beam-columns:

- For CSA S16:19, the overall reliability index (β^+) across all members, eccentricities, and effective lengths, ranges from 4.28 – 5.66, on average, which is greater than target value of β^+ = 3.0.
- For AISC 360-16, the overall β^+ ranges from 2.84 – 3.46, on average. Over the practical range of $1 \leq L/D \leq 3$, the resulting β^+ remains above 3.0.

- For Tousignant & Packer's Approach (i), the overall β^+ ranges from 3.08 – 3.67, on average, which is greater than the target value of 3.0.
- For Tousignant & Packer's Approach (ii), the overall β^+ ranges from 2.78 – 3.37, on average. As with AISC, over the practical range of $1 \leq L/D \leq 3$, it remains above 3.0.

With respect to the reliability indices obtained for concrete-filled CHS beam-columns:

- For CSA S16:19, the overall reliability index (β^+) across all members, eccentricities, and effective lengths, ranges from 3.12 – 3.76, on average, which is greater than target value of $\beta^+ = 3.0$.
- For AISC 360-16, the overall β^+ ranges from 3.04 – 3.91, on average.
- For Tousignant & Packer's Approach (i), the overall β^+ ranges from 3.20 – 3.81, on average, which is always greater than the target value of 3.0.
- For Tousignant & Packer's Approach (ii), the overall β^+ ranges from 3.23 – 3.84, on average, which is again always greater than 3.0.

Based on the above, it can be concluded that the two approaches proposed by Tousignant & Packer (2022a,b) for the design of concrete filled HSS beam-columns obtain a level of safety that would be acceptable in CSA S16 (CSA, 2019a).

5.3. RECOMMENDATIONS FOR FUTURE RESEARCH

Although the scope of this work is expansive, and has covered the probabilistic design of concrete-filled beam-columns, additional research in the following areas is recommended:

- Reliability analyses should be performed for a wider variety of KL/r and f'_c values, with corresponding tests included from the database. As discussed in Chapter 4, KL/r values higher than 200 and f'_c values grater than 70 MPa do not appear to result in unacceptable reliability indices. A further sensitivity study on their effects is recommended.
- While this thesis investigated the behaviour of concrete-filled HSS subjected to axial compression plus bending, it has made apparent that the tension plus bending load combination for concrete-filled HSS members requires attention.

REFERENCES

ACI. (2014). *Building code requirements for structural concrete and commentary. ACI 318-14.* Farmington Hills, MI, USA.

AISC. (2016). *Specification for structural steel buildings.* Chicago, IL, USA: AISC 360-16, American Institute of Steel Construction.

AISC. (2017). *Steel construction manual* (15th ed ed.). Chicago, IL, USA: American Institute of Steel Construction.

ASCE. (2016). *ASCE/SEI 7-16, Minimum Design Loads and Associated Criteria for Buildings and Other Structures.* Reston, Va: American Society of Civil Engineers.

ASTM. (2015). *Standard specification for coled-formed welded carbon steel hollow structural sections (HSS). ASTM A1085/A1085M-15.* West Conshohocken, PA, USA: American Society for Testing and Materials International.

Bartlett, F. (2007). Canadian Standards Asscociation Standard A23.3-04 resistance factor for concrete in compression. *Canadian Journal of Civil Engineering, 34*, 1029-1037.

Bartlett, F., & MacGregor, J. (1996). Statistical analysis of the compressive strength of concerete in compression. *ACI Materials Journal, 93*(2), 158-168.

BSC. (1984). *Construction with hollow steel sections* (1st ed.). Corby, UK: British Steel Corporation Tubes Division.

CEN. (2004a). *Design of composite steel and concrete structures - Part 1-1: General rules and rules for buildings.* Brussels, Belgium: European Committee for Standardization.

CIDECT. (1979). *Calcul des poteaux en profils creux remplis de béton. Fascicule 1: Méthode de calcul et technologie de mise en oeuvre; Fascicule 2: Abaques de calcul.* Geneva, Switzerland: CIDECT Monograph No. 5. Comité International pour le Développement et l'Étude de la Construction Tubulaire.

CISC. (2021). *Handbook of steel construction* (12th ed.). Toronto, ON, Canada: Canadian Institute of Steel Construction.

CSA. (1969). *Steel structures for Buildings.* Toronto, Canada: Canadian Standars Association.

CSA. (2001). *Limit state design of steel structures.* Toronto, ON, Canada: CAN/CSA S16-01, Canadian Standards Associations.

CSA. (2009). *Design of steel structures.* Toronto, ON, Canada: CSA S16-09, Canadian Standards Association.

CSA. (2011). *CSA S408-11: Guidelines for the development of limit states design standards.* Mississauga, ON, Canada: Canadian Standards Assocaition.

CSA. (2018). *General requirements for rolled or welded structural quality steel / Structural quality steel. CSA G40.20-13/G40.21-13 (R2018).* Toronto, ON, Canada: Canadian Standards Association.

CSA. (2018). *General requirements for rolled or welded structural quility steel / Structural quality steel. CSA G40.20- 13/G40.21- 13 (R2018).* Toronto, ON, Canada: Canadian Standards Association.

CSA. (2019a). *Design of Steel Structures.* Toronto, ON, Canada: CSA S16:19, Canadian Standards Association.

CSA. (2019b). *Design of concrete structures.* Toronto, ON, Canada: CSA A23.3:19, Canadian Standards Association.

Eamon, C., Thompson, M., & Liu, Z. (2005). Evaluation of accuracy and effciency of some simulation and sampling methods in structural reliability analysis. *Structural Safety*(27), 356-392.

Elchalakani, M., Zhao, X., & Grzebieta, R. (2001). Concrete-filled circular steel tubes subjected to pure bending. *Journal of Constructional Steel Research, 57*, 1141-1168.

Ellingwood, B., Galambos, T., MacGregor, J., & Cornell, C. (1980). Development of probability based load criterion for american national standard A58. *Special Publication 577*.

EN 1994-1-1. (2004). *Eurocode 4: Design of composite steel and concrete structures - Part 1-1: General rules and rules for buildings.* Brussels, Belgium: European Committee for Standardization.

Essa, H., & Kennedy, D. (2000). Proposed provisions for the design of steel beam-columns in S16-2001. *Canadian Journal of Civil Engineering, 27*, 610-619.

Galambos, T., & Raviranda, M. (1981). Load and resistance factor design. *Engineering Journal, AISC, 18*(3), 78 - 84.

Kennedy , D., & Baker, K. (1984). Resistance Factors for Steel Highway Bridges. *Canadian Journal of Civil Engineering, 11*, 324-334.

Kennedy, D., & Gad Aly, M. (1980). Limit state design of steel structures - performance factors. *Canadian Journal of Civil Engineering*, 7: 45-77.

Kennedy, D., Kulak, G., & Driver, R. (1994). Discussion to postbuckling behavior of steel-plate shear walls, by Elgaaly, M., Caccese, V., and Du., C. *Journal of Structural Engineering, ASCE, 120*(7), 2250 - 2251.

Lind, N. (1971). Consistent partial safety factors. *Journal of The Structural Division, ASCE, 97*(6), 1651 - 1670.

Liu, J. (2016). Updates to expected yield stress and tensile strength ratios for determination of expected member capacity in the 2016 AISC seismic provisions. *Engineering journal, 53*(4), 215-228.

Lu, Y., & Kennedy, D. (1994). The flexural behaviour of concrete-filled hollow structural sections. *Canadian Journal of Civil Engineering, 21*, 111-130.

Lundberg, J., & Galambos, T. (1996). Load and Resistance Factor Design of Composite Columns. *Structural Safety, 18*, 169-177.

MacPhedran, I., & Grondin, G. (2011). A simple steel beam desgin curve. *Canadian Journal of Civil Engineering, 38*(2), 141-153.

Melchers, R., & Beck, A. (2018). *Structural Reliability Analysis and Prediction* (3rd ed.). Hoboken, NJ: Wiley.

National Research Council of Canada (NRC). (2020). *NBCC 2020 Part 4.* Ottawa, ON, Canada: National building code of Canada.

Nowak, A., & Lind, N. (1979). Practical Bridge Code Calibration. *Journal of the Structural Division, ASCE, 105*(12), 2497 - 2510.

Pillai, U. (1974). Beam-columns of hollow structural sections. *Canadian Journal of Civil Engineering, 1*(2), 194-198.

Ravindra, M., & Galambos, T. (1978). Load and resistance factor design for steel. *Journal of the Structural Devisions, 104*(9), 1337-1353.

Schmidt, B., & Bartlett, F. (2002). Review of resistance factor for steel. *Canadian Journal of Civil Engineering, 29*, 109-118.

Schueller, G., Pradlwarter, H., & Koutsourelakis, P. (2004). A critical appraisal of reliability estimation procedures for high dimensions. *Probabilistic Engineering Mechanics*(19), 463-474.

Standard specification for coled-formed welded and seamless carbon steel structural tubing in rounds and shapes. ASTM A500/A500M-21a. (2021). West Conshohocken, PA, USA: American Society for Testing and Materials.

Thai, S., Thai, H., Uy, B., & Ngo, T. (2019). Concrete-filled steel tubular columns: Test database, design, and calibrations. *Journal of Constructional Steel Research, 157*, 161-181.

Tousignant, K., & Packer, J. (2022a). Concrete-filled hollow structural section. I: Materials, cross-section classification, and eccentrically loaded columns. *Canadian Journal of Civil Engineering, 49*(3), 368 - 383.

Tousignant, K., & Packer, J. (2022b). Concrete-filled hollow structural sections. II: Flexural members, beam columns, tension, and shear. *Canadian Journal of Civil Engineering, 49*(3), 384 - 400.

Tousignant, K., & Packer, J. (2022c). CSA S16:24 - Changes to concrete-filled HSS. *Proceedings, 49th Annual Conference* (pp. STR076-1 - STR076-11). Canadian Society for Civil Engineering.

Wardenier , J., Packer, J., Zhao, X., & van der Vegte, G. (2010). *Hollow sections in structural applications* (2nd ed.). Geneva, Switzerland: Comité International pour le Développement et l'Étude de la Construction Tubulaire, ISBN 978-90-72830-9.

Xi, Q., & Packer, J. (2021). Assesing the probabilistic assumptions behind structural reliability via simulations. *49th Annual Conference, Canadian Society for Civil Engineering*, (pp. STR230-1 - STR230-10).

Zhao, X., Packer, J., Wang, Y., & McCormick, J. (2019). *Design guide for concrete-filled hollow section columns under static, impact, blast, seismic and fire loading.* CIDECT Final Report 16H-4/19. Geneva, Switzerland: Comité International pour le Développement et l'Étude de la Construction Tubulaire.

Appendix A: DERIVATION OF THE CSA S16:19 M_{RC} EQUATION

In this appendix, derivation of the M_{rc} equation of CSA S16:19 for concrete-filled RHS beam-columns is explained.

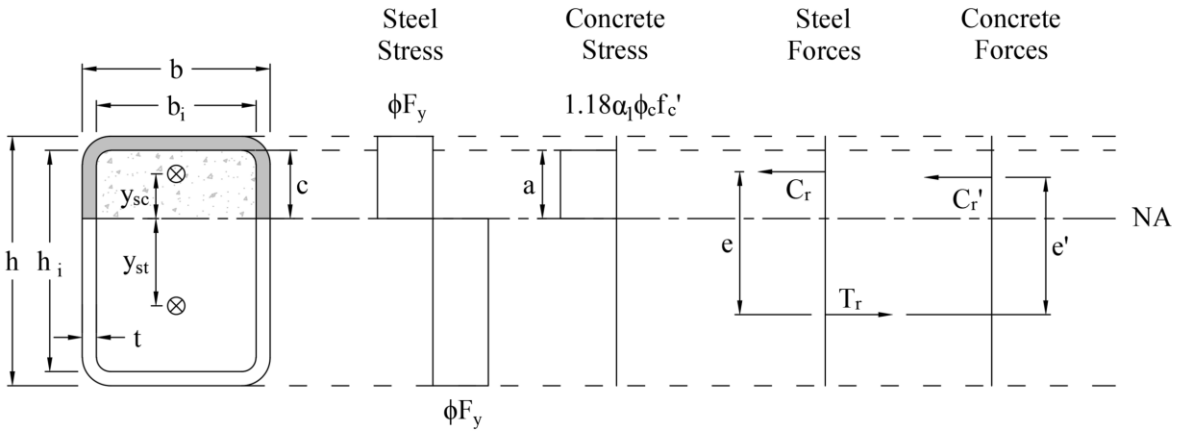

Figure A-1. Stress and force diagrams for calculating M_{rc} for concrete-filled RHS members

Assuming at failure the stress in concrete is $1.18\alpha_1 f_c'$ and setting c = a;

Compressive resistance of steel above the neutral axis (NA) is:

$$C_r = \phi A_{sc} F_y$$

where A_{sc} = area of steel in compression assuming rounded corners calculated as:

$$A_{sc} = 2\left[(a-t)t\right] + \left[(b_i - 2t)t\right] + \left[\frac{2\pi(\frac{3}{2}t)}{2}\right]t$$

hence:

$$C_r = 2\left[(a-t)t\right]\phi F_y + \left[(b_i - 2t)t\right]\phi F_y + \left[\frac{2\pi(\frac{3}{2}t)}{2}\right]t\phi F_y = 2at\phi F_y + (b_i - 4t + \frac{3\pi}{2}t)t\phi F_y$$

Tensile resistance of steel below the NA:

$$T_r = \phi A_{st} F_y$$

where A_{st} = area of steel in tension calculated as:

$$A_{st} = A_s - A_{sc}$$

hence:

$$T_r = 2\left[(h_i - t - a)t\right]\phi F_y + \left[(b_i - 2t) + \frac{3\pi}{2}t - 2t\right]t\phi F_y = 2h_i t\phi F_y - 2t^2\phi F_y - 2at\phi F_y$$

Compressive resistance of concrete above the NA assuming box section:

$$C_r' = A_{cc}(1.18\alpha_1\phi_c f_c')$$

where A_{cc} = area of concrete in compression; hence:

$$C_r' = ab_i(1.18\alpha_1\phi_c f_c')$$

Based on Figure A-1, equilibrium of forces can be written as:

$$C_r + C_r' = T_r$$

Substituting C_r, C_r' and T_r in the equilibrium:

$$2at\phi F_y + (b_i - 4t + \frac{3\pi}{2}t)t\phi F_y + ab_i(1.18\alpha_1\phi_c f_c') = 2h_i t\phi F_y - 2t^2\phi F_y - 2at\phi F_y$$

Solving for a:

$$a = \frac{2h_i t\phi F_y - 4t^2\phi F_y}{4t\phi F_y + 1.18\alpha_1 b_i\phi_c f_c'}$$

The factored bending resistance (M_{rc}) can be determined by summing the resaultant forces in the steel and concrete multiplied by their respective lever arms to the NA:

$$M_{rc} = C_r e + C_r' e$$

where e and e' are shown in Figure A-1 and calculated as:

$$e = y_{sc} + y_{st} \text{ and } e' = \frac{a}{2} + y_{st}$$

The distance between the centroid of the compressive steel and the NA (y_{sc}) is as follows:

$$y_{sc} = \frac{\left[2(a-t)t\right](\frac{a-t}{2}) + \left[(b_i - 2t)t\right](\frac{a+t}{2}) + \frac{3\pi}{2}t^2(\frac{28}{3\pi}t + a - t)}{2(a-t)t + (b_i - 2t)t + \frac{3\pi}{2}t^2}$$

$$= \frac{t(a-t)^2 + \frac{(b_i - 2t)(at + t^2)}{2} + (a-t)\frac{3\pi}{2}t^2 + 14t^3}{(2a + b_i)t - 4t^2 + \frac{3\pi}{2}t^2}$$

$$= \frac{t\left[(a-t)^2 + \frac{(b_i - 2t)(a+t)}{2} + (a-t)\frac{3\pi}{2}t + 14t^2\right]}{t\left[2a + b_i - 4t + \frac{3\pi}{2}t\right]}$$

$$= \frac{t\left[(a-t)^2 + \frac{(b_i-2t)(a+t)}{2} + (a-t)\frac{3\pi}{2}t + 14t^2\right]}{t\left[2a + b_i - 4t + \frac{3\pi}{2}t\right]}$$

$$= \frac{a(a+b_i) + (\frac{3\pi-4}{2}a + b_i - 2)t + (13 - \frac{3\pi}{2})t^2}{(2a + b_i + \frac{3\pi}{2}) - 4t}$$

The distance between the centroid of the tensile steel and the NA (y_{st}) is:

$$y_{st} = \frac{\left[2(h_i - t - a)t\right]\frac{h_i - t - a}{2} + (b_i - 2t)t\frac{h_i - a - t/2}{2} + \frac{3\pi}{2}t^2(\frac{28}{3\pi}t + h_i - t - a)}{2(h_i - t - a)t + (b_i - 2t)t + \frac{3\pi}{2}t^2}$$

$$= \frac{({h_i}^2 - 2ah_i + a^2 + \frac{b_i h_i}{2} - \frac{b_i a}{2}) + t(3a - 3h_i - \frac{b_i}{4} + \frac{3\pi}{2}h_i - \frac{3\pi}{2}a) + 2t^2(31 - 3\pi)}{(2h_i - 2a + b_i) + t(\frac{3\pi}{2} - 4)}$$

$$= \frac{(h_i - a)^2 + \frac{b_i}{2}(h_i - a) + t\left[a(3 - \frac{3\pi}{2}) + h_i(\frac{3\pi}{2} - 3) - \frac{b_i}{4}\right] + 2t^2(31 - 3\pi)}{(2h_i - 2a + b_i) + t(\frac{3\pi}{2} - 4)}$$

These derivations can be done in an easier way by assuming box sections for both the steel and concrete and summing the moments about the neutral axis; however, the result for M_{rc} obtained in this manner is optimistic when compared to the more rigorous approach (Tousignant & Packer 2022b).

Appendix B: DERIVATION OF C_F

Beam column interaction equation in CSA S16-19 is:

$$\frac{C_f}{C_{rc}} + \frac{\beta\omega_1 M_f}{M_{rc}(1-\frac{C_f}{C_{ec}})} \leq 1$$

Load effect S is required to find $G = R - S$. In order to find the load effect, the interaction equation should be solved for C_f at the optimum design state which means:

$$\frac{C_f}{C_{rc}} + \frac{\beta\omega_1 e C_f}{M_{rc}(1-\frac{C_f}{C_{ec}})} = 1$$

Which can be simplified to:

$$\frac{C_f}{C_{rc}} + \frac{\beta\omega_1 e C_f}{M_{rc}(\frac{C_{ec}-C_f}{C_{ec}})} = 1$$

That can be further simplified to:

$$\frac{C_f}{C_{rc}} + \frac{\beta\omega_1 e C_f C_{ec}}{M_{rc}(C_{ec}-C_f)} = 1$$

Now, a common denominator should be made as follow:

$$\frac{C_f M_{rc}(C_{ec}-C_f) + C_{rc}\beta\omega_1 e C_f C_{ec}}{C_{rc}M_{rc}(C_{ec}-C_f)} = 1$$

This equation can be further simplified to:

$$(M_{rc}C_{ec})C_f - (M_{rc})C_f{}^2 + (\beta\omega_1 e C_{rc}C_{ec})C_f = (C_{rc}M_{rc}C_{ec}) - (C_{rc}M_{rc})C_f$$

Factoring C_f and C_f^2 and transferring all terms to LHS the equation becomes:

$$(M_{rc})C_f{}^2 - (M_{rc}C_{ec} + \beta\omega_1 e C_{rc}C_{ec} + C_{rc}M_{rc})C_f + (C_{rc}M_{rc}C_{ec}) = 0$$

Now Δ should be calculated for finding roots of the equation.

$$\Delta = B^2 - 4AC = (M_{rc}C_{ec} + \beta\omega_1 e C_{rc}C_{ec} + C_{rc}M_{rc})^2 - 4M_{rc}{}^2 C_{rc}C_{ec}$$

Having Δ found, roots will be as follows:

$$C_f = \frac{-B \pm \sqrt{\Delta}}{2A} = \frac{(M_{rc}C_{ec} + \beta\omega_1 eC_{rc}C_{ec} + C_{rc}M_{rc}) \pm (M_{rc}C_{ec} + \beta\omega_1 eC_{rc}C_{ec} + C_{rc}M_{rc})^2 - 4{M_{rc}}^2 C_{rc}C_{ec}}{2M_{rc}}$$

Appendix C: DATABASE OF TESTS UNDER AXIAL COMPRESSION

Appendix Table C-1. Database of tests for concrete-filled RHS members subjected to axial compression in accordance with CSA S16:19

h (mm)	b (mm)	t (mm)	KL (mm)	F_y (MPa)	f_c' (MPa)	C_a (kN)	C_n (kN)	C_a/C_n
101.30	101.30	4.97	300.0	347.30	49.40	1310.00	962.01	1.36
103.60	103.60	4.90	300.0	347.30	49.40	1340.00	986.74	1.36
102.00	102.00	4.97	300.0	347.30	49.40	1370.00	971.76	1.41
142.00	142.00	5.11	420.0	347.30	49.40	2160.00	1613.02	1.34
142.00	142.00	5.08	420.0	347.30	49.40	2250.00	1608.42	1.40
141.40	141.40	5.07	420.0	347.30	49.40	2280.00	1596.61	1.43
142.10	142.10	2.01	420.0	305.10	44.90	1328.00	1010.31	1.31
142.10	142.10	2.01	420.0	305.10	44.90	1364.00	1010.31	1.35
140.90	140.90	2.02	420.0	305.10	44.90	1280.00	997.21	1.28
103.50	103.50	5.01	300.0	347.30	58.60	1500.00	1052.22	1.43
102.10	102.10	4.97	300.0	347.30	58.60	1330.00	1026.78	1.30
101.90	101.90	5.03	300.0	347.30	58.60	1440.00	1029.87	1.40
142.30	142.30	5.09	420.0	347.30	58.60	2520.00	1725.45	1.46
142.40	142.40	5.10	420.0	347.30	58.60	2610.00	1728.85	1.51
143.20	143.20	2.03	420.0	305.10	58.60	1990.00	1210.89	1.64
142.30	142.30	2.01	420.0	305.10	58.60	1855.00	1194.70	1.55
140.50	140.50	2.00	420.0	305.10	58.60	1780.00	1166.81	1.53
149.10	149.10	5.06	420.0	347.30	58.60	1700.00	1851.10	0.92
130.30	101.60	5.03	390.0	347.30	49.40	1580.00	1173.19	1.35
130.30	102.30	5.14	390.0	347.30	49.40	1600.00	1192.26	1.34
130.30	102.30	5.14	390.0	347.30	49.40	1640.00	1192.26	1.38
167.40	136.10	5.13	480.0	347.30	49.40	2510.00	1778.16	1.41
170.80	135.30	5.07	510.0	347.30	49.40	2470.00	1788.80	1.38
125.70	102.70	5.15	390.0	347.30	58.60	1840.00	1231.34	1.49
130.00	120.40	5.03	390.0	347.30	58.60	1820.00	1406.95	1.29
132.30	102.70	4.98	390.0	347.30	58.60	1725.00	1261.70	1.37
157.10	122.50	2.01	480.0	305.10	58.60	1800.00	1144.54	1.57
161.90	119.00	2.00	480.0	305.10	58.60	1740.00	1145.45	1.52
167.90	137.10	5.10	480.0	347.30	58.60	2600.00	1913.49	1.36
172.70	133.20	5.08	480.0	347.30	58.60	2700.00	1912.28	1.41
160.20	122.70	2.03	480.0	305.10	49.40	1400.00	1051.95	1.33
160.10	119.40	2.01	480.0	305.10	49.40	1420.00	1024.71	1.39
161.50	124.30	2.00	480.0	305.10	49.40	1320.00	1066.77	1.24
120.00	120.00	2.65	360.0	340.00	21.90	778.00	652.06	1.19

h (mm)	b (mm)	t (mm)	KL (mm)	F_y (MPa)	f_c' (MPa)	C_a (kN)	C_n (kN)	C_a/C_n
120.00	120.00	3.84	360.0	330.10	26.40	1080.00	846.00	1.28
120.00	120.00	3.84	360.0	330.10	28.20	1078.00	863.42	1.25
140.00	140.00	3.84	420.0	330.10	29.30	1499.40	1090.96	1.37
140.00	140.00	3.84	420.0	330.10	29.30	1470.00	1090.96	1.35
120.00	120.00	5.86	360.0	321.10	28.20	1460.20	1096.95	1.33
120.00	120.00	5.86	360.0	321.10	28.20	1372.00	1096.95	1.25
140.00	140.00	5.86	420.0	321.10	29.30	2009.00	1369.03	1.47
140.00	140.00	5.86	420.0	321.10	29.30	1906.10	1369.03	1.39
100.00	100.00	5.00	400.0	403.40	32.40	1195.00	949.82	1.26
100.00	100.00	5.00	400.0	403.40	32.40	1068.00	949.82	1.12
100.00	100.00	5.00	400.0	403.40	32.40	1294.00	949.82	1.36
100.00	100.00	5.00	400.0	403.40	32.40	1274.00	949.82	1.34
100.00	100.00	5.00	400.0	403.40	32.40	1313.00	949.82	1.38
100.00	100.00	5.00	400.0	403.40	32.40	1294.00	949.82	1.36
100.00	100.00	5.00	400.0	403.40	32.40	1244.60	949.82	1.31
100.00	100.00	5.00	400.0	403.40	32.40	1323.00	949.82	1.39
100.00	100.00	5.00	400.0	403.40	32.40	1313.00	949.82	1.38
100.00	100.00	5.00	400.0	403.40	32.40	1274.00	949.82	1.34
100.00	100.00	5.00	400.0	403.40	32.40	1244.60	949.82	1.31
100.00	100.00	2.20	300.0	339.40	21.40	511.00	447.73	1.14
100.00	100.00	2.20	300.0	339.40	21.40	510.00	447.73	1.14
250.00	250.00	8.00	500.0	379.00	33.00	4870.00	4317.41	1.13
152.40	152.40	4.43	300.0	389.00	46.20	1906.00	1742.81	1.09
152.40	152.40	8.95	300.0	432.00	45.40	3307.00	2769.05	1.19
153.40	152.00	6.17	300.0	377.00	43.60	3317.00	1999.16	1.66
153.00	152.20	9.04	300.0	394.00	47.20	4208.00	2625.23	1.60
200.30	200.30	4.35	601.0	323.00	29.60	1613.00	1960.41	0.82
300.50	300.50	6.10	902.0	395.00	26.50	2766.00	4583.11	0.60
200.10	200.10	4.35	601.0	323.00	57.90	2563.00	2702.26	0.95
300.60	300.60	6.10	902.0	395.00	58.90	5481.00	6529.90	0.84
200.20	200.20	4.35	601.0	323.00	63.70	2825.00	2846.44	0.99
200.30	200.30	4.35	601.0	323.00	29.60	2230.00	1960.41	1.14
300.50	300.50	6.10	902.0	395.00	26.50	5102.00	4583.11	1.11
200.10	200.10	4.35	601.0	323.00	57.90	3201.00	2702.26	1.18
300.70	300.70	6.10	902.0	395.00	52.20	6494.00	6152.54	1.06
200.30	200.30	4.35	601.0	323.00	63.70	3417.00	2848.85	1.20
100.70	100.70	9.60	301.0	400.00	24.64	1550.00	1435.52	1.08
101.00	101.00	9.60	300.0	400.00	74.88	2000.00	1673.86	1.19
100.10	100.10	4.20	301.0	333.00	27.76	700.00	709.66	0.99
100.00	100.00	4.20	302.0	333.00	27.76	680.00	708.69	0.96
100.00	100.00	4.10	299.0	333.00	77.76	1130.00	988.98	1.14
100.00	100.00	4.10	300.0	333.00	77.76	970.00	988.97	0.98
100.00	100.00	4.10	301.0	333.00	46.08	880.00	811.95	1.08
99.90	99.90	4.00	301.0	333.00	46.08	830.00	800.56	1.04
101.00	101.00	9.60	302.0	400.00	46.08	1800.00	1546.56	1.16
99.90	99.90	4.10	301.0	333.00	79.12	1130.00	994.40	1.14

h (mm)	b (mm)	t (mm)	KL (mm)	F_y (MPa)	f_c' (MPa)	C_a (kN)	C_n (kN)	C_a/C_n
200.00	200.00	3.00	600.0	303.50	46.80	2458.00	2083.58	1.18
200.00	200.00	3.00	601.0	303.50	46.80	2594.00	2083.58	1.24
200.00	200.00	3.00	602.0	303.50	46.80	2306.00	2083.58	1.11
200.00	200.00	3.00	603.0	303.50	46.80	2284.00	2083.58	1.10
200.00	200.00	3.00	604.0	303.50	46.80	2550.00	2083.58	1.22
200.00	200.00	3.00	605.0	303.50	46.80	2587.00	2083.58	1.24
149.80	149.80	4.27	600.0	412.00	31.90	1598.00	1514.42	1.06
149.80	149.80	4.27	1200.0	412.00	31.90	1586.00	1508.63	1.05
149.80	149.80	4.27	1800.0	412.00	31.90	1573.00	1488.26	1.06
149.80	149.80	4.27	2700.0	412.00	31.90	1356.00	1408.62	0.96
149.80	149.80	4.27	3600.0	412.00	31.90	1143.00	1259.53	0.91
149.80	149.80	4.27	4500.0	412.00	31.90	909.00	1066.70	0.85
120.00	120.00	5.86	2600.0	321.10	20.40	999.60	909.58	1.10
120.00	120.00	3.84	2600.0	330.10	29.30	980.00	790.54	1.24
140.00	140.00	3.84	2600.0	330.10	29.30	1323.00	1032.46	1.28
101.60	101.60	2.13	914.0	336.00	23.80	524.00	462.62	1.13
101.60	101.60	2.13	914.0	336.00	23.80	488.00	462.62	1.05
101.60	101.60	3.18	914.0	336.00	29.30	667.00	623.02	1.07
101.60	101.60	3.18	914.0	336.00	29.30	676.00	623.02	1.09
120.00	80.00	5.00	2760.0	386.30	44.00	600.00	566.34	1.06
120.00	80.00	5.00	2740.0	357.50	35.70	407.00	533.99	0.76
120.00	120.00	5.00	500.0	304.00	47.00	1440.00	1121.84	1.28
120.00	120.00	5.00	500.0	438.00	46.00	1690.00	1412.39	1.20
120.00	120.00	8.00	500.0	323.00	39.00	1550.00	1436.00	1.08
120.00	120.00	8.00	500.0	376.00	47.00	1990.00	1678.99	1.19
120.00	120.00	8.00	500.0	379.00	39.00	1800.00	1627.18	1.11
120.00	120.00	8.00	500.0	364.00	80.00	2300.00	1872.16	1.23
120.00	120.00	8.00	500.0	379.00	80.00	2290.00	1923.35	1.19
120.00	120.00	8.00	500.0	379.00	31.00	1680.00	1563.06	1.07
152.30	76.60	3.00	635.0	430.00	30.50	819.00	814.03	1.01
152.80	76.50	4.47	635.0	383.00	26.00	1006.00	934.86	1.08
152.40	101.80	4.32	635.0	413.00	26.00	1144.00	1136.53	1.01
152.70	102.80	4.57	635.0	365.00	23.80	1224.00	1060.95	1.15
151.40	101.30	5.72	635.0	324.00	23.80	1335.00	1108.56	1.20
151.40	102.10	7.34	635.0	358.00	23.80	1691.00	1433.39	1.18
127.30	127.30	3.15	635.0	356.00	30.50	917.00	906.16	1.01
126.90	126.90	4.34	635.0	357.00	26.00	1095.00	1035.85	1.06
127.00	126.90	4.55	635.0	322.00	23.80	1113.00	968.42	1.15
126.50	125.30	5.67	635.0	312.00	23.80	1202.00	1078.06	1.11
127.20	126.80	7.47	635.0	347.00	23.80	2069.00	1430.73	1.45
200.00	100.00	5.00	2000.0	360.00	33.40	1242.00	1369.42	0.91
200.00	100.00	5.00	2000.0	360.00	33.40	1242.00	1369.42	0.91
140.00	140.00	4.00	2100.0	366.00	33.40	1011.00	1228.33	0.82
140.00	140.00	5.00	2100.0	362.00	33.40	1248.00	1365.91	0.91
150.00	90.00	3.00	2250.0	320.00	33.40	691.00	674.08	1.03
150.00	90.00	3.00	2251.0	320.00	33.40	638.00	673.96	0.95

h (mm)	b (mm)	t (mm)	KL (mm)	F_y (MPa)	f_c' (MPa)	C_a (kN)	C_n (kN)	C_a/C_n
150.00	90.00	3.00	2256.0	320.00	33.40	738.00	673.35	1.10
150.00	90.00	3.00	2257.0	320.00	33.40	625.00	673.22	0.93
200.00	200.00	3.00	2310.0	303.50	46.80	1986.00	2072.84	0.96
200.00	200.00	3.00	2311.0	303.50	46.80	2045.00	2072.82	0.99
200.00	200.00	3.00	2312.0	303.50	46.80	2280.00	2072.80	1.10
200.00	200.00	3.00	2313.0	303.50	46.80	2173.00	2072.78	1.05
200.00	200.00	3.00	2314.0	303.50	46.80	2258.00	2072.77	1.09
150.20	150.20	2.91	1110.0	319.30	68.50	2352.00	1605.02	1.47
149.50	149.50	2.89	2200.0	319.30	68.50	2077.00	1567.08	1.33
148.60	148.60	2.93	3101.0	319.30	68.50	1558.00	1499.40	1.04
151.40	151.40	4.77	1085.0	316.60	68.50	2597.00	1893.20	1.37
150.00	150.00	4.90	2201.0	316.60	68.50	2381.00	1845.48	1.29
150.70	150.70	4.89	3100.0	316.60	68.50	1627.00	1771.14	0.92
175.70	134.90	2.91	993.0	319.30	68.50	2401.00	1679.44	1.43
176.50	136.30	2.91	1980.0	319.30	68.50	2283.00	1679.85	1.36
199.30	124.60	2.92	921.0	319.30	68.50	2636.00	1759.63	1.50
199.90	125.90	2.90	1829.0	319.30	68.50	2303.00	1755.09	1.31
160.80	102.70	2.04	480.0	305.10	49.40	1080.00	911.74	1.18
159.10	103.30	4.80	480.0	347.30	49.40	1875.00	1357.79	1.38
156.70	102.40	4.80	480.0	347.30	49.40	1915.00	1333.08	1.44
158.80	104.40	4.85	480.0	347.30	49.40	1820.00	1372.77	1.33
188.40	121.60	4.88	480.0	347.30	49.40	2260.00	1761.00	1.28
190.90	120.40	4.83	570.0	347.30	49.40	2510.00	1758.85	1.43
160.20	102.10	2.00	570.0	305.10	58.60	1555.00	995.89	1.56
162.80	99.60	2.13	480.0	305.10	58.60	1460.00	1006.57	1.45
162.30	98.50	2.00	480.0	305.10	58.60	1545.00	977.95	1.58
156.90	103.40	4.71	480.0	347.30	58.60	2090.00	1418.43	1.47
162.00	106.90	4.81	480.0	347.30	58.60	2320.00	1506.09	1.54
158.90	102.60	4.74	480.0	347.30	58.60	2060.00	1429.52	1.44
194.80	121.00	4.72	570.0	347.30	49.40	2700.00	1775.59	1.52
189.60	121.70	4.81	570.0	347.30	49.40	2680.00	1758.91	1.52
197.00	197.00	6.40	600.0	437.88	20.91	2730.00	2670.02	1.02
198.50	198.50	6.10	600.0	437.88	20.23	3010.00	2588.38	1.16
201.00	201.00	10.30	600.0	381.68	20.91	3980.00	3449.41	1.15
201.00	201.00	10.00	600.0	381.68	20.23	3920.00	3359.15	1.17
150.00	100.00	4.50	1855.0	379.80	29.00	1344.80	1002.63	1.34
150.00	100.00	4.50	1855.0	379.80	29.00	1281.30	1002.63	1.28
150.00	100.00	4.50	1855.0	379.80	29.00	1320.20	1002.63	1.32
150.00	100.00	4.50	1855.0	379.80	29.00	1367.60	1002.63	1.36
150.00	100.00	4.50	1855.0	379.80	63.00	1756.10	1297.18	1.35
150.00	100.00	4.50	1855.0	379.80	63.00	1702.80	1297.18	1.31
150.00	100.00	4.50	1855.0	379.80	63.00	1762.70	1297.18	1.36
150.00	100.00	4.50	1855.0	379.80	63.00	1737.50	1297.18	1.34
150.00	100.00	4.50	1855.0	379.80	63.00	1669.20	1297.18	1.29
150.00	100.00	4.50	1855.0	379.80	63.00	1705.80	1297.18	1.32
150.00	100.00	4.50	1855.0	379.80	70.00	1894.60	1352.76	1.40

h (mm)	b (mm)	t (mm)	KL (mm)	F_y (MPa)	f_c' (MPa)	C_a (kN)	C_n (kN)	C_a/C_n
150.00	100.00	4.50	1855.0	379.80	70.00	1889.20	1352.76	1.40
150.00	100.00	4.50	1855.0	379.80	70.00	1885.60	1352.76	1.39
150.00	100.00	4.50	1855.0	379.80	70.00	1891.60	1352.76	1.40
150.00	100.00	4.50	1855.0	379.80	70.00	1862.30	1352.76	1.38
150.00	100.00	4.50	1855.0	379.80	70.00	1889.80	1352.76	1.40
125.00	125.00	4.00	300.0	342.59	46.67	1159.20	1146.91	1.01
190.00	190.00	2.50	570.0	342.00	58.08	2480.00	2151.77	1.15
190.00	190.00	2.50	570.0	342.00	58.08	2430.00	2151.77	1.13
150.20	150.20	2.98	401.0	392.00	47.67	2360.00	1450.66	1.63
150.00	150.40	3.00	400.6	392.00	47.67	2300.00	1454.63	1.58
100.50	200.50	2.97	402.0	392.00	47.67	2160.00	1360.56	1.59
60.00	60.00	2.00	180.0	404.00	42.91	318.00	288.85	1.10
60.00	60.00	2.00	180.0	404.00	42.91	322.00	288.85	1.11
100.00	100.00	2.00	300.0	404.00	42.91	770.00	623.06	1.24
100.00	100.00	2.00	300.0	404.00	42.91	772.00	623.06	1.24
60.00	60.00	2.00	180.0	404.00	71.55	422.00	349.71	1.21
60.00	60.00	2.00	180.0	404.00	71.55	406.00	349.71	1.16

Appendix Table C-2. Database of tests for concrete-filled RHS members subjected to axial compression in accordance with AISC 360-16

h (mm)	b (mm)	t (mm)	KL (mm)	F_y (MPa)	f_c' (MPa)	C_a (kN)	C_n (kN)	C_a/C_n
101.30	101.30	4.97	300.0	347.30	49.40	1310.00	987.58	1.33
103.60	103.60	4.90	300.0	347.30	49.40	1340.00	1014.06	1.32
102.00	102.00	4.97	300.0	347.30	49.40	1370.00	997.83	1.37
142.00	142.00	5.11	420.0	347.30	49.40	2160.00	1668.11	1.29
142.00	142.00	5.08	420.0	347.30	49.40	2250.00	1663.58	1.35
141.40	141.40	5.07	420.0	347.30	49.40	2280.00	1651.20	1.38
103.50	103.50	5.01	300.0	347.30	58.60	1500.00	1091.70	1.37
102.10	102.10	4.97	300.0	347.30	58.60	1330.00	1064.99	1.25
101.90	101.90	5.03	300.0	347.30	58.60	1440.00	1067.74	1.35
142.30	142.30	5.09	420.0	347.30	58.60	2520.00	1805.70	1.40
142.40	142.40	5.10	420.0	347.30	58.60	2610.00	1809.20	1.44
149.10	149.10	5.06	420.0	347.30	58.60	1700.00	1941.01	0.88
130.30	101.60	5.03	390.0	347.30	49.40	1580.00	1203.80	1.31
130.30	102.30	5.14	390.0	347.30	49.40	1600.00	1222.97	1.31
130.30	102.30	5.14	390.0	347.30	49.40	1640.00	1222.97	1.34
167.40	136.10	5.13	480.0	347.30	49.40	2510.00	1837.59	1.37
170.80	135.30	5.07	510.0	347.30	49.40	2470.00	1847.57	1.34
125.70	102.70	5.15	390.0	347.30	58.60	1840.00	1275.64	1.44
130.00	120.40	5.03	390.0	347.30	58.60	1820.00	1465.99	1.24
132.30	102.70	4.98	390.0	347.30	58.60	1725.00	1309.29	1.32
167.90	137.10	5.10	480.0	347.30	58.60	2600.00	2001.80	1.30
172.70	133.20	5.08	480.0	347.30	58.60	2700.00	1999.79	1.35
120.00	120.00	2.65	360.0	340.00	21.90	778.00	658.57	1.18
120.00	120.00	3.84	360.0	330.10	26.40	1080.00	855.42	1.26
120.00	120.00	3.84	360.0	330.10	28.20	1078.00	874.57	1.23
140.00	140.00	3.84	420.0	330.10	29.30	1499.40	1108.42	1.35
140.00	140.00	3.84	420.0	330.10	29.30	1470.00	1108.42	1.33
120.00	120.00	5.86	360.0	321.10	28.20	1460.20	1106.12	1.32
120.00	120.00	5.86	360.0	321.10	28.20	1372.00	1106.12	1.24
140.00	140.00	5.86	420.0	321.10	29.30	2009.00	1384.21	1.45
140.00	140.00	5.86	420.0	321.10	29.30	1906.10	1384.21	1.38
100.00	100.00	5.00	400.0	403.40	32.40	1195.00	953.83	1.25
100.00	100.00	5.00	400.0	403.40	32.40	1068.00	953.83	1.12
100.00	100.00	5.00	400.0	403.40	32.40	1294.00	953.83	1.36
100.00	100.00	5.00	400.0	403.40	32.40	1274.00	953.83	1.34
100.00	100.00	5.00	400.0	403.40	32.40	1313.00	953.83	1.38
100.00	100.00	5.00	400.0	403.40	32.40	1294.00	953.83	1.36
100.00	100.00	5.00	400.0	403.40	32.40	1244.60	953.83	1.30
100.00	100.00	5.00	400.0	403.40	32.40	1323.00	953.83	1.39
100.00	100.00	5.00	400.0	403.40	32.40	1313.00	953.83	1.38
100.00	100.00	5.00	400.0	403.40	32.40	1274.00	953.83	1.34
100.00	100.00	5.00	400.0	403.40	32.40	1244.60	953.83	1.30
100.00	100.00	2.20	300.0	339.40	21.40	511.00	452.09	1.13
100.00	100.00	2.20	300.0	339.40	21.40	510.00	452.09	1.13
250.00	250.00	8.00	500.0	379.00	33.00	4870.00	4396.87	1.11
152.40	152.40	4.43	300.0	389.00	46.20	1906.00	1804.49	1.06
152.40	152.40	8.95	300.0	432.00	45.40	3307.00	2817.69	1.17
153.40	152.00	6.17	300.0	377.00	43.60	3317.00	2050.73	1.62

h (mm)	b (mm)	t (mm)	KL (mm)	F_y (MPa)	f_c' (MPa)	C_a (kN)	C_n (kN)	C_a/C_n
153.00	152.20	9.04	300.0	394.00	47.20	4208.00	2679.00	1.57
200.30	200.30	4.35	601.0	323.00	29.60	1613.00	1999.19	0.81
300.50	300.50	6.10	902.0	395.00	26.50	2766.00	4646.55	0.60
200.10	200.10	4.35	601.0	323.00	57.90	2563.00	2869.08	0.89
300.60	300.60	6.10	902.0	395.00	58.90	5481.00	6916.39	0.79
200.20	200.20	4.35	601.0	323.00	63.70	2825.00	3050.38	0.93
200.30	200.30	4.35	601.0	323.00	29.60	2230.00	1999.19	1.12
300.50	300.50	6.10	902.0	395.00	26.50	5102.00	4646.55	1.10
200.10	200.10	4.35	601.0	323.00	57.90	3201.00	2869.08	1.12
300.70	300.70	6.10	902.0	395.00	52.20	6494.00	6451.50	1.01
200.30	200.30	4.35	601.0	323.00	63.70	3417.00	3053.02	1.12
100.70	100.70	9.60	301.0	400.00	24.64	1550.00	1433.46	1.08
100.10	100.10	4.20	301.0	333.00	27.76	700.00	716.21	0.98
100.00	100.00	4.20	302.0	333.00	27.76	680.00	715.19	0.95
100.00	100.00	4.10	301.0	333.00	46.08	880.00	834.65	1.05
99.90	99.90	4.00	301.0	333.00	46.08	830.00	823.37	1.01
101.00	101.00	9.60	302.0	400.00	46.08	1800.00	1558.43	1.16
149.80	149.80	4.27	600.0	412.00	31.90	1598.00	1530.53	1.04
149.80	149.80	4.27	1200.0	412.00	31.90	1586.00	1486.81	1.07
149.80	149.80	4.27	1800.0	412.00	31.90	1573.00	1416.71	1.11
149.80	149.80	4.27	2700.0	412.00	31.90	1356.00	1270.84	1.07
149.80	149.80	4.27	3600.0	412.00	31.90	1143.00	1091.49	1.05
149.80	149.80	4.27	4500.0	412.00	31.90	909.00	897.58	1.01
120.00	120.00	5.86	2600.0	321.10	20.40	999.60	828.57	1.21
120.00	120.00	3.84	2600.0	330.10	29.30	980.00	701.90	1.40
140.00	140.00	3.84	2600.0	330.10	29.30	1323.00	931.96	1.42
101.60	101.60	2.13	914.0	336.00	23.80	524.00	453.35	1.16
101.60	101.60	2.13	914.0	336.00	23.80	488.00	453.35	1.08
101.60	101.60	3.18	914.0	336.00	29.30	667.00	611.89	1.09
101.60	101.60	3.18	914.0	336.00	29.30	676.00	611.89	1.10
120.00	80.00	5.00	2760.0	386.30	44.00	600.00	509.96	1.18
120.00	80.00	5.00	2740.0	357.50	35.70	407.00	487.54	0.83
120.00	120.00	5.00	500.0	304.00	47.00	1440.00	1151.63	1.25
120.00	120.00	5.00	500.0	438.00	46.00	1690.00	1435.01	1.18
120.00	120.00	8.00	500.0	323.00	39.00	1550.00	1447.67	1.07
120.00	120.00	8.00	500.0	376.00	47.00	1990.00	1697.28	1.17
120.00	120.00	8.00	500.0	379.00	39.00	1800.00	1635.40	1.10
120.00	120.00	8.00	500.0	379.00	31.00	1680.00	1563.42	1.07
152.30	76.60	3.00	635.0	430.00	30.50	819.00	800.14	1.02
152.80	76.50	4.47	635.0	383.00	26.00	1006.00	918.88	1.09
152.40	101.80	4.32	635.0	413.00	26.00	1144.00	1129.22	1.01
152.70	102.80	4.57	635.0	365.00	23.80	1224.00	1054.49	1.16
151.40	101.30	5.72	635.0	324.00	23.80	1335.00	1101.45	1.21
151.40	102.10	7.34	635.0	358.00	23.80	1691.00	1418.89	1.19
127.30	127.30	3.15	635.0	356.00	30.50	917.00	913.59	1.00
126.90	126.90	4.34	635.0	357.00	26.00	1095.00	1036.67	1.06
127.00	126.90	4.55	635.0	322.00	23.80	1113.00	969.39	1.15
126.50	125.30	5.67	635.0	312.00	23.80	1202.00	1077.14	1.12
127.20	126.80	7.47	635.0	347.00	23.80	2069.00	1424.18	1.45
200.00	100.00	5.00	2000.0	360.00	33.40	1242.00	1260.17	0.99

h (mm)	b (mm)	t (mm)	KL (mm)	F_y (MPa)	f_c' (MPa)	C_a (kN)	C_n (kN)	C_a/C_n
200.00	100.00	5.00	2000.0	360.00	33.40	1242.00	1260.17	0.99
140.00	140.00	4.00	2100.0	366.00	33.40	1011.00	1171.83	0.86
140.00	140.00	5.00	2100.0	362.00	33.40	1248.00	1283.64	0.97
150.00	90.00	3.00	2250.0	320.00	33.40	691.00	578.02	1.20
150.00	90.00	3.00	2251.0	320.00	33.40	638.00	577.86	1.10
150.00	90.00	3.00	2256.0	320.00	33.40	738.00	577.07	1.28
150.00	90.00	3.00	2257.0	320.00	33.40	625.00	576.92	1.08
150.20	150.20	2.91	1110.0	319.30	68.50	2352.00	1683.49	1.40
149.50	149.50	2.89	2200.0	319.30	68.50	2077.00	1476.38	1.41
148.60	148.60	2.93	3101.0	319.30	68.50	1558.00	1246.56	1.25
151.40	151.40	4.77	1085.0	316.60	68.50	2597.00	1971.76	1.32
150.00	150.00	4.90	2201.0	316.60	68.50	2381.00	1765.45	1.35
150.70	150.70	4.89	3100.0	316.60	68.50	1627.00	1557.42	1.04
175.70	134.90	2.91	993.0	319.30	68.50	2401.00	1764.43	1.36
159.10	103.30	4.80	480.0	347.30	49.40	1875.00	1393.07	1.35
156.70	102.40	4.80	480.0	347.30	49.40	1915.00	1367.10	1.40
158.80	104.40	4.85	480.0	347.30	49.40	1820.00	1408.60	1.29
188.40	121.60	4.88	480.0	347.30	49.40	2260.00	1818.51	1.24
190.90	120.40	4.83	570.0	347.30	49.40	2510.00	1810.15	1.39
156.90	103.40	4.71	480.0	347.30	58.60	2090.00	1471.91	1.42
162.00	106.90	4.81	480.0	347.30	58.60	2320.00	1564.56	1.48
158.90	102.60	4.74	480.0	347.30	58.60	2060.00	1482.94	1.39
194.80	121.00	4.72	570.0	347.30	49.40	2700.00	1828.98	1.48
189.60	121.70	4.81	570.0	347.30	49.40	2680.00	1810.94	1.48
197.00	197.00	6.40	600.0	437.88	20.91	2730.00	2678.03	1.02
198.50	198.50	6.10	600.0	437.88	20.23	3010.00	2596.15	1.16
201.00	201.00	10.30	600.0	381.68	20.91	3980.00	3454.32	1.15
201.00	201.00	10.00	600.0	381.68	20.23	3920.00	3363.39	1.17
150.00	100.00	4.50	1855.0	379.80	29.00	1344.80	916.67	1.47
150.00	100.00	4.50	1855.0	379.80	29.00	1281.30	916.67	1.40
150.00	100.00	4.50	1855.0	379.80	29.00	1320.20	916.67	1.44
150.00	100.00	4.50	1855.0	379.80	29.00	1367.60	916.67	1.49
150.00	100.00	4.50	1855.0	379.80	63.00	1756.10	1175.46	1.49
150.00	100.00	4.50	1855.0	379.80	63.00	1702.80	1175.46	1.45
150.00	100.00	4.50	1855.0	379.80	63.00	1762.70	1175.46	1.50
150.00	100.00	4.50	1855.0	379.80	63.00	1737.50	1175.46	1.48
150.00	100.00	4.50	1855.0	379.80	63.00	1669.20	1175.46	1.42
150.00	100.00	4.50	1855.0	379.80	63.00	1705.80	1175.46	1.45
150.00	100.00	4.50	1855.0	379.80	70.00	1894.60	1226.21	1.55
150.00	100.00	4.50	1855.0	379.80	70.00	1889.20	1226.21	1.54
150.00	100.00	4.50	1855.0	379.80	70.00	1885.60	1226.21	1.54
150.00	100.00	4.50	1855.0	379.80	70.00	1891.60	1226.21	1.54
150.00	100.00	4.50	1855.0	379.80	70.00	1862.30	1226.21	1.52
150.00	100.00	4.50	1855.0	379.80	70.00	1889.80	1226.21	1.54
125.00	125.00	4.00	300.0	342.59	46.67	1159.20	1187.77	0.98
150.20	150.20	2.98	401.0	392.00	47.67	2360.00	1514.15	1.56
150.00	150.40	3.00	400.6	392.00	47.67	2300.00	1518.11	1.52
60.00	60.00	2.00	180.0	404.00	42.91	318.00	295.91	1.07
60.00	60.00	2.00	180.0	404.00	42.91	322.00	295.91	1.09
100.00	100.00	2.00	300.0	404.00	42.91	770.00	644.69	1.19

h (mm)	b (mm)	t (mm)	KL (mm)	F_y (MPa)	f_c' (MPa)	C_a (kN)	C_n (kN)	C_a/C_n
100.00	100.00	2.00	300.0	404.00	42.91	772.00	644.69	1.20

Appendix Table C-3. Database of tests for concrete-filled RHS members subjected to axial compression in accordance with Tousignant & Packer (2022a,b)

h (mm)	b (mm)	t (mm)	KL (mm)	F_y (MPa)	f_c' (MPa)	C_a (kN)	C_n (kN)	C_a/C_n
101.30	101.30	4.97	300.0	347.30	49.40	1310.00	961.90	1.36
103.60	103.60	4.90	300.0	347.30	49.40	1340.00	986.63	1.36
102.00	102.00	4.97	300.0	347.30	49.40	1370.00	971.65	1.41
142.00	142.00	5.11	420.0	347.30	49.40	2160.00	1612.80	1.34
142.00	142.00	5.08	420.0	347.30	49.40	2250.00	1608.19	1.40
141.40	141.40	5.07	420.0	347.30	49.40	2280.00	1596.38	1.43
142.10	142.10	2.01	420.0	305.10	44.90	1328.00	1010.09	1.31
142.10	142.10	2.01	420.0	305.10	44.90	1364.00	1010.09	1.35
140.90	140.90	2.02	420.0	305.10	44.90	1280.00	996.99	1.28
103.50	103.50	5.01	300.0	347.30	58.60	1500.00	1052.09	1.43
102.10	102.10	4.97	300.0	347.30	58.60	1330.00	1026.65	1.30
101.90	101.90	5.03	300.0	347.30	58.60	1440.00	1029.74	1.40
142.30	142.30	5.09	420.0	347.30	58.60	2520.00	1725.17	1.46
142.40	142.40	5.10	420.0	347.30	58.60	2610.00	1728.56	1.51
143.20	143.20	2.03	420.0	305.10	58.60	1990.00	1210.56	1.64
142.30	142.30	2.01	420.0	305.10	58.60	1855.00	1194.37	1.55
140.50	140.50	2.00	420.0	305.10	58.60	1780.00	1166.47	1.53
149.10	149.10	5.06	420.0	347.30	58.60	1700.00	1850.83	0.92
130.30	101.60	5.03	390.0	347.30	49.40	1580.00	1172.87	1.35
130.30	102.30	5.14	390.0	347.30	49.40	1600.00	1191.94	1.34
130.30	102.30	5.14	390.0	347.30	49.40	1640.00	1191.94	1.38
167.40	136.10	5.13	480.0	347.30	49.40	2510.00	1777.70	1.41
170.80	135.30	5.07	510.0	347.30	49.40	2470.00	1788.21	1.38
125.70	102.70	5.15	390.0	347.30	58.60	1840.00	1230.95	1.49
130.00	120.40	5.03	390.0	347.30	58.60	1820.00	1406.66	1.29
132.30	102.70	4.98	390.0	347.30	58.60	1725.00	1261.29	1.37
157.10	122.50	2.01	480.0	305.10	58.60	1800.00	1143.71	1.57
161.90	119.00	2.00	480.0	305.10	58.60	1740.00	1144.54	1.52
167.90	137.10	5.10	480.0	347.30	58.60	2600.00	1912.92	1.36
172.70	133.20	5.08	480.0	347.30	58.60	2700.00	1911.66	1.41
160.20	122.70	2.03	480.0	305.10	49.40	1400.00	1051.32	1.33
160.10	119.40	2.01	480.0	305.10	49.40	1420.00	1024.03	1.39
161.50	124.30	2.00	480.0	305.10	49.40	1320.00	1066.15	1.24
120.00	120.00	2.65	360.0	340.00	21.90	778.00	652.00	1.19
120.00	120.00	3.84	360.0	330.10	26.40	1080.00	845.93	1.28
120.00	120.00	3.84	360.0	330.10	28.20	1078.00	863.34	1.25
140.00	140.00	3.84	420.0	330.10	29.30	1499.40	1090.85	1.37
140.00	140.00	3.84	420.0	330.10	29.30	1470.00	1090.85	1.35
120.00	120.00	5.86	360.0	321.10	28.20	1460.20	1096.88	1.33
120.00	120.00	5.86	360.0	321.10	28.20	1372.00	1096.88	1.25
140.00	140.00	5.86	420.0	321.10	29.30	2009.00	1368.93	1.47
140.00	140.00	5.86	420.0	321.10	29.30	1906.10	1368.93	1.39
100.00	100.00	5.00	400.0	403.40	32.40	1195.00	949.59	1.26
100.00	100.00	5.00	400.0	403.40	32.40	1068.00	949.59	1.12
100.00	100.00	5.00	400.0	403.40	32.40	1294.00	949.59	1.36
100.00	100.00	5.00	400.0	403.40	32.40	1274.00	949.59	1.34
100.00	100.00	5.00	400.0	403.40	32.40	1313.00	949.59	1.38
100.00	100.00	5.00	400.0	403.40	32.40	1294.00	949.59	1.36

h (mm)	b (mm)	t (mm)	KL (mm)	F_y (MPa)	f_c' (MPa)	C_a (kN)	C_n (kN)	C_a/C_n
100.00	100.00	5.00	400.0	403.40	32.40	1244.60	949.59	1.31
100.00	100.00	5.00	400.0	403.40	32.40	1323.00	949.59	1.39
100.00	100.00	5.00	400.0	403.40	32.40	1313.00	949.59	1.38
100.00	100.00	5.00	400.0	403.40	32.40	1274.00	949.59	1.34
100.00	100.00	5.00	400.0	403.40	32.40	1244.60	949.59	1.31
100.00	100.00	2.20	300.0	339.40	21.40	511.00	447.70	1.14
100.00	100.00	2.20	300.0	339.40	21.40	510.00	447.70	1.14
250.00	250.00	8.00	500.0	379.00	33.00	4870.00	4317.29	1.13
152.40	152.40	4.43	300.0	389.00	46.20	1906.00	1742.75	1.09
152.40	152.40	8.95	300.0	432.00	45.40	3307.00	2768.98	1.19
153.40	152.00	6.17	300.0	377.00	43.60	3317.00	1999.11	1.66
153.00	152.20	9.04	300.0	394.00	47.20	4208.00	2625.17	1.60
200.30	200.30	4.35	601.0	323.00	29.60	1613.00	1960.17	0.82
300.50	300.50	6.10	902.0	395.00	26.50	2766.00	4582.52	0.60
200.10	200.10	4.35	601.0	323.00	57.90	2563.00	2701.63	0.95
300.60	300.60	6.10	902.0	395.00	58.90	5481.00	6528.13	0.84
200.20	200.20	4.35	601.0	323.00	63.70	2825.00	2845.72	0.99
200.30	200.30	4.35	601.0	323.00	29.60	2230.00	1960.17	1.14
300.50	300.50	6.10	902.0	395.00	26.50	5102.00	4582.52	1.11
200.10	200.10	4.35	601.0	323.00	57.90	3201.00	2701.63	1.18
300.70	300.70	6.10	902.0	395.00	52.20	6494.00	6151.05	1.06
200.30	200.30	4.35	601.0	323.00	63.70	3417.00	2848.12	1.20
100.70	100.70	9.60	301.0	400.00	24.64	1550.00	1435.46	1.08
100.10	100.10	4.20	301.0	333.00	27.76	700.00	709.60	0.99
100.00	100.00	4.20	302.0	333.00	27.76	680.00	708.63	0.96
100.00	100.00	4.10	301.0	333.00	46.08	880.00	811.85	1.08
99.90	99.90	4.00	301.0	333.00	46.08	830.00	800.46	1.04
101.00	101.00	9.60	302.0	400.00	46.08	1800.00	1546.44	1.16
200.00	200.00	3.00	600.0	303.50	46.80	2458.00	2083.10	1.18
200.00	200.00	3.00	601.0	303.50	46.80	2594.00	2083.10	1.25
200.00	200.00	3.00	602.0	303.50	46.80	2306.00	2083.10	1.11
200.00	200.00	3.00	603.0	303.50	46.80	2284.00	2083.09	1.10
200.00	200.00	3.00	604.0	303.50	46.80	2550.00	2083.09	1.22
200.00	200.00	3.00	605.0	303.50	46.80	2587.00	2083.09	1.24
149.80	149.80	4.27	600.0	412.00	31.90	1598.00	1513.88	1.06
149.80	149.80	4.27	1200.0	412.00	31.90	1586.00	1502.16	1.06
149.80	149.80	4.27	1800.0	412.00	31.90	1573.00	1461.96	1.08
149.80	149.80	4.27	2700.0	412.00	31.90	1356.00	1318.01	1.03
149.80	149.80	4.27	3600.0	412.00	31.90	1143.00	1092.05	1.05
149.80	149.80	4.27	4500.0	412.00	31.90	909.00	856.39	1.06
120.00	120.00	5.86	2600.0	321.10	20.40	999.60	869.50	1.15
120.00	120.00	3.84	2600.0	330.10	29.30	980.00	723.23	1.36
140.00	140.00	3.84	2600.0	330.10	29.30	1323.00	969.41	1.36
101.60	101.60	2.13	914.0	336.00	23.80	524.00	460.25	1.14
101.60	101.60	2.13	914.0	336.00	23.80	488.00	460.25	1.06
101.60	101.60	3.18	914.0	336.00	29.30	667.00	620.01	1.08
101.60	101.60	3.18	914.0	336.00	29.30	676.00	620.01	1.09
120.00	80.00	5.00	2760.0	386.30	44.00	600.00	478.99	1.25
120.00	80.00	5.00	2740.0	357.50	35.70	407.00	465.27	0.87
120.00	120.00	5.00	500.0	304.00	47.00	1440.00	1121.41	1.28

h (mm)	b (mm)	t (mm)	KL (mm)	F_y (MPa)	f_c' (MPa)	C_a (kN)	C_n (kN)	C_a/C_n
120.00	120.00	5.00	500.0	438.00	46.00	1690.00	1411.73	1.20
120.00	120.00	8.00	500.0	323.00	39.00	1550.00	1435.66	1.08
120.00	120.00	8.00	500.0	376.00	47.00	1990.00	1678.47	1.19
120.00	120.00	8.00	500.0	379.00	39.00	1800.00	1626.75	1.11
120.00	120.00	8.00	500.0	379.00	31.00	1680.00	1562.74	1.08
152.30	76.60	3.00	635.0	430.00	30.50	819.00	811.06	1.01
152.80	76.50	4.47	635.0	383.00	26.00	1006.00	933.69	1.08
152.40	101.80	4.32	635.0	413.00	26.00	1144.00	1135.52	1.01
152.70	102.80	4.57	635.0	365.00	23.80	1224.00	1060.17	1.15
151.40	101.30	5.72	635.0	324.00	23.80	1335.00	1107.94	1.20
151.40	102.10	7.34	635.0	358.00	23.80	1691.00	1432.87	1.18
127.30	127.30	3.15	635.0	356.00	30.50	917.00	905.38	1.01
126.90	126.90	4.34	635.0	357.00	26.00	1095.00	1035.26	1.06
127.00	126.90	4.55	635.0	322.00	23.80	1113.00	968.01	1.15
126.50	125.30	5.67	635.0	312.00	23.80	1202.00	1077.67	1.12
127.20	126.80	7.47	635.0	347.00	23.80	2069.00	1430.28	1.45
200.00	100.00	5.00	2000.0	360.00	33.40	1242.00	1312.17	0.95
200.00	100.00	5.00	2000.0	360.00	33.40	1242.00	1312.17	0.95
140.00	140.00	4.00	2100.0	366.00	33.40	1011.00	1206.72	0.84
140.00	140.00	5.00	2100.0	362.00	33.40	1248.00	1331.19	0.94
150.00	90.00	3.00	2250.0	320.00	33.40	691.00	584.81	1.18
150.00	90.00	3.00	2251.0	320.00	33.40	638.00	584.61	1.09
150.00	90.00	3.00	2256.0	320.00	33.40	738.00	583.61	1.26
150.00	90.00	3.00	2257.0	320.00	33.40	625.00	583.41	1.07
200.00	200.00	3.00	2310.0	303.50	46.80	1986.00	2016.45	0.98
200.00	200.00	3.00	2311.0	303.50	46.80	2045.00	2016.35	1.01
200.00	200.00	3.00	2312.0	303.50	46.80	2280.00	2016.25	1.13
200.00	200.00	3.00	2313.0	303.50	46.80	2173.00	2016.15	1.08
200.00	200.00	3.00	2314.0	303.50	46.80	2258.00	2016.04	1.12
150.20	150.20	2.91	1110.0	319.30	68.50	2352.00	1593.16	1.48
149.50	149.50	2.89	2200.0	319.30	68.50	2077.00	1445.40	1.44
148.60	148.60	2.93	3101.0	319.30	68.50	1558.00	1193.18	1.31
151.40	151.40	4.77	1085.0	316.60	68.50	2597.00	1884.12	1.38
150.00	150.00	4.90	2201.0	316.60	68.50	2381.00	1743.38	1.37
150.70	150.70	4.89	3100.0	316.60	68.50	1627.00	1508.18	1.08
175.70	134.90	2.91	993.0	319.30	68.50	2401.00	1667.83	1.44
176.50	136.30	2.91	1980.0	319.30	68.50	2283.00	1559.70	1.46
199.30	124.60	2.92	921.0	319.30	68.50	2636.00	1747.83	1.51
199.90	125.90	2.90	1829.0	319.30	68.50	2303.00	1634.05	1.41
160.80	102.70	2.04	480.0	305.10	49.40	1080.00	910.80	1.19
159.10	103.30	4.80	480.0	347.30	49.40	1875.00	1357.01	1.38
156.70	102.40	4.80	480.0	347.30	49.40	1915.00	1332.29	1.44
158.80	104.40	4.85	480.0	347.30	49.40	1820.00	1372.01	1.33
188.40	121.60	4.88	480.0	347.30	49.40	2260.00	1760.37	1.28
190.90	120.40	4.83	570.0	347.30	49.40	2510.00	1757.64	1.43
160.20	102.10	2.00	570.0	305.10	58.60	1555.00	993.57	1.57
162.80	99.60	2.13	480.0	305.10	58.60	1460.00	1005.26	1.45
162.30	98.50	2.00	480.0	305.10	58.60	1545.00	976.58	1.58
156.90	103.40	4.71	480.0	347.30	58.60	2090.00	1417.45	1.47
162.00	106.90	4.81	480.0	347.30	58.60	2320.00	1505.16	1.54

h (mm)	b (mm)	t (mm)	KL (mm)	F_y (MPa)	f_c' (MPa)	C_a (kN)	C_n (kN)	C_a/C_n
158.90	102.60	4.74	480.0	347.30	58.60	2060.00	1428.52	1.44
194.80	121.00	4.72	570.0	347.30	49.40	2700.00	1774.36	1.52
189.60	121.70	4.81	570.0	347.30	49.40	2680.00	1757.72	1.52
197.00	197.00	6.40	600.0	437.88	20.91	2730.00	2669.79	1.02
198.50	198.50	6.10	600.0	437.88	20.23	3010.00	2588.16	1.16
201.00	201.00	10.30	600.0	381.68	20.91	3980.00	3449.23	1.15
201.00	201.00	10.00	600.0	381.68	20.23	3920.00	3358.98	1.17
150.00	100.00	4.50	1855.0	379.80	29.00	1344.80	952.08	1.41
150.00	100.00	4.50	1855.0	379.80	29.00	1281.30	952.08	1.35
150.00	100.00	4.50	1855.0	379.80	29.00	1320.20	952.08	1.39
150.00	100.00	4.50	1855.0	379.80	29.00	1367.60	952.08	1.44
150.00	100.00	4.50	1855.0	379.80	63.00	1756.10	1161.17	1.51
150.00	100.00	4.50	1855.0	379.80	63.00	1702.80	1161.17	1.47
150.00	100.00	4.50	1855.0	379.80	63.00	1762.70	1161.17	1.52
150.00	100.00	4.50	1855.0	379.80	63.00	1737.50	1161.17	1.50
150.00	100.00	4.50	1855.0	379.80	63.00	1669.20	1161.17	1.44
150.00	100.00	4.50	1855.0	379.80	63.00	1705.80	1161.17	1.47
150.00	100.00	4.50	1855.0	379.80	70.00	1894.60	1197.98	1.58
150.00	100.00	4.50	1855.0	379.80	70.00	1889.20	1197.98	1.58
150.00	100.00	4.50	1855.0	379.80	70.00	1885.60	1197.98	1.57
150.00	100.00	4.50	1855.0	379.80	70.00	1891.60	1197.98	1.58
150.00	100.00	4.50	1855.0	379.80	70.00	1862.30	1197.98	1.55
150.00	100.00	4.50	1855.0	379.80	70.00	1889.80	1197.98	1.58
125.00	125.00	4.00	300.0	342.59	46.67	1159.20	1146.84	1.01
190.00	190.00	2.50	570.0	342.00	58.08	2480.00	2151.11	1.15
190.00	190.00	2.50	570.0	342.00	58.08	2430.00	2151.11	1.13
150.20	150.20	2.98	401.0	392.00	47.67	2360.00	1450.45	1.63
150.00	150.40	3.00	400.6	392.00	47.67	2300.00	1454.42	1.58
200.50	100.50	2.97	402.0	392.00	47.67	2160.00	1359.63	1.59
60.00	60.00	2.00	180.0	404.00	42.91	318.00	288.81	1.10
60.00	60.00	2.00	180.0	404.00	42.91	322.00	288.81	1.11
100.00	100.00	2.00	300.0	404.00	42.91	770.00	622.94	1.24
100.00	100.00	2.00	300.0	404.00	42.91	772.00	622.94	1.24

Appendix Table C-4. Database of tests for concrete-filled CHS members subjected to axial compression in accordance with CSA S16:19

d (mm)	t (mm)	KL (mm)	F_y (MPa)	f_c' (MPa)	C_a (kN)	C_n (kN)	C_a/C_n
140.40	4.93	406.0	302.00	33.20	1824.00	1392.16	1.31
219.10	5.00	600.0	380.00	51.60	3118.00	3514.99	0.89
219.10	10.00	600.0	381.00	51.60	5241.00	5283.56	0.99
219.10	5.00	600.0	380.00	51.60	3118.00	3514.99	0.89
219.10	10.00	600.0	381.00	51.60	5241.00	5283.56	0.99
168.30	2.80	300.0	317.80	37.71	1282.50	1436.04	0.89
159.00	3.00	300.0	336.28	33.39	1185.70	1354.20	0.88
120.00	2.50	300.0	445.52	41.44	879.20	1038.14	0.85
100.00	3.00	300.0	432.09	34.04	724.00	837.78	0.86
101.60	3.00	300.0	425.03	34.04	703.30	845.86	0.83
157.00	2.48	314.0	326.00	73.20	2117.00	1669.41	1.27
157.00	2.48	314.0	326.00	73.20	2058.00	1669.41	1.23
157.00	2.48	314.0	326.00	73.20	2068.00	1669.41	1.24
282.00	4.36	564.0	322.00	73.20	6811.00	5318.82	1.28
282.00	4.36	564.0	322.00	73.20	6380.00	5318.82	1.20
282.00	4.36	564.0	322.00	73.20	6860.00	5318.82	1.29
474.00	7.42	948.0	317.00	73.20	17787.00	14997.14	1.19
474.00	7.42	948.0	317.00	73.20	18306.00	14997.14	1.22
474.00	7.42	948.0	317.00	73.20	17885.00	14997.14	1.19
153.00	3.64	306.0	320.00	73.20	2264.00	1845.46	1.23
153.00	3.64	306.0	320.00	73.20	2274.00	1845.46	1.23
153.00	3.64	306.0	320.00	73.20	2205.00	1845.46	1.19
393.00	9.38	786.0	312.00	73.20	13936.00	12037.23	1.16
393.00	9.38	786.0	312.00	73.20	14406.00	12037.23	1.20
393.00	9.38	786.0	312.00	73.20	14161.00	12037.23	1.18
477.00	11.36	954.0	310.00	73.20	20237.00	17659.13	1.15
477.00	11.36	954.0	310.00	73.20	20462.00	17659.13	1.16
477.00	11.36	954.0	310.00	73.20	19854.00	17659.13	1.12
168.30	4.47	813.0	302.00	23.40	1744.00	1452.18	1.20
108.00	4.50	445.0	409.64	28.60	970.20	1104.15	0.88
60.00	2.00	180.0	404.00	75.63	427.00	377.64	1.13
60.00	2.00	180.0	404.00	75.63	415.00	377.64	1.10
100.00	2.00	300.0	404.00	75.63	930.00	818.48	1.14
100.00	2.00	300.0	404.00	75.63	920.00	818.48	1.12
129.00	3.00	387.0	306.00	45.52	1068.00	1026.68	1.04
129.00	3.00	387.0	306.00	47.01	1093.00	1039.31	1.05
129.00	3.00	387.0	306.00	47.95	1118.00	1047.18	1.07
129.00	3.00	387.0	306.00	50.30	1162.00	1066.79	1.09
131.00	4.00	393.0	306.00	45.52	1280.00	1224.58	1.05
131.00	4.00	393.0	306.00	47.01	1360.00	1237.21	1.10
131.00	4.00	393.0	306.00	47.95	1403.00	1245.09	1.13
131.00	4.00	393.0	306.00	50.30	1459.00	1264.69	1.15
133.00	5.00	399.0	306.00	45.52	1454.00	1420.97	1.02
133.00	5.00	399.0	306.00	47.01	1470.00	1433.60	1.03

d (mm)	t (mm)	KL (mm)	F_y (MPa)	f_c' (MPa)	C_a (kN)	C_n (kN)	C_a/C_n
133.00	5.00	399.0	306.00	47.95	1518.00	1441.48	1.05
133.00	5.00	399.0	306.00	50.30	1569.00	1461.08	1.07
129.00	3.00	387.0	306.00	52.28	1095.00	1083.16	1.01
129.00	3.00	387.0	306.00	53.70	1128.00	1094.80	1.03
129.00	3.00	387.0	306.00	55.22	1147.00	1107.16	1.04
129.00	3.00	387.0	306.00	57.31	1192.00	1124.07	1.06
131.00	4.00	393.0	306.00	52.28	1320.00	1281.06	1.03
131.00	4.00	393.0	306.00	53.70	1389.00	1292.70	1.07
131.00	4.00	393.0	306.00	55.22	1430.00	1305.07	1.10
131.00	4.00	393.0	306.00	57.31	1452.00	1321.98	1.10
133.00	5.00	399.0	306.00	52.28	1548.00	1477.45	1.05
133.00	5.00	399.0	306.00	53.70	1581.00	1489.09	1.06
133.00	5.00	399.0	306.00	55.22	1609.00	1501.46	1.07
133.00	5.00	399.0	306.00	57.31	1661.00	1518.37	1.09
129.00	3.00	387.0	306.00	60.66	1266.00	1150.76	1.10
129.00	3.00	387.0	306.00	62.48	1287.00	1165.13	1.10
129.00	3.00	387.0	306.00	65.36	1301.00	1187.65	1.10
129.00	3.00	387.0	306.00	67.10	1356.00	1201.06	1.13
131.00	4.00	393.0	306.00	60.66	1469.00	1348.67	1.09
131.00	4.00	393.0	306.00	62.48	1482.00	1363.04	1.09
131.00	4.00	393.0	306.00	65.36	1496.00	1385.56	1.08
131.00	4.00	393.0	306.00	67.10	1542.00	1398.97	1.10
133.00	5.00	399.0	306.00	60.66	1659.00	1545.06	1.07
133.00	5.00	399.0	306.00	62.48	1673.00	1559.44	1.07
133.00	5.00	399.0	306.00	65.36	1712.00	1581.96	1.08
133.00	5.00	399.0	306.00	67.10	1774.00	1595.37	1.11
169.30	2.62	1830.0	338.10	37.10	756.00	1154.01	0.66
169.30	2.62	1830.0	338.10	34.10	689.00	1111.56	0.62
168.80	5.00	2135.0	302.40	33.40	1130.00	1366.89	0.83
168.80	5.00	2135.0	302.40	27.80	1165.00	1292.85	0.90
200.00	3.00	2000.0	303.50	46.80	1830.00	1744.84	1.05
200.00	3.00	2001.0	303.50	46.80	1806.00	1744.61	1.04
200.00	3.00	2002.0	303.50	46.80	1882.00	1744.38	1.08
200.00	3.00	2003.0	303.50	46.80	2060.00	1744.14	1.18
200.00	3.00	2004.0	303.50	46.80	2115.00	1743.91	1.21
95.00	3.66	860.0	332.00	25.30	656.00	569.82	1.15
95.00	3.68	860.0	392.00	25.30	686.00	649.90	1.06
95.00	3.40	860.0	340.00	25.30	656.00	551.68	1.19
95.00	3.86	1420.0	332.00	25.30	567.00	480.50	1.18
95.00	3.91	1420.0	392.00	25.30	606.00	540.37	1.12
95.00	3.58	1420.0	340.00	25.30	576.00	463.81	1.24
95.00	3.76	1980.0	332.00	25.30	536.00	381.78	1.40
95.00	3.78	1980.0	392.00	25.30	567.00	415.25	1.37
95.00	3.51	1980.0	340.00	25.30	488.00	368.83	1.32
216.00	4.11	2220.0	304.00	23.20	1834.00	1665.54	1.10
216.00	6.05	2220.0	395.00	23.20	2462.00	2530.82	0.97

d (mm)	t (mm)	KL (mm)	F_y (MPa)	f_c' (MPa)	C_a (kN)	C_n (kN)	C_a/C_n
216.00	5.97	2220.0	399.00	23.20	2421.00	2525.80	0.96
216.00	6.30	2220.0	411.00	30.20	2932.00	2839.24	1.03
95.00	3.86	1980.0	337.00	24.40	498.00	389.04	1.28
95.00	3.40	1980.0	343.00	24.40	473.00	360.12	1.31
95.00	3.58	1980.0	360.00	24.40	473.00	381.74	1.24
95.00	3.73	1980.0	332.00	24.40	413.00	377.25	1.09
121.00	3.73	1050.0	333.00	21.40	746.00	777.54	0.96
121.00	3.76	1050.0	313.00	24.60	837.00	770.77	1.09
121.00	3.99	1050.0	332.00	24.60	867.00	837.12	1.04
121.00	5.61	1050.0	349.00	21.40	998.00	1079.48	0.92
121.00	5.41	1050.0	348.00	21.40	1018.00	1048.89	0.97
121.00	5.46	1050.0	336.00	24.60	1099.00	1048.96	1.05
121.00	5.56	1050.0	327.00	24.60	1079.00	1039.66	1.04
121.00	3.76	2310.0	333.00	21.40	629.00	543.13	1.16
121.00	3.71	2310.0	313.00	24.60	695.00	538.15	1.29
121.00	3.86	2310.0	332.00	24.60	755.00	568.68	1.33
121.00	5.69	2310.0	349.00	21.40	786.00	744.08	1.06
121.00	5.49	2310.0	348.00	21.40	816.00	723.98	1.13
121.00	5.64	2310.0	336.00	24.60	874.00	738.68	1.18
121.00	5.44	2310.0	327.00	24.60	865.00	709.45	1.22
114.30	3.18	914.0	420.00	29.40	712.00	842.27	0.85
114.30	3.18	914.0	420.00	29.40	756.00	842.27	0.90
355.60	11.18	1880.0	361.00	38.60	11460.00	9221.65	1.24
355.60	11.18	1880.0	361.00	33.30	10710.00	8882.06	1.21
355.60	7.98	2083.0	361.00	23.80	7433.00	6438.05	1.15
127.30	1.63	711.0	334.00	67.20	1285.00	931.32	1.38
127.10	2.95	711.0	376.00	67.20	1305.00	1225.82	1.06
127.10	2.95	711.0	334.00	67.20	1305.00	1154.20	1.13
168.20	4.52	813.0	302.00	31.90	2006.00	1590.59	1.26
168.40	4.52	813.0	302.00	43.80	2233.00	1767.18	1.26
168.20	4.52	813.0	302.00	43.80	2113.00	1763.85	1.20
88.90	5.84	1727.0	406.00	41.50	614.70	601.12	1.02
88.90	5.84	1422.0	406.00	41.50	711.70	695.27	1.02
88.90	5.84	1118.0	406.00	41.50	715.20	799.40	0.89
88.90	5.84	813.0	406.00	41.50	918.50	909.78	1.01
88.90	5.84	508.0	406.00	41.50	991.90	1021.21	0.97
88.90	5.84	508.0	406.00	41.50	889.60	1021.21	0.87
108.00	4.50	4158.0	348.10	25.40	342.00	240.38	1.42
108.00	4.50	4158.0	348.10	25.40	292.00	240.38	1.21
108.00	4.50	4158.0	348.10	37.40	298.00	248.77	1.20
108.00	4.50	4158.0	348.10	37.40	280.00	248.77	1.13
108.00	4.50	4023.0	348.10	37.40	318.00	263.15	1.21
108.00	4.50	4023.0	348.10	37.40	320.00	263.15	1.22
108.00	4.50	3807.0	348.10	25.40	350.00	277.71	1.26
108.00	4.50	3807.0	348.10	25.40	370.00	277.71	1.33
108.00	4.50	3510.0	348.10	25.40	400.00	314.65	1.27

d (mm)	t (mm)	KL (mm)	F_y (MPa)	f_c' (MPa)	C_a (kN)	C_n (kN)	C_a/C_n
108.00	4.50	3510.0	348.10	25.40	390.00	314.65	1.24
108.00	4.50	3510.0	348.10	37.40	440.00	328.02	1.34
114.00	4.44	850.0	332.00	37.00	902.00	945.23	0.95
114.00	4.49	2750.0	332.00	31.00	657.00	495.43	1.33
215.90	6.00	2220.0	392.00	22.90	2442.00	2488.12	0.98
215.90	6.00	2220.0	350.00	30.00	2869.00	2461.91	1.17
120.90	3.76	1050.0	312.00	21.10	721.00	740.58	0.97
120.90	3.76	2310.0	312.00	21.10	636.00	517.35	1.23
120.90	5.53	1050.0	343.00	21.10	1010.00	1048.36	0.96
120.90	5.53	1050.0	343.00	24.20	1090.00	1070.35	1.02
95.00	3.65	1370.0	350.00	25.00	667.00	484.42	1.38
95.00	3.65	1420.0	350.00	25.00	583.00	474.76	1.23
95.00	3.65	1980.0	350.00	25.00	529.00	378.14	1.40
165.00	4.30	2440.0	317.70	43.30	1149.00	1265.64	0.91
160.00	4.50	2420.0	317.70	43.30	1561.00	1220.88	1.28
165.00	4.30	3640.0	317.70	43.30	987.00	943.93	1.05
166.00	5.00	870.0	313.60	42.24	1827.70	1830.35	1.00
166.00	5.00	1700.0	313.60	42.24	1460.20	1586.25	0.92
108.00	4.00	648.0	338.88	28.99	825.16	825.50	1.00
108.00	4.00	648.0	338.88	28.99	828.10	825.50	1.00
108.00	4.00	864.0	338.88	28.99	766.36	774.75	0.99
108.00	4.00	864.0	338.88	28.99	801.64	774.75	1.03
108.00	4.00	864.0	338.88	28.99	869.26	774.75	1.12
108.00	4.00	1080.0	338.88	28.99	836.92	724.52	1.16
108.00	4.00	1080.0	338.88	28.99	783.02	724.52	1.08
108.00	4.00	1620.0	338.88	28.99	707.56	604.36	1.17
108.00	4.00	1620.0	338.88	28.99	646.80	604.36	1.07
108.00	4.00	1620.0	338.88	28.99	643.86	604.36	1.07
108.00	4.00	2160.0	338.88	28.99	672.28	499.09	1.35
108.00	4.00	2160.0	338.88	28.99	697.76	499.09	1.40
108.00	4.00	2160.0	338.88	28.99	676.20	499.09	1.35
108.00	4.00	2700.0	338.88	28.99	648.76	411.10	1.58
108.00	4.00	3240.0	338.88	28.99	559.58	329.02	1.70
108.00	4.00	3240.0	338.88	28.99	478.24	329.02	1.45
108.00	4.00	3240.0	338.88	28.99	600.74	329.02	1.83
108.00	4.00	4320.0	338.88	28.99	373.38	209.84	1.78
108.00	4.00	4320.0	338.88	28.99	345.94	209.84	1.65
108.00	4.00	4320.0	338.88	28.99	294.00	209.84	1.40
108.00	4.00	5400.0	338.88	28.99	225.40	140.42	1.61
108.00	4.00	5400.0	338.88	28.99	210.70	140.42	1.50
108.00	4.00	5560.0	338.88	28.99	212.50	132.95	1.60
104.00	2.00	524.0	344.00	32.65	540.00	545.83	0.99
105.00	2.50	530.0	344.00	35.65	613.00	647.56	0.95
106.00	3.00	536.0	344.00	33.47	674.00	718.78	0.94
107.00	3.50	542.0	379.80	31.87	835.00	854.21	0.98
107.00	4.00	542.0	379.80	31.87	889.00	934.74	0.95

d (mm)	t (mm)	KL (mm)	F_y (MPa)	f_c' (MPa)	C_a (kN)	C_n (kN)	C_a/C_n
108.00	4.50	548.0	344.00	33.50	917.00	957.05	0.96
108.00	5.00	548.0	379.80	33.50	1084.00	1111.69	0.98
160.00	2.50	960.0	433.20	32.22	1426.00	1283.95	1.11
140.00	2.50	840.0	433.20	38.88	1124.00	1132.85	0.99
140.00	3.00	840.0	426.30	33.06	1208.00	1185.55	1.02
100.00	2.50	600.0	433.20	45.77	750.00	739.41	1.01
100.00	3.00	600.0	426.30	29.13	723.00	732.00	0.99
140.00	5.30	840.0	378.30	21.86	1326.00	1462.89	0.91
140.00	5.00	840.0	378.30	30.58	1379.00	1489.67	0.93
140.00	5.00	840.0	378.30	34.92	1501.00	1532.28	0.98
140.00	5.30	840.0	378.30	51.50	1664.00	1746.53	0.95
140.00	5.00	840.0	378.30	42.25	1539.00	1602.51	0.96
108.00	4.00	540.0	327.10	39.23	836.00	887.66	0.94
108.00	4.00	756.0	337.60	35.33	785.00	834.42	0.94
108.00	4.00	972.0	337.60	33.54	736.00	773.13	0.95
108.00	4.00	1188.0	327.10	34.03	686.00	709.98	0.97
108.00	4.00	1404.0	332.00	33.15	686.00	663.57	1.03
108.00	4.00	1620.0	347.70	33.15	672.00	633.05	1.06
165.20	4.17	1322.0	358.70	40.90	1445.00	1637.88	0.88
165.20	4.17	1982.0	358.70	40.90	1305.00	1435.96	0.91
165.20	4.17	2974.0	358.70	40.90	1180.00	1131.85	1.04
165.20	4.17	3965.0	358.70	40.90	956.00	867.38	1.10
165.20	4.17	4956.0	358.70	40.90	800.00	647.87	1.23
165.00	4.70	2475.0	355.00	26.93	1058.00	1224.86	0.86
165.00	4.70	2476.0	355.00	26.93	1037.00	1224.59	0.85
110.00	1.90	2200.0	350.00	26.93	437.00	335.64	1.30
110.00	1.90	2200.0	350.00	26.93	368.00	335.64	1.10
110.00	1.90	2200.0	350.00	26.93	355.00	335.64	1.06
110.00	1.90	2200.0	350.00	26.93	374.00	335.64	1.11
108.00	4.00	540.0	332.02	40.40	835.90	903.96	0.92
108.00	4.50	485.0	409.64	28.60	1205.40	1091.28	1.10
140.00	5.00	840.0	378.28	45.10	1667.00	1629.16	1.02
140.00	5.50	840.0	333.20	42.90	1379.80	1557.45	0.89
164.00	6.00	1700.0	356.82	31.50	1633.70	1729.02	0.94
95.00	3.50	860.0	348.88	26.20	665.40	576.97	1.15
95.00	3.50	1420.0	348.88	26.20	582.10	464.99	1.25
121.00	4.00	1050.0	311.15	22.20	702.70	780.52	0.90
121.00	4.00	1050.0	317.03	26.50	851.60	823.75	1.03
121.00	6.00	1050.0	349.37	22.20	1007.40	1138.79	0.88
121.00	6.00	1050.0	325.85	26.50	1088.80	1105.31	0.99
216.00	6.00	2220.0	391.02	24.10	2440.20	2513.75	0.97
216.00	6.00	2220.0	379.26	31.40	2865.50	2628.31	1.09
153.00	3.20	1679.0	413.56	21.80	901.60	1030.17	0.88
121.00	4.80	1048.0	449.82	33.90	1146.60	1270.67	0.90
121.00	4.80	1048.0	449.82	29.10	1078.00	1237.55	0.87
121.00	4.80	1048.0	449.82	25.60	940.80	1212.94	0.78

d (mm)	t (mm)	KL (mm)	F_y (MPa)	f_c' (MPa)	C_a (kN)	C_n (kN)	C_a/C_n
318.50	6.90	4200.0	301.84	47.00	5494.90	4635.07	1.19
108.00	4.00	756.0	337.61	36.30	785.00	839.96	0.93
108.00	4.00	972.0	337.61	34.50	737.00	778.49	0.95
108.00	4.00	1404.0	332.02	34.10	686.00	668.34	1.03
108.00	4.00	1620.0	351.23	34.10	637.00	641.06	0.99
140.00	5.00	840.0	378.28	23.10	1283.80	1414.37	0.91
140.00	5.00	840.0	378.28	31.60	1391.60	1499.69	0.93
140.00	5.00	840.0	378.28	45.10	1685.60	1629.16	1.03
108.00	4.00	1188.0	327.12	35.00	686.00	715.17	0.96
169.00	7.50	690.0	360.00	70.80	3080.00	3090.30	1.00
169.00	7.50	690.0	360.00	70.80	4190.00	3090.30	1.36
169.00	7.50	1768.0	360.00	70.80	2870.00	2550.00	1.13
219.00	6.00	1000.0	325.00	58.00	2989.00	3514.47	0.85
219.00	4.00	1000.0	325.00	47.60	1931.00	2677.70	0.72
219.00	4.00	1000.0	325.00	52.30	1980.00	2791.98	0.71
114.30	6.00	571.5	342.95	32.68	1016.60	1245.20	0.82
114.30	6.00	800.0	342.95	32.68	1057.10	1169.20	0.90
114.30	6.00	1143.0	342.95	32.68	872.20	1056.55	0.83
114.30	6.00	571.5	342.95	58.68	1263.20	1396.24	0.90
114.30	6.00	800.0	342.95	58.68	1190.00	1317.55	0.90
114.30	6.00	1143.0	342.95	58.68	1120.60	1196.71	0.94
114.30	6.00	571.5	342.95	73.30	1308.50	1473.83	0.89
114.30	6.00	800.0	342.95	22.50	925.90	1106.48	0.84
114.30	6.00	1143.0	342.95	58.20	1126.90	1194.28	0.94
108.00	4.50	4158.0	348.10	25.51	342.00	242.17	1.41
108.00	4.50	4158.0	348.10	25.51	292.00	242.17	1.21
108.00	4.50	4158.0	348.10	39.11	298.00	251.62	1.18
108.00	4.50	4158.0	348.10	39.11	280.00	251.62	1.11
108.00	4.50	4023.0	348.10	39.11	318.00	266.17	1.19
108.00	4.50	4023.0	348.10	39.11	320.00	266.17	1.20
108.00	4.50	3807.0	348.10	25.51	350.00	279.68	1.25
108.00	4.50	3807.0	348.10	25.51	370.00	279.68	1.32
108.00	4.50	3510.0	348.10	25.51	400.00	316.76	1.26
108.00	4.50	3510.0	348.10	25.51	390.00	316.76	1.23
108.00	4.50	3510.0	348.10	39.11	440.00	331.83	1.33

Appendix Table C-5. Database of tests for concrete-filled CHS members subjected to axial compression in accordance with AISC 360-16

d (mm)	t (mm)	KL (mm)	F_y (MPa)	f_c' (MPa)	C_a (kN)	C_n (kN)	C_a/C_n
140.40	4.93	406.0	302.00	33.20	1824.00	1049.94	1.74
219.10	5.00	600.0	380.00	51.60	3118.00	2940.45	1.06
219.10	10.00	600.0	381.00	51.60	5241.00	4004.65	1.31
219.10	5.00	600.0	380.00	51.60	3118.00	2940.45	1.06
219.10	10.00	600.0	381.00	51.60	5241.00	4004.65	1.31
168.30	2.80	300.0	317.80	37.71	1282.50	1204.27	1.06
159.00	3.00	300.0	336.28	33.39	1185.70	1074.60	1.10
120.00	2.50	300.0	445.52	41.44	879.20	815.22	1.08
100.00	3.00	300.0	432.09	34.04	724.00	614.82	1.18
101.60	3.00	300.0	425.03	34.04	703.30	622.61	1.13
168.30	4.47	813.0	302.00	23.40	1744.00	1121.48	1.56
108.00	4.50	445.0	409.64	28.60	970.20	797.78	1.22
129.00	3.00	387.0	306.00	45.52	1068.00	870.76	1.23
129.00	3.00	387.0	306.00	47.01	1093.00	887.45	1.23
129.00	3.00	387.0	306.00	47.95	1118.00	897.91	1.25
129.00	3.00	387.0	306.00	50.30	1162.00	924.11	1.26
131.00	4.00	393.0	306.00	45.52	1280.00	995.37	1.29
131.00	4.00	393.0	306.00	47.01	1360.00	1012.08	1.34
131.00	4.00	393.0	306.00	47.95	1403.00	1022.54	1.37
131.00	4.00	393.0	306.00	50.30	1459.00	1048.77	1.39
133.00	5.00	399.0	306.00	45.52	1454.00	1121.79	1.30
133.00	5.00	399.0	306.00	47.01	1470.00	1138.51	1.29
133.00	5.00	399.0	306.00	47.95	1518.00	1148.98	1.32
133.00	5.00	399.0	306.00	50.30	1569.00	1175.22	1.34
129.00	3.00	387.0	306.00	52.28	1095.00	946.19	1.16
129.00	3.00	387.0	306.00	53.70	1128.00	962.01	1.17
129.00	3.00	387.0	306.00	55.22	1147.00	978.91	1.17
129.00	3.00	387.0	306.00	57.31	1192.00	1002.22	1.19
131.00	4.00	393.0	306.00	52.28	1320.00	1070.88	1.23
131.00	4.00	393.0	306.00	53.70	1389.00	1086.71	1.28
131.00	4.00	393.0	306.00	55.22	1430.00	1103.64	1.30
131.00	4.00	393.0	306.00	57.31	1452.00	1126.96	1.29
133.00	5.00	399.0	306.00	52.28	1548.00	1197.35	1.29
133.00	5.00	399.0	306.00	53.70	1581.00	1213.19	1.30
133.00	5.00	399.0	306.00	55.22	1609.00	1230.12	1.31
133.00	5.00	399.0	306.00	57.31	1661.00	1253.47	1.33
129.00	3.00	387.0	306.00	60.66	1266.00	1039.42	1.22
129.00	3.00	387.0	306.00	62.48	1287.00	1059.69	1.21
129.00	3.00	387.0	306.00	65.36	1301.00	1091.77	1.19
129.00	3.00	387.0	306.00	67.10	1356.00	1111.07	1.22
131.00	4.00	393.0	306.00	60.66	1469.00	1164.21	1.26
131.00	4.00	393.0	306.00	62.48	1482.00	1184.50	1.25
131.00	4.00	393.0	306.00	65.36	1496.00	1216.63	1.23
131.00	4.00	393.0	306.00	67.10	1542.00	1235.96	1.25

d (mm)	t (mm)	KL (mm)	F_y (MPa)	f_c' (MPa)	C_a (kN)	C_n (kN)	C_a/C_n
133.00	5.00	399.0	306.00	60.66	1659.00	1290.75	1.29
133.00	5.00	399.0	306.00	62.48	1673.00	1311.05	1.28
133.00	5.00	399.0	306.00	65.36	1712.00	1343.21	1.27
133.00	5.00	399.0	306.00	67.10	1774.00	1362.55	1.30
169.30	2.62	1830.0	338.10	37.10	756.00	1088.85	0.69
169.30	2.62	1830.0	338.10	34.10	689.00	1038.16	0.66
168.80	5.00	2135.0	302.40	33.40	1130.00	1262.74	0.89
168.80	5.00	2135.0	302.40	27.80	1165.00	1174.58	0.99
200.00	3.00	2000.0	303.50	46.80	1830.00	1708.31	1.07
200.00	3.00	2001.0	303.50	46.80	1806.00	1708.15	1.06
200.00	3.00	2002.0	303.50	46.80	1882.00	1707.99	1.10
200.00	3.00	2003.0	303.50	46.80	2060.00	1707.83	1.21
200.00	3.00	2004.0	303.50	46.80	2115.00	1707.66	1.24
95.00	3.66	860.0	332.00	25.30	656.00	468.57	1.40
95.00	3.68	860.0	392.00	25.30	686.00	526.76	1.30
95.00	3.40	860.0	340.00	25.30	656.00	454.44	1.44
95.00	3.86	1420.0	332.00	25.30	567.00	442.69	1.28
95.00	3.91	1420.0	392.00	25.30	606.00	495.20	1.22
95.00	3.58	1420.0	340.00	25.30	576.00	428.09	1.35
95.00	3.76	1980.0	332.00	25.30	536.00	380.45	1.41
95.00	3.78	1980.0	392.00	25.30	567.00	415.78	1.36
95.00	3.51	1980.0	340.00	25.30	488.00	368.27	1.33
216.00	4.11	2220.0	304.00	23.20	1834.00	1472.23	1.25
216.00	6.05	2220.0	395.00	23.20	2462.00	2125.01	1.16
216.00	5.97	2220.0	399.00	23.20	2421.00	2120.56	1.14
216.00	6.30	2220.0	411.00	30.20	2932.00	2427.10	1.21
95.00	3.86	1980.0	337.00	24.40	498.00	386.60	1.29
95.00	3.40	1980.0	343.00	24.40	473.00	359.05	1.32
95.00	3.58	1980.0	360.00	24.40	473.00	380.82	1.24
95.00	3.73	1980.0	332.00	24.40	413.00	375.30	1.10
121.00	3.73	1050.0	333.00	21.40	746.00	632.45	1.18
121.00	3.76	1050.0	313.00	24.60	837.00	638.95	1.31
121.00	3.99	1050.0	332.00	24.60	867.00	687.11	1.26
121.00	5.61	1050.0	349.00	21.40	998.00	858.96	1.16
121.00	5.41	1050.0	348.00	21.40	1018.00	835.65	1.22
121.00	5.46	1050.0	336.00	24.60	1099.00	846.22	1.30
121.00	5.56	1050.0	327.00	24.60	1079.00	840.02	1.28
121.00	3.76	2310.0	333.00	21.40	629.00	529.08	1.19
121.00	3.71	2310.0	313.00	24.60	695.00	528.68	1.31
121.00	3.86	2310.0	332.00	24.60	755.00	558.11	1.35
121.00	5.69	2310.0	349.00	21.40	786.00	718.35	1.09
121.00	5.49	2310.0	348.00	21.40	816.00	699.67	1.17
121.00	5.64	2310.0	336.00	24.60	874.00	717.40	1.22
121.00	5.44	2310.0	327.00	24.60	865.00	689.79	1.25
114.30	3.18	914.0	420.00	29.40	712.00	685.09	1.04
114.30	3.18	914.0	420.00	29.40	756.00	685.09	1.10

d (mm)	t (mm)	KL (mm)	F_y (MPa)	f_c' (MPa)	C_a (kN)	C_n (kN)	C_a/C_n
355.60	11.18	1880.0	361.00	38.60	11460.00	7401.99	1.55
355.60	11.18	1880.0	361.00	33.30	10710.00	6978.05	1.53
355.60	7.98	2083.0	361.00	23.80	7433.00	5066.24	1.47
127.30	1.63	711.0	376.00	67.20	1285.00	974.00	1.32
127.30	1.63	711.0	334.00	67.20	1285.00	949.03	1.35
127.10	2.95	711.0	376.00	67.20	1305.00	1131.57	1.15
127.10	2.95	711.0	334.00	67.20	1305.00	1086.26	1.20
168.20	4.52	813.0	302.00	31.90	2006.00	1283.99	1.56
168.40	4.52	813.0	302.00	43.80	2233.00	1505.48	1.48
168.20	4.52	813.0	302.00	43.80	2113.00	1502.54	1.41
88.90	5.84	1727.0	406.00	41.50	614.70	594.75	1.03
88.90	5.84	1422.0	406.00	41.50	711.70	655.26	1.09
88.90	5.84	1118.0	406.00	41.50	715.20	708.33	1.01
88.90	5.84	813.0	406.00	41.50	918.50	751.69	1.22
88.90	5.84	508.0	406.00	41.50	991.90	782.87	1.27
88.90	5.84	508.0	406.00	41.50	889.60	782.87	1.14
108.00	4.50	4158.0	348.10	25.40	342.00	250.69	1.36
108.00	4.50	4158.0	348.10	25.40	292.00	250.69	1.16
108.00	4.50	4158.0	348.10	37.40	298.00	262.24	1.14
108.00	4.50	4158.0	348.10	37.40	280.00	262.24	1.07
108.00	4.50	4023.0	348.10	37.40	318.00	280.14	1.14
108.00	4.50	4023.0	348.10	37.40	320.00	280.14	1.14
108.00	4.50	3807.0	348.10	25.40	350.00	296.14	1.18
108.00	4.50	3807.0	348.10	25.40	370.00	296.14	1.25
108.00	4.50	3510.0	348.10	25.40	400.00	336.56	1.19
108.00	4.50	3510.0	348.10	25.40	390.00	336.56	1.16
108.00	4.50	3510.0	348.10	37.40	440.00	358.56	1.23
114.00	4.44	850.0	332.00	37.00	902.00	780.71	1.16
114.00	4.49	2750.0	332.00	31.00	657.00	514.59	1.28
215.90	6.00	2220.0	392.00	22.90	2442.00	2088.67	1.17
215.90	6.00	2220.0	350.00	30.00	2869.00	2141.02	1.34
120.90	3.76	1050.0	312.00	21.10	721.00	604.86	1.19
120.90	3.76	2310.0	312.00	21.10	636.00	504.58	1.26
120.90	5.53	1050.0	343.00	21.10	1010.00	834.50	1.21
120.90	5.53	1050.0	343.00	24.20	1090.00	860.23	1.27
95.00	3.65	1370.0	350.00	25.00	667.00	442.24	1.51
95.00	3.65	1420.0	350.00	25.00	583.00	437.57	1.33
95.00	3.65	1980.0	350.00	25.00	529.00	378.59	1.40
165.00	4.30	2440.0	317.70	43.30	1149.00	1242.83	0.92
160.00	4.50	2420.0	317.70	43.30	1561.00	1199.79	1.30
165.00	4.30	3640.0	317.70	43.30	987.00	1003.41	0.98
166.00	5.00	870.0	313.60	42.24	1827.70	1527.93	1.20
166.00	5.00	1700.0	313.60	42.24	1460.20	1440.85	1.01
108.00	4.00	648.0	338.88	28.99	825.16	642.97	1.28
108.00	4.00	648.0	338.88	28.99	828.10	642.97	1.29
108.00	4.00	864.0	338.88	28.99	766.36	630.63	1.22

d (mm)	t (mm)	KL (mm)	F_y (MPa)	f_c' (MPa)	C_a (kN)	C_n (kN)	C_a/C_n
108.00	4.00	864.0	338.88	28.99	801.64	630.63	1.27
108.00	4.00	864.0	338.88	28.99	869.26	630.63	1.38
108.00	4.00	1080.0	338.88	28.99	836.92	615.12	1.36
108.00	4.00	1080.0	338.88	28.99	783.02	615.12	1.27
108.00	4.00	1620.0	338.88	28.99	707.56	564.15	1.25
108.00	4.00	1620.0	338.88	28.99	646.80	564.15	1.15
108.00	4.00	1620.0	338.88	28.99	643.86	564.15	1.14
108.00	4.00	2160.0	338.88	28.99	672.28	499.81	1.35
108.00	4.00	2160.0	338.88	28.99	697.76	499.81	1.40
108.00	4.00	2160.0	338.88	28.99	676.20	499.81	1.35
108.00	4.00	2700.0	338.88	28.99	648.76	427.75	1.52
108.00	4.00	3240.0	338.88	28.99	559.58	353.63	1.58
108.00	4.00	3240.0	338.88	28.99	478.24	353.63	1.35
108.00	4.00	3240.0	338.88	28.99	600.74	353.63	1.70
108.00	4.00	4320.0	338.88	28.99	373.38	218.56	1.71
108.00	4.00	4320.0	338.88	28.99	345.94	218.56	1.58
108.00	4.00	4320.0	338.88	28.99	294.00	218.56	1.35
108.00	4.00	5400.0	338.88	28.99	225.40	139.88	1.61
108.00	4.00	5400.0	338.88	28.99	210.70	139.88	1.51
108.00	4.00	5560.0	338.88	28.99	212.50	131.94	1.61
104.00	2.00	524.0	344.00	32.65	540.00	454.63	1.19
105.00	2.50	530.0	344.00	35.65	613.00	532.05	1.15
106.00	3.00	536.0	344.00	33.47	674.00	572.55	1.18
107.00	3.50	542.0	379.80	31.87	835.00	656.88	1.27
107.00	4.00	542.0	379.80	31.87	889.00	710.64	1.25
108.00	4.50	548.0	344.00	33.50	917.00	734.65	1.25
108.00	5.00	548.0	379.80	33.50	1084.00	837.78	1.29
160.00	2.50	960.0	433.20	32.22	1426.00	1076.31	1.32
140.00	2.50	840.0	433.20	38.88	1124.00	962.17	1.17
140.00	3.00	840.0	426.30	33.06	1208.00	962.07	1.26
100.00	2.50	600.0	433.20	45.77	750.00	618.27	1.21
100.00	3.00	600.0	426.30	29.13	723.00	564.74	1.28
140.00	5.30	840.0	378.30	21.86	1326.00	1093.14	1.21
140.00	5.00	840.0	378.30	30.58	1379.00	1155.92	1.19
140.00	5.00	840.0	378.30	34.92	1501.00	1208.26	1.24
140.00	5.30	840.0	378.30	51.50	1664.00	1447.00	1.15
140.00	5.00	840.0	378.30	42.25	1539.00	1296.47	1.19
108.00	4.00	540.0	327.10	39.23	836.00	707.23	1.18
108.00	4.00	756.0	337.60	35.33	785.00	680.35	1.15
108.00	4.00	972.0	337.60	33.54	736.00	652.69	1.13
108.00	4.00	1188.0	327.10	34.03	686.00	626.00	1.10
108.00	4.00	1404.0	332.00	33.15	686.00	604.93	1.13
108.00	4.00	1620.0	347.70	33.15	672.00	596.24	1.13
165.20	4.17	1322.0	358.70	40.90	1445.00	1428.89	1.01
165.20	4.17	1982.0	358.70	40.90	1305.00	1336.45	0.98
165.20	4.17	2974.0	358.70	40.90	1180.00	1149.39	1.03

d (mm)	t (mm)	KL (mm)	F_y (MPa)	f_c' (MPa)	C_a (kN)	C_n (kN)	C_a/C_n
165.20	4.17	3965.0	358.70	40.90	956.00	930.84	1.03
165.20	4.17	4956.0	358.70	40.90	800.00	709.78	1.13
165.00	4.70	2475.0	355.00	26.93	1058.00	1143.44	0.93
165.00	4.70	2476.0	355.00	26.93	1037.00	1143.30	0.91
110.00	1.90	2200.0	350.00	26.93	437.00	336.78	1.30
110.00	1.90	2200.0	350.00	26.93	368.00	336.78	1.09
110.00	1.90	2200.0	350.00	26.93	355.00	336.78	1.05
110.00	1.90	2200.0	350.00	26.93	374.00	336.78	1.11
108.00	4.00	540.0	332.02	40.40	835.90	721.90	1.16
108.00	4.50	485.0	409.64	28.60	1205.40	795.78	1.51
140.00	5.00	840.0	378.28	45.10	1667.00	1330.67	1.25
140.00	5.50	840.0	333.20	42.90	1379.80	1272.42	1.08
164.00	6.00	1700.0	356.82	31.50	1633.70	1484.64	1.10
95.00	3.50	860.0	348.88	26.20	665.40	474.67	1.40
95.00	3.50	1420.0	348.88	26.20	582.10	430.36	1.35
121.00	4.00	1050.0	311.15	22.20	702.70	638.14	1.10
121.00	4.00	1050.0	317.03	26.50	851.60	683.82	1.25
121.00	6.00	1050.0	349.37	22.20	1007.40	906.29	1.11
121.00	6.00	1050.0	325.85	26.50	1088.80	895.39	1.22
216.00	6.00	2220.0	391.02	24.10	2440.20	2119.67	1.15
216.00	6.00	2220.0	379.26	31.40	2865.50	2278.93	1.26
153.00	3.20	1679.0	413.56	21.80	901.60	883.83	1.02
121.00	4.80	1048.0	449.82	33.90	1146.60	1033.00	1.11
121.00	4.80	1048.0	449.82	29.10	1078.00	992.76	1.09
121.00	4.80	1048.0	449.82	25.60	940.80	963.32	0.98
318.50	6.90	4200.0	301.84	47.00	5494.90	4565.49	1.20
108.00	4.00	756.0	337.61	36.30	785.00	687.18	1.14
108.00	4.00	972.0	337.61	34.50	737.00	659.21	1.12
108.00	4.00	1404.0	332.02	34.10	686.00	610.76	1.12
108.00	4.00	1620.0	351.23	34.10	637.00	604.91	1.05
140.00	5.00	840.0	378.28	23.10	1283.80	1065.46	1.20
140.00	5.00	840.0	378.28	31.60	1391.60	1168.19	1.19
140.00	5.00	840.0	378.28	45.10	1685.60	1330.67	1.27
108.00	4.00	1188.0	327.12	35.00	686.00	632.31	1.08
219.00	6.00	1000.0	325.00	58.00	2989.00	3100.42	0.96
219.00	4.00	1000.0	325.00	47.60	1931.00	2411.51	0.80
219.00	4.00	1000.0	325.00	52.30	1980.00	2562.49	0.77
114.30	6.00	571.5	342.95	32.68	1016.60	938.36	1.08
114.30	6.00	800.0	342.95	32.68	1057.10	922.40	1.15
114.30	6.00	1143.0	342.95	32.68	872.20	889.37	0.98
114.30	6.00	571.5	342.95	58.68	1263.20	1134.95	1.11
114.30	6.00	800.0	342.95	58.68	1190.00	1112.99	1.07
114.30	6.00	1143.0	342.95	58.68	1120.60	1067.69	1.05
114.30	6.00	800.0	342.95	22.50	925.90	847.21	1.09
114.30	6.00	1143.0	342.95	58.20	1126.90	1064.43	1.06
108.00	4.50	4158.0	348.10	25.51	342.00	252.76	1.35

d (mm)	t (mm)	KL (mm)	F_y (MPa)	f_c' (MPa)	C_a (kN)	C_n (kN)	C_a/C_n
108.00	4.50	4158.0	348.10	25.51	292.00	252.76	1.16
108.00	4.50	4158.0	348.10	39.11	298.00	265.69	1.12
108.00	4.50	4158.0	348.10	39.11	280.00	265.69	1.05
108.00	4.50	4023.0	348.10	39.11	318.00	283.82	1.12
108.00	4.50	4023.0	348.10	39.11	320.00	283.82	1.13
108.00	4.50	3807.0	348.10	25.51	350.00	298.28	1.17
108.00	4.50	3807.0	348.10	25.51	370.00	298.28	1.24
108.00	4.50	3510.0	348.10	25.51	400.00	338.67	1.18
108.00	4.50	3510.0	348.10	25.51	390.00	338.67	1.15
108.00	4.50	3510.0	348.10	39.11	440.00	363.49	1.21

Appendix Table C-6. Database of tests for concrete-filled CHS members subjected to axial compression in accordance with Tousignant & Packer (2022a,b)

d (mm)	t (mm)	KL (mm)	F_y (MPa)	f_c' (MPa)	C_a (kN)	C_n (kN)	C_a/C_n
140.40	4.93	406.0	302.00	33.20	1824.00	1392.16	1.31
219.10	5.00	600.0	380.00	51.60	3118.00	3514.99	0.89
219.10	10.00	600.0	381.00	51.60	5241.00	5283.56	0.99
219.10	5.00	600.0	380.00	51.60	3118.00	3514.99	0.89
219.10	10.00	600.0	381.00	51.60	5241.00	5283.56	0.99
168.30	2.80	300.0	317.80	37.71	1282.50	1436.04	0.89
159.00	3.00	300.0	336.28	33.39	1185.70	1354.20	0.88
120.00	2.50	300.0	445.52	41.44	879.20	1038.14	0.85
100.00	3.00	300.0	432.09	34.04	724.00	837.78	0.86
101.60	3.00	300.0	425.03	34.04	703.30	845.86	0.83
168.30	4.47	813.0	302.00	23.40	1744.00	1452.18	1.20
108.00	4.50	445.0	409.64	28.60	970.20	1104.15	0.88
129.00	3.00	387.0	306.00	45.52	1068.00	1026.68	1.04
129.00	3.00	387.0	306.00	47.01	1093.00	1039.31	1.05
129.00	3.00	387.0	306.00	47.95	1118.00	1047.18	1.07
129.00	3.00	387.0	306.00	50.30	1162.00	1066.79	1.09
131.00	4.00	393.0	306.00	45.52	1280.00	1224.58	1.05
131.00	4.00	393.0	306.00	47.01	1360.00	1237.21	1.10
131.00	4.00	393.0	306.00	47.95	1403.00	1245.09	1.13
131.00	4.00	393.0	306.00	50.30	1459.00	1264.69	1.15
133.00	5.00	399.0	306.00	45.52	1454.00	1420.97	1.02
133.00	5.00	399.0	306.00	47.01	1470.00	1433.60	1.03
133.00	5.00	399.0	306.00	47.95	1518.00	1441.48	1.05
133.00	5.00	399.0	306.00	50.30	1569.00	1461.08	1.07
129.00	3.00	387.0	306.00	52.28	1095.00	1083.16	1.01
129.00	3.00	387.0	306.00	53.70	1128.00	1094.80	1.03
129.00	3.00	387.0	306.00	55.22	1147.00	1107.16	1.04
129.00	3.00	387.0	306.00	57.31	1192.00	1124.07	1.06
131.00	4.00	393.0	306.00	52.28	1320.00	1281.06	1.03
131.00	4.00	393.0	306.00	53.70	1389.00	1292.70	1.07
131.00	4.00	393.0	306.00	55.22	1430.00	1305.07	1.10
131.00	4.00	393.0	306.00	57.31	1452.00	1321.98	1.10
133.00	5.00	399.0	306.00	52.28	1548.00	1477.45	1.05
133.00	5.00	399.0	306.00	53.70	1581.00	1489.09	1.06
133.00	5.00	399.0	306.00	55.22	1609.00	1501.46	1.07
133.00	5.00	399.0	306.00	57.31	1661.00	1518.37	1.09
129.00	3.00	387.0	306.00	60.66	1266.00	1150.76	1.10
129.00	3.00	387.0	306.00	62.48	1287.00	1165.13	1.10
129.00	3.00	387.0	306.00	65.36	1301.00	1187.65	1.10
129.00	3.00	387.0	306.00	67.10	1356.00	1201.06	1.13
131.00	4.00	393.0	306.00	60.66	1469.00	1348.67	1.09
131.00	4.00	393.0	306.00	62.48	1482.00	1363.04	1.09
131.00	4.00	393.0	306.00	65.36	1496.00	1385.56	1.08
131.00	4.00	393.0	306.00	67.10	1542.00	1398.97	1.10
133.00	5.00	399.0	306.00	60.66	1659.00	1545.06	1.07
133.00	5.00	399.0	306.00	62.48	1673.00	1559.44	1.07
133.00	5.00	399.0	306.00	65.36	1712.00	1581.96	1.08
133.00	5.00	399.0	306.00	67.10	1774.00	1595.37	1.11

d (mm)	t (mm)	KL (mm)	F_y (MPa)	f_c' (MPa)	C_a (kN)	C_n (kN)	C_a/C_n
169.30	2.62	1830.0	338.10	37.10	756.00	1154.01	0.66
169.30	2.62	1830.0	338.10	34.10	689.00	1111.56	0.62
168.80	5.00	2135.0	302.40	33.40	1130.00	1366.89	0.83
168.80	5.00	2135.0	302.40	27.80	1165.00	1292.85	0.90
200.00	3.00	2000.0	303.50	46.80	1830.00	1744.84	1.05
200.00	3.00	2001.0	303.50	46.80	1806.00	1744.61	1.04
200.00	3.00	2002.0	303.50	46.80	1882.00	1744.38	1.08
200.00	3.00	2003.0	303.50	46.80	2060.00	1744.14	1.18
200.00	3.00	2004.0	303.50	46.80	2115.00	1743.91	1.21
95.00	3.66	860.0	332.00	25.30	656.00	569.82	1.15
95.00	3.68	860.0	392.00	25.30	686.00	649.90	1.06
95.00	3.40	860.0	340.00	25.30	656.00	551.68	1.19
95.00	3.86	1420.0	332.00	25.30	567.00	480.50	1.18
95.00	3.91	1420.0	392.00	25.30	606.00	540.37	1.12
95.00	3.58	1420.0	340.00	25.30	576.00	463.81	1.24
95.00	3.76	1980.0	332.00	25.30	536.00	381.78	1.40
95.00	3.78	1980.0	392.00	25.30	567.00	415.25	1.37
95.00	3.51	1980.0	340.00	25.30	488.00	368.83	1.32
216.00	4.11	2220.0	304.00	23.20	1834.00	1665.54	1.10
216.00	6.05	2220.0	395.00	23.20	2462.00	2530.82	0.97
216.00	5.97	2220.0	399.00	23.20	2421.00	2525.80	0.96
216.00	6.30	2220.0	411.00	30.20	2932.00	2839.24	1.03
95.00	3.86	1980.0	337.00	24.40	498.00	389.04	1.28
95.00	3.40	1980.0	343.00	24.40	473.00	360.12	1.31
95.00	3.58	1980.0	360.00	24.40	473.00	381.74	1.24
95.00	3.73	1980.0	332.00	24.40	413.00	377.25	1.09
121.00	3.73	1050.0	333.00	21.40	746.00	777.54	0.96
121.00	3.76	1050.0	313.00	24.60	837.00	770.77	1.09
121.00	3.99	1050.0	332.00	24.60	867.00	837.12	1.04
121.00	5.61	1050.0	349.00	21.40	998.00	1079.48	0.92
121.00	5.41	1050.0	348.00	21.40	1018.00	1048.89	0.97
121.00	5.46	1050.0	336.00	24.60	1099.00	1048.96	1.05
121.00	5.56	1050.0	327.00	24.60	1079.00	1039.66	1.04
121.00	3.76	2310.0	333.00	21.40	629.00	543.13	1.16
121.00	3.71	2310.0	313.00	24.60	695.00	538.15	1.29
121.00	3.86	2310.0	332.00	24.60	755.00	568.68	1.33
121.00	5.69	2310.0	349.00	21.40	786.00	744.08	1.06
121.00	5.49	2310.0	348.00	21.40	816.00	723.98	1.13
121.00	5.64	2310.0	336.00	24.60	874.00	738.68	1.18
121.00	5.44	2310.0	327.00	24.60	865.00	709.45	1.22
114.30	3.18	914.0	420.00	29.40	712.00	842.27	0.85
114.30	3.18	914.0	420.00	29.40	756.00	842.27	0.90
355.60	11.18	1880.0	361.00	38.60	11460.00	9221.65	1.24
355.60	11.18	1880.0	361.00	33.30	10710.00	8882.06	1.21
355.60	7.98	2083.0	361.00	23.80	7433.00	6438.05	1.15
127.30	1.63	711.0	376.00	67.20	1285.00	971.91	1.32
127.30	1.63	711.0	334.00	67.20	1285.00	931.32	1.38
127.10	2.95	711.0	376.00	67.20	1305.00	1225.82	1.06
127.10	2.95	711.0	334.00	67.20	1305.00	1154.20	1.13
168.20	4.52	813.0	302.00	31.90	2006.00	1590.59	1.26

d (mm)	t (mm)	KL (mm)	F_y (MPa)	f_c' (MPa)	C_a (kN)	C_n (kN)	C_a/C_n
168.40	4.52	813.0	302.00	43.80	2233.00	1767.18	1.26
168.20	4.52	813.0	302.00	43.80	2113.00	1763.85	1.20
88.90	5.84	1727.0	406.00	41.50	614.70	601.12	1.02
88.90	5.84	1422.0	406.00	41.50	711.70	695.27	1.02
88.90	5.84	1118.0	406.00	41.50	715.20	799.40	0.89
88.90	5.84	813.0	406.00	41.50	918.50	909.78	1.01
88.90	5.84	508.0	406.00	41.50	991.90	1021.21	0.97
88.90	5.84	508.0	406.00	41.50	889.60	1021.21	0.87
108.00	4.50	4158.0	348.10	25.40	342.00	240.38	1.42
108.00	4.50	4158.0	348.10	25.40	292.00	240.38	1.21
108.00	4.50	4158.0	348.10	37.40	298.00	248.77	1.20
108.00	4.50	4158.0	348.10	37.40	280.00	248.77	1.13
108.00	4.50	4023.0	348.10	37.40	318.00	263.15	1.21
108.00	4.50	4023.0	348.10	37.40	320.00	263.15	1.22
108.00	4.50	3807.0	348.10	25.40	350.00	277.71	1.26
108.00	4.50	3807.0	348.10	25.40	370.00	277.71	1.33
108.00	4.50	3510.0	348.10	25.40	400.00	314.65	1.27
108.00	4.50	3510.0	348.10	25.40	390.00	314.65	1.24
108.00	4.50	3510.0	348.10	37.40	440.00	328.02	1.34
114.00	4.44	850.0	332.00	37.00	902.00	945.23	0.95
114.00	4.49	2750.0	332.00	31.00	657.00	495.43	1.33
215.90	6.00	2220.0	392.00	22.90	2442.00	2488.12	0.98
215.90	6.00	2220.0	350.00	30.00	2869.00	2461.91	1.17
120.90	3.76	1050.0	312.00	21.10	721.00	740.58	0.97
120.90	3.76	2310.0	312.00	21.10	636.00	517.35	1.23
120.90	5.53	1050.0	343.00	21.10	1010.00	1048.36	0.96
120.90	5.53	1050.0	343.00	24.20	1090.00	1070.35	1.02
95.00	3.65	1370.0	350.00	25.00	667.00	484.42	1.38
95.00	3.65	1420.0	350.00	25.00	583.00	474.76	1.23
95.00	3.65	1980.0	350.00	25.00	529.00	378.14	1.40
165.00	4.30	2440.0	317.70	43.30	1149.00	1265.64	0.91
160.00	4.50	2420.0	317.70	43.30	1561.00	1220.88	1.28
165.00	4.30	3640.0	317.70	43.30	987.00	943.93	1.05
166.00	5.00	870.0	313.60	42.24	1827.70	1830.35	1.00
166.00	5.00	1700.0	313.60	42.24	1460.20	1586.25	0.92
108.00	4.00	648.0	338.88	28.99	825.16	825.50	1.00
108.00	4.00	648.0	338.88	28.99	828.10	825.50	1.00
108.00	4.00	864.0	338.88	28.99	766.36	774.75	0.99
108.00	4.00	864.0	338.88	28.99	801.64	774.75	1.03
108.00	4.00	864.0	338.88	28.99	869.26	774.75	1.12
108.00	4.00	1080.0	338.88	28.99	836.92	724.52	1.16
108.00	4.00	1080.0	338.88	28.99	783.02	724.52	1.08
108.00	4.00	1620.0	338.88	28.99	707.56	604.36	1.17
108.00	4.00	1620.0	338.88	28.99	646.80	604.36	1.07
108.00	4.00	1620.0	338.88	28.99	643.86	604.36	1.07
108.00	4.00	2160.0	338.88	28.99	672.28	499.09	1.35
108.00	4.00	2160.0	338.88	28.99	697.76	499.09	1.40
108.00	4.00	2160.0	338.88	28.99	676.20	499.09	1.35
108.00	4.00	2700.0	338.88	28.99	648.76	411.10	1.58
108.00	4.00	3240.0	338.88	28.99	559.58	329.02	1.70

d (mm)	t (mm)	KL (mm)	F_y (MPa)	f_c' (MPa)	C_a (kN)	C_n (kN)	C_a/C_n
108.00	4.00	3240.0	338.88	28.99	478.24	329.02	1.45
108.00	4.00	3240.0	338.88	28.99	600.74	329.02	1.83
108.00	4.00	4320.0	338.88	28.99	373.38	209.84	1.78
108.00	4.00	4320.0	338.88	28.99	345.94	209.84	1.65
108.00	4.00	4320.0	338.88	28.99	294.00	209.84	1.40
108.00	4.00	5400.0	338.88	28.99	225.40	140.42	1.61
108.00	4.00	5400.0	338.88	28.99	210.70	140.42	1.50
108.00	4.00	5560.0	338.88	28.99	212.50	132.95	1.60
104.00	2.00	524.0	344.00	32.65	540.00	545.83	0.99
105.00	2.50	530.0	344.00	35.65	613.00	647.56	0.95
106.00	3.00	536.0	344.00	33.47	674.00	718.78	0.94
107.00	3.50	542.0	379.80	31.87	835.00	854.21	0.98
107.00	4.00	542.0	379.80	31.87	889.00	934.74	0.95
108.00	4.50	548.0	344.00	33.50	917.00	957.05	0.96
108.00	5.00	548.0	379.80	33.50	1084.00	1111.69	0.98
160.00	2.50	960.0	433.20	32.22	1426.00	1283.95	1.11
140.00	2.50	840.0	433.20	38.88	1124.00	1132.85	0.99
140.00	3.00	840.0	426.30	33.06	1208.00	1185.55	1.02
100.00	2.50	600.0	433.20	45.77	750.00	739.41	1.01
100.00	3.00	600.0	426.30	29.13	723.00	732.00	0.99
140.00	5.30	840.0	378.30	21.86	1326.00	1462.89	0.91
140.00	5.00	840.0	378.30	30.58	1379.00	1489.67	0.93
140.00	5.00	840.0	378.30	34.92	1501.00	1532.28	0.98
140.00	5.30	840.0	378.30	51.50	1664.00	1746.53	0.95
140.00	5.00	840.0	378.30	42.25	1539.00	1602.51	0.96
108.00	4.00	540.0	327.10	39.23	836.00	887.66	0.94
108.00	4.00	756.0	337.60	35.33	785.00	834.42	0.94
108.00	4.00	972.0	337.60	33.54	736.00	773.13	0.95
108.00	4.00	1188.0	327.10	34.03	686.00	709.98	0.97
108.00	4.00	1404.0	332.00	33.15	686.00	663.57	1.03
108.00	4.00	1620.0	347.70	33.15	672.00	633.05	1.06
165.20	4.17	1322.0	358.70	40.90	1445.00	1637.88	0.88
165.20	4.17	1982.0	358.70	40.90	1305.00	1435.96	0.91
165.20	4.17	2974.0	358.70	40.90	1180.00	1131.85	1.04
165.20	4.17	3965.0	358.70	40.90	956.00	867.38	1.10
165.20	4.17	4956.0	358.70	40.90	800.00	647.87	1.23
165.00	4.70	2475.0	355.00	26.93	1058.00	1224.86	0.86
165.00	4.70	2476.0	355.00	26.93	1037.00	1224.59	0.85
110.00	1.90	2200.0	350.00	26.93	437.00	335.64	1.30
110.00	1.90	2200.0	350.00	26.93	368.00	335.64	1.10
110.00	1.90	2200.0	350.00	26.93	355.00	335.64	1.06
110.00	1.90	2200.0	350.00	26.93	374.00	335.64	1.11
108.00	4.00	540.0	332.02	40.40	835.90	903.96	0.92
108.00	4.50	485.0	409.64	28.60	1205.40	1091.28	1.10
140.00	5.00	840.0	378.28	45.10	1667.00	1629.16	1.02
140.00	5.50	840.0	333.20	42.90	1379.80	1557.45	0.89
164.00	6.00	1700.0	356.82	31.50	1633.70	1729.02	0.94
95.00	3.50	860.0	348.88	26.20	665.40	576.97	1.15
95.00	3.50	1420.0	348.88	26.20	582.10	464.99	1.25
121.00	4.00	1050.0	311.15	22.20	702.70	780.52	0.90

d (mm)	t (mm)	KL (mm)	F_y (MPa)	f_c' (MPa)	C_a (kN)	C_n (kN)	C_a/C_n
121.00	4.00	1050.0	317.03	26.50	851.60	823.75	1.03
121.00	6.00	1050.0	349.37	22.20	1007.40	1138.79	0.88
121.00	6.00	1050.0	325.85	26.50	1088.80	1105.31	0.99
216.00	6.00	2220.0	391.02	24.10	2440.20	2513.75	0.97
216.00	6.00	2220.0	379.26	31.40	2865.50	2628.31	1.09
153.00	3.20	1679.0	413.56	21.80	901.60	1030.17	0.88
121.00	4.80	1048.0	449.82	33.90	1146.60	1270.67	0.90
121.00	4.80	1048.0	449.82	29.10	1078.00	1237.55	0.87
121.00	4.80	1048.0	449.82	25.60	940.80	1212.94	0.78
318.50	6.90	4200.0	301.84	47.00	5494.90	4635.07	1.19
108.00	4.00	756.0	337.61	36.30	785.00	839.96	0.93
108.00	4.00	972.0	337.61	34.50	737.00	778.49	0.95
108.00	4.00	1404.0	332.02	34.10	686.00	668.34	1.03
108.00	4.00	1620.0	351.23	34.10	637.00	641.06	0.99
140.00	5.00	840.0	378.28	23.10	1283.80	1414.37	0.91
140.00	5.00	840.0	378.28	31.60	1391.60	1499.69	0.93
140.00	5.00	840.0	378.28	45.10	1685.60	1629.16	1.03
108.00	4.00	1188.0	327.12	35.00	686.00	715.17	0.96
219.00	6.00	1000.0	325.00	58.00	2989.00	3514.47	0.85
219.00	4.00	1000.0	325.00	47.60	1931.00	2677.70	0.72
219.00	4.00	1000.0	325.00	52.30	1980.00	2791.98	0.71
114.30	6.00	571.5	342.95	32.68	1016.60	1245.20	0.82
114.30	6.00	800.0	342.95	32.68	1057.10	1169.20	0.90
114.30	6.00	1143.0	342.95	32.68	872.20	1056.55	0.83
114.30	6.00	571.5	342.95	58.68	1263.20	1396.24	0.90
114.30	6.00	800.0	342.95	58.68	1190.00	1317.55	0.90
114.30	6.00	1143.0	342.95	58.68	1120.60	1196.71	0.94
114.30	6.00	800.0	342.95	22.50	925.90	1106.48	0.84
114.30	6.00	1143.0	342.95	58.20	1126.90	1194.28	0.94
108.00	4.50	4158.0	348.10	25.51	342.00	242.17	1.41
108.00	4.50	4158.0	348.10	25.51	292.00	242.17	1.21
108.00	4.50	4158.0	348.10	39.11	298.00	251.62	1.18
108.00	4.50	4158.0	348.10	39.11	280.00	251.62	1.11
108.00	4.50	4023.0	348.10	39.11	318.00	266.17	1.19
108.00	4.50	4023.0	348.10	39.11	320.00	266.17	1.20
108.00	4.50	3807.0	348.10	25.51	350.00	279.68	1.25
108.00	4.50	3807.0	348.10	25.51	370.00	279.68	1.32
108.00	4.50	3510.0	348.1	25.51	400.00	316.76	1.26
108.00	4.50	3510.0	348.1	25.51	390.00	316.76	1.23
108.00	4.50	3510.0	348.1	39.11	440.00	331.83	1.33

Appendix D: DATABASE OF TESTS UNDER AXIAL COMPRESSION PLUS BENDING

Appendix Table D-1. Database of tests for concrete-filled RHS members subjected to axial compression plus bending in accordance with CSA S16:19

h (mm)	b (mm)	t (mm)	KL (mm)	e (mm)	F_y (MPa)	f_c' (MPa)	C_a (kN)	C_n (kN)	C_a/C_n
120.00	120.00	3.84	2600.0	40.0	330.10	25.46	421.40	346.74	1.22
120.00	120.00	3.84	2600.0	40.0	330.10	25.46	417.50	347.42	1.20
120.00	120.00	3.84	2600.0	50.0	330.10	36.60	423.40	349.56	1.21
140.00	140.00	3.84	2600.0	15.0	330.10	23.55	833.00	661.41	1.26
140.00	140.00	3.84	2600.0	40.0	330.10	23.55	615.40	484.42	1.27
140.00	140.00	3.84	2600.0	60.0	330.10	23.55	509.60	405.66	1.26
140.00	140.00	3.84	2600.0	40.0	330.10	25.46	558.60	504.90	1.11
140.00	140.00	3.84	2600.0	60.0	330.10	36.60	539.00	477.92	1.13
120.00	120.00	5.86	2600.0	15.0	321.10	23.55	754.60	600.99	1.26
120.00	120.00	5.86	2600.0	30.0	321.10	23.55	548.80	491.75	1.12
120.00	120.00	5.86	2600.0	50.0	321.10	23.55	510.60	385.15	1.33
200.00	200.00	5.86	2600.0	30.0	321.10	26.77	1793.40	1475.36	1.22
200.00	200.00	5.86	2600.0	50.0	321.10	22.79	1425.90	1179.45	1.21
200.00	200.00	5.86	2600.0	80.0	321.10	26.77	1200.50	1010.72	1.19

Appendix Table D-2. Database of tests for concrete-filled RHS members subjected to axial compression plus bending in accordance with AISC 360-16

h (mm)	b (mm)	t (mm)	KL (mm)	e (mm)	F_y (MPa)	f_c' (MPa)	C_a (kN)	C_n (kN)	C_a/C_n
150.00	100.00	5.00	2940.0	45.0	331.50	48.10	470.00	535.42	0.88
150.00	100.00	5.00	2940.0	75.0	321.60	47.40	339.00	394.88	0.86
150.00	100.00	5.00	4000.0	6.0	360.80	47.00	667.00	797.02	0.84
150.00	100.00	5.00	4000.0	15.0	355.50	47.70	650.00	701.19	0.93
150.00	100.00	5.00	4000.0	45.0	350.50	48.30	443.00	499.82	0.89
150.00	100.00	5.00	4000.0	75.0	342.50	48.20	344.00	382.99	0.90
150.00	100.00	5.00	4910.0	6.0	360.80	45.70	536.00	648.11	0.83
150.00	100.00	5.00	4910.0	15.0	342.50	46.30	558.00	576.00	0.97
150.00	100.00	5.00	4910.0	45.0	368.00	47.30	356.00	447.92	0.79
150.00	100.00	5.00	4910.0	75.0	350.50	47.50	293.00	350.41	0.84
150.00	100.00	5.00	2940.0	30.0	324.30	51.50	402.00	638.60	0.63
150.00	100.00	5.00	4000.0	30.0	368.00	45.70	349.00	591.27	0.59
150.00	100.00	5.00	4910.0	30.0	355.50	47.20	273.00	502.80	0.54
120.00	120.00	3.84	2600.0	40.0	330.10	25.46	421.40	360.18	1.17
120.00	120.00	3.84	2600.0	40.0	330.10	25.46	417.50	360.18	1.16
120.00	120.00	3.84	2600.0	50.0	330.10	36.60	423.40	344.38	1.23
140.00	140.00	3.84	2600.0	15.0	330.10	23.55	833.00	665.96	1.25
140.00	140.00	3.84	2600.0	40.0	330.10	23.55	615.40	479.98	1.28
140.00	140.00	3.84	2600.0	60.0	330.10	23.55	509.60	392.33	1.30
140.00	140.00	3.84	2600.0	40.0	330.10	25.46	558.60	487.62	1.15
140.00	140.00	3.84	2600.0	60.0	330.10	36.60	539.00	426.74	1.26
120.00	120.00	5.86	2600.0	15.0	321.10	23.55	754.60	653.37	1.15
120.00	120.00	5.86	2600.0	30.0	321.10	23.55	548.80	530.42	1.03
120.00	120.00	5.86	2600.0	50.0	321.10	23.55	510.60	424.04	1.20
200.00	200.00	5.86	2600.0	30.0	321.10	26.77	1793.40	1396.69	1.28
200.00	200.00	5.86	2600.0	50.0	321.10	22.79	1425.90	1111.38	1.28
200.00	200.00	5.86	2600.0	80.0	321.10	26.77	1200.50	908.95	1.32
150.20	150.20	2.91	1110.0	1.1	319.30	68.50	2352.00	1610.71	1.46
149.50	149.50	2.89	2200.0	3.5	319.30	68.50	2077.00	1308.72	1.59
148.60	148.60	2.93	3101.0	2.5	319.30	68.50	1558.00	1157.10	1.35
151.40	151.40	4.77	1085.0	1.1	316.60	68.50	2597.00	1906.25	1.36
150.00	150.00	4.90	2201.0	2.0	316.60	68.50	2381.00	1672.08	1.42
150.70	150.70	4.89	3100.0	3.5	316.60	68.50	1627.00	1434.78	1.13
175.70	134.90	2.91	993.0	1.0	319.30	68.50	2401.00	1727.51	1.39
149.40	149.40	2.89	1090.0	43.0	319.30	68.50	1147.00	599.69	1.91
150.40	150.40	2.91	1115.0	22.0	319.30	68.50	1597.00	886.50	1.80
149.80	149.80	2.92	2203.0	23.5	319.30	68.50	1274.00	801.47	1.59
148.30	148.30	2.87	3101.0	26.0	319.30	68.50	941.00	679.57	1.38
152.10	152.10	4.82	1105.0	41.5	316.60	68.50	1416.00	871.49	1.62
150.60	150.60	4.88	1100.0	21.1	316.60	68.50	1901.00	1190.02	1.60
150.80	150.80	4.86	2199.0	21.0	316.60	68.50	1519.00	1120.10	1.36
150.40	150.40	4.86	3100.0	25.5	316.60	68.50	1103.00	952.30	1.16
176.20	135.70	2.91	988.0	20.5	319.30	68.50	1911.00	1030.59	1.85
173.50	134.10	2.93	989.0	41.0	319.30	68.50	1343.00	703.92	1.91
174.90	134.80	2.93	988.0	72.0	319.30	68.50	823.00	491.10	1.68
174.60	136.40	2.89	1982.0	21.0	319.30	68.50	1588.00	966.49	1.64
176.20	137.20	4.82	990.0	20.0	316.60	68.50	2058.00	1348.38	1.53
175.10	137.20	4.83	1980.0	22.0	316.60	68.50	1813.00	1243.40	1.46

Appendix Table D-3. Database of tests for concrete-filled RHS members subjected to axial compression plus bending in accordance with Tousignant & Packer (2022a,b) Approach (i)

h (mm)	b (mm)	t (mm)	KL (mm)	e (mm)	F_y (MPa)	f_c' (MPa)	C_a (kN)	C_n (kN)	C_a/C_n
150.00	100.00	5.00	2940.0	45.0	331.50	48.10	470.00	560.63	0.84
150.00	100.00	5.00	2940.0	75.0	321.60	47.40	339.00	437.57	0.77
150.00	100.00	5.00	4000.0	6.0	360.80	47.00	667.00	713.59	0.93
150.00	100.00	5.00	4000.0	15.0	355.50	47.70	650.00	594.51	1.09
150.00	100.00	5.00	4000.0	45.0	350.50	48.30	443.00	450.30	0.98
150.00	100.00	5.00	4000.0	75.0	342.50	48.20	344.00	367.97	0.93
150.00	100.00	5.00	4910.0	6.0	360.80	45.70	536.00	538.69	1.00
150.00	100.00	5.00	4910.0	15.0	342.50	46.30	558.00	419.37	1.33
150.00	100.00	5.00	4910.0	45.0	368.00	47.30	356.00	369.39	0.96
150.00	100.00	5.00	4910.0	75.0	350.50	47.50	293.00	305.77	0.96
150.00	100.00	5.00	2940.0	30.0	324.30	51.50	402.00	678.41	0.59
150.00	100.00	5.00	4000.0	30.0	368.00	45.70	349.00	556.09	0.63
150.00	100.00	5.00	4910.0	30.0	355.50	47.20	273.00	450.69	0.61
120.00	120.00	3.84	2600.0	40.0	330.10	25.46	421.40	346.74	1.22
120.00	120.00	3.84	2600.0	40.0	330.10	25.46	417.50	347.42	1.20
120.00	120.00	3.84	2600.0	50.0	330.10	36.60	423.40	349.56	1.21
140.00	140.00	3.84	2600.0	15.0	330.10	23.55	833.00	661.41	1.26
140.00	140.00	3.84	2600.0	40.0	330.10	23.55	615.40	484.42	1.27
140.00	140.00	3.84	2600.0	60.0	330.10	23.55	509.60	405.66	1.26
140.00	140.00	3.84	2600.0	40.0	330.10	25.46	558.60	504.90	1.11
140.00	140.00	3.84	2600.0	60.0	330.10	36.60	539.00	477.92	1.13
120.00	120.00	5.86	2600.0	15.0	321.10	23.55	754.60	600.99	1.26
120.00	120.00	5.86	2600.0	30.0	321.10	23.55	548.80	491.75	1.12
120.00	120.00	5.86	2600.0	50.0	321.10	23.55	510.60	385.15	1.33
200.00	200.00	5.86	2600.0	30.0	321.10	26.77	1793.40	1475.36	1.22
200.00	200.00	5.86	2600.0	50.0	321.10	22.79	1425.90	1179.45	1.21
200.00	200.00	5.86	2600.0	80.0	321.10	26.77	1200.50	1010.72	1.19
150.20	150.20	2.91	1110.0	1.1	319.30	68.50	2352.00	1566.17	1.50
149.50	149.50	2.89	2200.0	3.5	319.30	68.50	2077.00	1327.06	1.57
148.60	148.60	2.93	3101.0	2.5	319.30	68.50	1558.00	1066.58	1.46
151.40	151.40	4.77	1085.0	1.1	316.60	68.50	2597.00	1849.03	1.40
150.00	150.00	4.90	2201.0	2.0	316.60	68.50	2381.00	1657.38	1.44
150.70	150.70	4.89	3100.0	3.5	316.60	68.50	1627.00	1363.88	1.19
175.70	134.90	2.91	993.0	1.0	319.30	68.50	2401.00	1654.43	1.45
149.40	149.40	2.89	1090.0	43.0	319.30	68.50	1147.00	971.83	1.18
150.40	150.40	2.91	1115.0	22.0	319.30	68.50	1597.00	1203.91	1.33
149.80	149.80	2.92	2203.0	23.5	319.30	68.50	1274.00	1023.15	1.25
148.30	148.30	2.87	3101.0	26.0	319.30	68.50	941.00	778.19	1.21
152.10	152.10	4.82	1105.0	41.5	316.60	68.50	1416.00	1137.91	1.24
150.60	150.60	4.88	1100.0	21.1	316.60	68.50	1901.00	1387.48	1.37
150.80	150.80	4.86	2199.0	21.0	316.60	68.50	1519.00	1238.57	1.23
150.40	150.40	4.86	3100.0	25.5	316.60	68.50	1103.00	979.52	1.13
176.20	135.70	2.91	988.0	20.5	319.30	68.50	1911.00	1346.09	1.42
173.50	134.10	2.93	989.0	41.0	319.30	68.50	1343.00	1093.33	1.23
174.90	134.80	2.93	988.0	72.0	319.30	68.50	823.00	893.92	0.92
174.60	136.40	2.89	1982.0	21.0	319.30	68.50	1588.00	1237.01	1.28
176.20	137.20	4.82	990.0	20.0	316.60	68.50	2058.00	1548.96	1.33
175.10	137.20	4.83	1980.0	22.0	316.60	68.50	1813.00	1410.88	1.29

Appendix Table D-4. Database of tests for concrete-filled RHS members subjected to axial compression plus bending in accordance with Tousignant & Packer (2022a,b) Approach (ii)

h (mm)	b (mm)	t (mm)	KL (mm)	e (mm)	F_y (MPa)	f_c' (MPa)	C_a (kN)	C_n (kN)	C_a/C_n
150.00	100.00	5.00	2940.0	45.0	331.50	48.10	470.00	444.97	1.06
150.00	100.00	5.00	2940.0	75.0	321.60	47.40	339.00	329.66	1.03
150.00	100.00	5.00	4000.0	6.0	360.80	47.00	667.00	666.60	1.00
150.00	100.00	5.00	4000.0	15.0	355.50	47.70	650.00	518.62	1.25
150.00	100.00	5.00	4000.0	45.0	350.50	48.30	443.00	362.44	1.22
150.00	100.00	5.00	4000.0	75.0	342.50	48.20	344.00	282.95	1.22
150.00	100.00	5.00	4910.0	6.0	360.80	45.70	536.00	501.46	1.07
150.00	100.00	5.00	4910.0	15.0	342.50	46.30	558.00	356.88	1.56
150.00	100.00	5.00	4910.0	45.0	368.00	47.30	356.00	305.46	1.17
150.00	100.00	5.00	4910.0	75.0	350.50	47.50	293.00	240.50	1.22
150.00	100.00	5.00	2940.0	30.0	324.30	51.50	402.00	557.41	0.72
150.00	100.00	5.00	4000.0	30.0	368.00	45.70	349.00	480.23	0.73
150.00	100.00	5.00	4910.0	30.0	355.50	47.20	273.00	392.08	0.70
120.00	120.00	3.84	2600.0	40.0	330.10	25.46	421.40	315.32	1.34
120.00	120.00	3.84	2600.0	40.0	330.10	25.46	417.50	315.99	1.32
120.00	120.00	3.84	2600.0	50.0	330.10	36.60	423.40	293.31	1.44
140.00	140.00	3.84	2600.0	15.0	330.10	23.55	833.00	621.79	1.34
140.00	140.00	3.84	2600.0	40.0	330.10	23.55	615.40	436.76	1.41
140.00	140.00	3.84	2600.0	60.0	330.10	23.55	509.60	359.21	1.42
140.00	140.00	3.84	2600.0	40.0	330.10	25.46	558.60	450.31	1.24
140.00	140.00	3.84	2600.0	60.0	330.10	36.60	539.00	383.85	1.40
120.00	120.00	5.86	2600.0	15.0	321.10	23.55	754.60	590.88	1.28
120.00	120.00	5.86	2600.0	30.0	321.10	23.55	548.80	480.42	1.14
120.00	120.00	5.86	2600.0	50.0	321.10	23.55	510.60	373.96	1.37
200.00	200.00	5.86	2600.0	30.0	321.10	26.77	1793.40	1363.36	1.32
200.00	200.00	5.86	2600.0	50.0	321.10	22.79	1425.90	1086.63	1.31
200.00	200.00	5.86	2600.0	80.0	321.10	26.77	1200.50	886.24	1.35
150.20	150.20	2.91	1110.0	1.1	319.30	68.50	2352.00	1520.50	1.55
149.50	149.50	2.89	2200.0	3.5	319.30	68.50	2077.00	1158.33	1.79
148.60	148.60	2.93	3101.0	2.5	319.30	68.50	1558.00	901.47	1.73
151.40	151.40	4.77	1085.0	1.1	316.60	68.50	2597.00	1819.67	1.43
150.00	150.00	4.90	2201.0	2.0	316.60	68.50	2381.00	1592.90	1.49
150.70	150.70	4.89	3100.0	3.5	316.60	68.50	1627.00	1263.67	1.29
175.70	134.90	2.91	993.0	1.0	319.30	68.50	2401.00	1607.73	1.49
149.40	149.40	2.89	1090.0	43.0	319.30	68.50	1147.00	577.98	1.98
150.40	150.40	2.91	1115.0	22.0	319.30	68.50	1597.00	837.78	1.91
149.80	149.80	2.92	2203.0	23.5	319.30	68.50	1274.00	672.44	1.89
148.30	148.30	2.87	3101.0	26.0	319.30	68.50	941.00	485.39	1.94
152.10	152.10	4.82	1105.0	41.5	316.60	68.50	1416.00	845.50	1.67
150.60	150.60	4.88	1100.0	21.1	316.60	68.50	1901.00	1138.76	1.67
150.80	150.80	4.86	2199.0	21.0	316.60	68.50	1519.00	993.53	1.53
150.40	150.40	4.86	3100.0	25.5	316.60	68.50	1103.00	760.21	1.45
176.20	135.70	2.91	988.0	20.5	319.30	68.50	1911.00	914.62	2.09
173.50	134.10	2.93	989.0	41.0	319.30	68.50	1343.00	619.67	2.17
174.90	134.80	2.93	988.0	72.0	319.30	68.50	823.00	433.70	1.90
174.60	136.40	2.89	1982.0	21.0	319.30	68.50	1588.00	798.54	1.99
176.20	137.20	4.82	990.0	20.0	316.60	68.50	2058.00	1222.47	1.68
175.10	137.20	4.83	1980.0	22.0	316.60	68.50	1813.00	1071.12	1.69

Appendix Table D-5. Database of tests for concrete-filled CHS members subjected to axial compression plus bending in accordance with CSA S16:19

d (mm)	t (mm)	KL (mm)	e (mm)	F_y (MPa)	f_c' (MPa)	C_a (kN)	C_n (kN)	C_a/C_n
169.00	5.10	3327.0	47.6	309.00	37.80	622.00	643.09	0.97
169.00	5.26	3327.0	38.1	309.00	36.80	702.00	698.02	1.01
169.00	7.19	3327.0	47.6	312.00	21.80	653.00	663.95	0.98
169.00	7.29	3327.0	38.1	312.00	22.60	739.00	734.72	1.01
169.00	8.81	3302.0	47.6	323.00	22.50	758.00	781.19	0.97
132.00	4.50	2050.0	98.4	341.33	24.80	225.40	255.71	0.88
132.00	4.50	2050.0	73.8	341.33	24.80	307.72	303.62	1.01
132.00	4.50	2060.0	86.1	341.33	24.80	270.48	277.12	0.98
132.00	4.50	2050.0	48.2	341.33	24.80	405.72	379.31	1.07
108.00	4.50	2700.0	8.4	341.33	37.30	443.94	359.74	1.23
108.00	4.16	2380.0	35.9	341.33	37.30	250.88	262.23	0.96
108.00	4.00	2520.0	59.3	341.33	37.30	188.16	199.35	0.94
108.00	4.00	2440.0	78.5	341.33	37.30	148.96	177.55	0.84
108.00	4.00	2960.0	10.0	341.33	37.30	276.36	291.70	0.95
108.00	4.00	2940.0	38.8	341.33	37.30	205.80	207.08	0.99
108.00	4.00	2890.0	60.0	341.33	37.30	145.04	177.48	0.82
108.00	4.00	2910.0	77.5	341.33	37.30	135.24	157.18	0.86
166.00	5.00	710.0	20.0	329.28	38.21	1568.00	1268.30	1.24
166.00	5.00	710.0	40.0	313.60	38.21	1038.80	932.31	1.11
166.00	5.00	2700.0	20.0	329.28	27.80	808.50	828.16	0.98
166.00	5.00	2700.0	20.0	329.28	27.81	784.00	828.23	0.95
166.00	5.00	3700.0	100.0	303.80	27.81	303.80	364.52	0.83

Appendix Table D-6. Database of tests for concrete-filled CHS members subjected to axial compression plus bending in accordance with AISC 360-16

d (mm)	t (mm)	KL (mm)	e (mm)	F_y (MPa)	f_c' (MPa)	C_a (kN)	C_n (kN)	C_a/C_n
169.00	5.26	3327.0	38.1	309.00	36.80	702.00	656.67	1.07
169.00	7.19	3327.0	47.6	312.00	21.80	653.00	672.28	0.97
169.00	7.29	3327.0	38.1	312.00	22.60	739.00	749.58	0.99
169.00	8.81	3302.0	47.6	323.00	22.50	758.00	806.72	0.94
108.00	4.50	2700.0	8.4	341.33	37.30	443.94	409.89	1.08
108.00	4.16	2380.0	35.9	341.33	37.30	250.88	265.70	0.94
108.00	4.00	2520.0	59.3	341.33	37.30	188.16	192.65	0.98
108.00	4.00	2440.0	78.5	341.33	37.30	148.96	162.41	0.92
108.00	4.00	2960.0	10.0	341.33	37.30	276.36	342.57	0.81
108.00	4.00	2940.0	38.8	341.33	37.30	205.80	226.12	0.91
108.00	4.00	2890.0	60.0	341.33	37.30	145.04	181.70	0.80
108.00	4.00	2910.0	77.5	341.33	37.30	135.24	154.92	0.87

Appendix Table D-7. Database of tests for concrete-filled CHS members subjected to axial compression plus bending in accordance with Tousignant & Packer (2022a,b) Approach (i)

d (mm)	t (mm)	KL (mm)	e (mm)	F_y (MPa)	f_c' (MPa)	C_a (kN)	C_n (kN)	C_a/C_n
169.00	5.26	3327.0	38.1	309.00	36.80	702.00	630.36	1.11
169.00	7.19	3327.0	47.6	312.00	21.80	653.00	620.38	1.05
169.00	7.29	3327.0	38.1	312.00	22.60	739.00	687.88	1.07
169.00	8.81	3302.0	47.6	323.00	22.50	758.00	734.06	1.03
108.00	4.50	2700.0	8.4	341.33	37.30	443.94	310.31	1.43
108.00	4.16	2380.0	35.9	341.33	37.30	250.88	239.83	1.05
108.00	4.00	2520.0	59.3	341.33	37.30	188.16	178.76	1.05
108.00	4.00	2440.0	78.5	341.33	37.30	148.96	160.42	0.93
108.00	4.00	2960.0	10.0	341.33	37.30	276.36	282.70	0.98
108.00	4.00	2940.0	38.8	341.33	37.30	205.80	187.67	1.10
108.00	4.00	2890.0	60.0	341.33	37.30	145.04	166.20	0.87
108.00	4.00	2910.0	77.5	341.33	37.30	135.24	143.20	0.94

Appendix Table D-8. Database of tests for concrete-filled CHS members subjected to axial compression plus bending in accordance with Tousignant & Packer (2022a,b) Approach (ii)

d (mm)	t (mm)	KL (mm)	e (mm)	F_y (MPa)	f_c' (MPa)	C_a (kN)	C_n (kN)	C_a/C_n
169.00	5.26	3327.0	38.1	309.00	36.80	702.00	533.11	1.32
169.00	7.19	3327.0	47.6	312.00	21.80	653.00	598.29	1.09
169.00	7.29	3327.0	38.1	312.00	22.60	739.00	664.24	1.11
169.00	8.81	3302.0	47.6	323.00	22.50	758.00	725.08	1.05
108.00	4.50	2700.0	8.4	341.33	37.30	443.94	290.86	1.53
108.00	4.16	2380.0	35.9	341.33	37.30	250.88	212.90	1.18
108.00	4.00	2520.0	59.3	341.33	37.30	188.16	154.11	1.22
108.00	4.00	2440.0	78.5	341.33	37.30	148.96	136.66	1.09
108.00	4.00	2960.0	10.0	341.33	37.30	276.36	264.56	1.04
108.00	4.00	2940.0	38.8	341.33	37.30	205.80	165.73	1.24
108.00	4.00	2890.0	60.0	341.33	37.30	145.04	144.68	1.00
108.00	4.00	2910.0	77.5	341.33	37.30	135.24	123.20	1.10

Appendix E: SAMPLE MCS CODE IN ACCORDANCE WITH APPROACH (I)

This appendix explains a sample of MCS code for concrete-filled RHS beam-columns in accordance with Approach (i).

```
%VARIABLES
Fc = [20,50,70,90]; %concrete strength
e = [100,200,300,500]; %eccentricity
h = [355.6,355.6,304.8,304.8,254,254,203.42,203.2,177.8,177.8,152.4,152.4]; %column height
b = [355.6,355.6,304.8,304.8,254,254,203.42,203.2,177.8,177.8,152.4,152.4]; %column width
t = [12.7,6.35,12.7,6.35,12.7,6.35,12.7,6.35,12.7,6.35,12.7,6.35]; %column thickness
KL_r = [20,50,100,150,200,250,300]; %effective length

PhiR = 0.9; %steel resistance factor
PhiC = 0.65; %concrete resistance factor
Fy = 350; %Yield strength
K = 1.0; %effective length factor
Es = 200000; %modulus of Elasticity
Gamma = 2400; %concrete density
Ec = (3300*sqrt(Fc)+6900)*(Gamma/2300)^2; %modulus of elasticity of concrete

L_D = [0,0.1,0.135,0.2,0.3,0.4,0.5,0.6,0.8,1.0,1.2,1.5,1.7,2.0,2.3,2.5,2.8,3.0]; %live to dead load ratio
for i = 1:length(L_D)
   if L_D(i) <= 0.135
      alphaD(i,1) = 1.4; %dead load factor
      alphaL(i,1) = 0; %live load factor
   else
      alphaD(i,1) = 1.25;  %dead load factor
      alphaL(i,1) = 1.5;  %live load factor
   end
end
```

```
N = 1000000; %number of simulations
B_length = length(h)*length(KL_r)*length(Fc)*length(e)*length(L_D);
q = 0;

R = zeros(N,1); %resistance array for simulations
S = zeros(N,1); %load array for simulations

mPF = 1.17; %mean ratio professional factor
COVPF = 0.19; %COV professional factor

locPF= log(mPF^2/sqrt((mPF*COVPF)^2 + mPF^2)); %lognormal mean Professional factor
scalePF= sqrt(log(1 + ((mPF*COVPF)/mPF)^2)); %lognormal std. Professional factor
rPF = lognrnd(locPF,scalePF,N,1); %random Professional factor actual/predicted ratio

mD = 1.05; %mean ratio dead load from Schmidt & Bartlett
COVD = 0.1; %COV dead load from Schmidt & Bartlett

mL = 0.78; %mean ratio live load from Schmidt & Bartlett
COVL = 0.32; %COV live load from Schmidt & Bartlett

mEs= 1.00; %mean ratio modulus of elasticity
COVEs= 0.019; %COV modulus of elasticity

mFy = 1.178; %mean ratio yield strength from Xi & Packer
COVFy = 0.086; %COV yield strength from Xi & Packer

mFc = 1.270; %mean ratio concrete strength from Bartlett
COVFc = 0.122; %COV concrete strength from Bartlett

mH = 1.0016; %mean actual/predicted ratio cross sectional depth from Kennedy and Gad Aly
COVH = 0.0026; %COV actual/predicted ratio cross sectional depth from Kennedy and Gad Aly

mB = 1.0016; %mean actual/predicted ratio cross sectional width from Kennedy and Gad Aly
COVB = 0.0026; %COV actual/predicted cross sectional width from Kennedy and Gad Aly
```

```
mt = 0.975; %mean actual/predicted ratio cross sectional thickness from Kennedy and Gad Aly
COVt = 0.025; %COV actual/predicted cross sectional thickness from Kennedy and Gad Aly

%RANDOM SAMPLES

locD= log(mD^2/sqrt((mD*COVD)^2 + mD^2)); %lognormal mean dead load
scaleD= sqrt(log(1 + ((mD*COVD)/mD)^2)); %lognormal std. dead load
rD = lognrnd(locD,scaleD,N,1); %random dead load actual/predicted ratios

locL= log(mL^2/sqrt((mL*COVL)^2 + mL^2)); %lognormal mean live load
scaleL= sqrt(log(1 + ((mL*COVL)/mL)^2)); %lognormal std. live load
rL = lognrnd(locL,scaleL,N,1); %random live load actual/predicted ratios

locEs= log(mEs^2/sqrt((mEs*COVEs)^2 + mEs^2)); %lognormal mean modulus of elasticity
scaleEs= sqrt(log(1 + ((mEs*COVEs)/mEs)^2)); %lognormal std. modulus of elasticity
rEs = lognrnd(locEs,scaleEs,N,1); %random modulus of elasticity actual/predicted ratios

j = 1;
NN = N;
while NN>0
   NN = (N + 1) - j;
   locFy= log(mFy^2/sqrt((mFy*COVFy)^2 + mFy^2)); %lognormal mean concrete yield strength
   scaleFy= sqrt(log(1 + ((mFy*COVFy)/mFy)^2)); %lognormal std. yield strength
   rFy_Temp = lognrnd(locFy,scaleFy,NN,1); %random yield strength actual/predicted ratios
   for i = 1:NN
      if rFy_Temp(i)>=1
         rFy(j,1) = rFy_Temp(i);
         j = j + 1;
      end
   end
end

j = 1;
NN = N;
while NN>0
```

```
    NN = (N + 1) - j;
    locFc= log(mFc^2/sqrt((mFc*COVFc)^2 + mFc^2)); %lognormal mean concrete strength
    scaleFc= sqrt(log(1 + ((mFc*COVFc)/mFc)^2)); %lognormal std. concrete strength
    rFc_Temp = lognrnd(locFc,scaleFc,NN,1); %random concrete strength actual/predicted ratios
    for i = 1:NN
        if rFc_Temp(i)>=1
            rFc(j,1) = rFc_Temp(i);
            j = j + 1;
        end
    end
end

loch = log(mh^2/sqrt((mh*COVh)^2 + mh^2)); %lognormal mean cross sectional depth
scaleh = sqrt(log(1 + ((mh*COVh)/mh)^2)); %lognormal std. cross sectional depth
rh = lognrnd(loch,scaleh,N,1); %random cross sectional depth actual/predicted ratios

locb = log(mb^2/sqrt((mb*COVb)^2 + mb^2)); %lognormal mean cross sectional width
scaleb = sqrt(log(1 + ((mb*COVb)/mb)^2)); %lognormal std. cross sectional width
rb = lognrnd(locb,scaleb,N,1); %random cross sectional width actual/predicted ratios

loct= log(mt^2/sqrt((mt*COVt)^2 + mt^2)); %lognormal mean cross sectional thickness
scalet= sqrt(log(1 + ((mt*COVt)/mt)^2)); %lognormal std. cross sectional thickness
rt = lognrnd(loct,scalet,N,1); %random cross sectional thickness actual/predicted ratios

%% SAMPLES R AND S RECORDER INITIAL DEFINITIONS

R_UP = 7500;
R_LOW = 0;
R_BIN_SIZE = 100;
R_N_REC = (R_UP - R_LOW)/R_BIN_SIZE;
R_Rec = zeros(R_N_REC,1);
o = 0;

S_UP = 7500;
S_LOW = 0;
S_BIN_SIZE = 100;
```

```
S_N_REC = (S_UP - S_LOW)/S_BIN_SIZE;
S_Rec = zeros(S_N_REC,1);
p = 0;

%SOLUTION (Functions tabulated here can be found at the end of the code)

for i = 1:length(h) %Section Varies%
    for j = 1:length(KL_r) %KL/r Varies%
        for m = 1:length(Fc) %Fc Varies%
            [Cr_nominal(j,m,i),Cec_nominal(j,m,i),Crco_nominal(j,m,i),Crcm_nominal(j,m,i)]=
            AxialFactoredResistanceA1R(h(i),b(i),t(i),Fy,Fc(m),KL_r(j),PhiR,PhiC,Es,Ec(m));
            % Factored resistance equation for compression using nominal values
            Mr_nominal(j,m,i)=BendingFactoredResistanceA1R(h(i),b(i),t(i),Fy,Fc(m),PhiR,Phi
            C); %Factored resistance equation for flexure using nominal values
            Betha_nominal(j,m,i)=(Crco_nominal(j,m,i)-
            Crcm_nominal(j,m,i))/Crco_nominal(j,m,i);
                for k = 1:length(e) %E(ey) Varies%
                delta_nominal(k,j,m,i)=(Mr_nominal(j,m,i)*Cec_nominal(j,m,i)+Mr_nomin
                al(j,m,i)*Cr_nominal(j,m,i)+Betha_nominal(j,m,i)*e(k)*Cr_nominal(j,m,i)*
                Cec_nominal(j,m,i))^2-
                4*(Mr_nominal(j,m,i))^2*Cr_nominal(j,m,i)*Cec_nominal(j,m,i);
                Rf_nominal(k,j,m,i)=((Mr_nominal(j,m,i)*Cec_nominal(j,m,i)+Mr_nominal
                (j,m,i)*Cr_nominal(j,m,i)+
                Betha_nominal(j,m,i)*e(k)*Cr_nominal(j,m,i)*Cec_nominal(j,m,i))-
                sqrt(delta_nominal(k,j,m,i))) / (2*Mr_nominal(j,m,i)); %Factored resistance
                equation using nominal values
                    for n = 1:length(L_D) %Sampling for the variant%
                    [L,D]=NominalLiveDeadLoadA1R(alphaD(n),alphaL(n),L_D(n),Rf
                    _nominal(k,j,m,i)); %nominal dead and live loads
                        for c = 1:N %Sample Resistance R%

%Compression

As(c,1)=2*(t(i)*rt(c,1))*((b(i)*rb(c,1))+(h(i)*rh(c,1))-2*t(i)*rt(c,1))-(pi)*(((2*(t(i)*rt(c,1)))^2)-
((t(i)*rt(c,1))^2)); %cross sectional area of steel
```

```
Ac(c,1)=((b(i)*rb(c,1))-2*(t(i)*rt(c,1)))*((h(i)*rh(c,1))-2*(t(i)*rt(c,1)))-(4-pi)*((t(i)*rt(c,1))^2);%cross sectional area of concrete
alphaC(c,1) = max(0.85-0.0015*(Fc(m)*rFc(c,1)),0.73);
Cp(c,1) = As(c,1)*(Fy*rFy(c,1))+alphaC(c,1)*Ac(c,1)*(Fc(m)*rFc(c,1));  %Plastic section capacity
Ig(c,1) = (1/3 - pi/16 - 1/(3*(12-3*pi)))*(2*(t(i)*rt(c,1)))^4;
Ag(c,1) = (1-pi/4)*(2*(t(i)*rt(c,1)))^2;
hgh(c,1) = (h(i)*rh(c,1))/2 - ((10-3*pi)/(12-3*pi))*2*(t(i)*rt(c,1));
Ie(c,1) = (1/3 - pi/16 - 1/(3*(12-3*pi)))*(t(i)*rt(c,1))^4;
Ae(c,1) = (1-pi/4)*(t(i)*rt(c,1))^2;
heh(c,1) = ((h(i)*rh(c,1))-2*(t(i)*rt(c,1)))/2 - ((10-3*pi)/(12-3*pi))*(t(i)*rt(c,1));
Is(c,1) = ((b(i)*rb(c,1))*(h(i)*rh(c,1))^3)/12 - (((b(i)*rb(c,1))-2*(t(i)*rt(c,1)))*((h(i)*rh(c,1))-2*(t(i)*rt(c,1)))^3)/12 - 4*(Ig(c,1)+Ag(c,1)*hgh(c,1)^2)+4*(Ie(c,1)+Ae(c,1)*heh(c,1)^2); %moment of inertia of steel
Ic(c,1)=(((b(i)*rb(c,1))-2*(t(i)*rt(c,1)))*((h(i)*rh(c,1))-2*(t(i)*rt(c,1)))^3)/12+4*(Ie(c,1)+Ae(c,1)*heh(c,1)^2); %moment of inertia of concrete
r(c,1) = sqrt(Is(c,1)/As(c,1)); %radius of gyration
EIe(c,1) = ((Es*rEs(c,1))*Is(c,1)+0.6*Ec(m)*Ic(c,1)); %effective flexural stiffness for the whole composite section
Cec_sample(c,1)  = (pi^2)*EIe(c,1)/(r(c,1)*KL_r(j))^2; %euler buckling load
lambda(c,1) = sqrt(Cp(c,1)/Cec_sample(c,1));
tau(c,1) = 1;
taup(c,1) = 1;
Crco_sample(c,1) = (tau(c,1)*1*As(c,1)*(Fy*rFy(c,1)) + taup(c,1)*alphaC(c,1)*1*Ac(c,1)*(Fc(m)*rFc(c,1))) / (1)^(1/1.8); %axial nominal resistance with lambda=0
Crcm_sample(c,1) = 1.18*alphaC(c,1)*Ac(c,1)*(Fc(m)*rFc(c,1));

Cr_sample(c,1) = (tau(c,1)*1*As(c,1)*(Fy*rFy(c,1)) + taup(c,1)*alphaC(c,1)*1*Ac(c,1)*(Fc(m)*rFc(c,1))) / (1+lambda(c,1)^(2*1.8))^(1/1.8); %axial factored resistance equation

%Flexure
fc(c,1) = 1.18*alphaC(c,1)*(Fc(m)*rFc(c,1));
Zs(c,1) = (b(i)*rb(c,1))*(h(i)*rh(c,1))^2/4 - ((b(i)*rb(c,1))-2*(t(i)*rt(c,1)))*((h(i)*rh(c,1))-2*(t(i)*rt(c,1)))^2/4 - (4*Ag(c,1)*hgh(c,1)) + (4*Ae(c,1)*heh(c,1)); %plastic modulus of the steel alone
Zc(c,1)= ((b(i)*rb(c,1))-2*(t(i)*rt(c,1)))*((h(i)*rh(c,1))-2*(t(i)*rt(c,1)))^2/4 - 0.429*(t(i)*rt(c,1))^2*((h(i)*rh(c,1))-2*(t(i)*rt(c,1))) + 0.192*(t(i)*rt(c,1))^3; %plastic modulus of concrete alone
```

```
a(c,1) = ((h(i)*rh(c,1))-2*(t(i)*rt(c,1)))/2 - (Ac(c,1)*1*fc(c,1))/(8*(t(i)*rt(c,1))*1*(Fy*rFy(c,1)) + 2*((B(i)*rB(c,1))-2*(t(i)*rt(c,1)))*fc(c,1)*1); %depth of concrete compression zone

Mr_sample(c,1) = Zs(c,1)*1*(Fy*rFy(c,1)) - 2*(t(i)*rt(c,1))*(((h(i)*rh(c,1))-2*(t(i)*rt(c,1)))/2-a(c,1))^2*1*(Fy*rFy(c,1)) + Zc(c,1)/2*1*fc(c,1) - ((b(i)*rb(c,1))-2*(t(i)*rt(c,1)))/2*(((h(i)*rh(c,1))-2*(t(i)*rt(c,1)))/2-a(c,1))^2*1*fc(c,1); %Flexural factored equation

% Resistance equation
Betha_sample(c,1) = (Crco_sample(c,1)-Crcm_sample(c,1))/Crco_sample(c,1);

delta_sample(c,1) = (Mr_sample(c,1)*Cec_sample(c,1) + Mr_sample(c,1)*Cr_sample(c,1) + Betha_sample(c,1)*e(k)*Cr_sample(c,1)*Cec_sample(c,1))^2 - 4*(Mr_sample(c,1))^2*Cr_sample(c,1)*Cec_sample(c,1);
R(c,1) =rPF(c,1)*(((Mr_sample(c,1)*Cec_sample(c,1) + Mr_sample(c,1)*Cr_sample(c,1) + Betha_sample(c,1)*e(k)*Cr_sample(c,1)*Cec_sample(c,1)) - sqrt(delta_sample(c,1))) / (2*Mr_sample(c,1)));
%Factored resistance equation using nominal values


        end

        %LOAD EFFECT

        for c =1:N
          S(c,1) = (D*rD(c,1))+(L*rL(c,1)); %Load equation

          % FREQUENCY RECORDE FOR S HISTOGRAM
          if i==5 && j==3 && m==2 && k==1 && n==10
              S_BIN_NO = fix((S(c,1)/1000)/S_BIN_SIZE) + 1; %divided by 1000 convert to kN
              S_Rec(S_BIN_NO,1) = S_Rec(S_BIN_NO,1) + 1;
              p = p + 1;
              S_Rec_Data(p,1) = S(c,1)/1000;
          end

        end

        %RELIABILITY
```

```
            G = log(R) - log(S);
            q = q + 1;
            beta_plus(q,1) = mean(G)/std(G) %Reliability index

        end
      end
    end
  end
end

%% CONVERT S AND R HISTOGRAM VALUES TO FREQUENCIES
R_Rec_Freq = R_Rec/sum(R_Rec,'all')*100;
S_Rec_Freq = S_Rec/sum(S_Rec,'all')*100;

%AXIAL RESISTANCE FUNCTION

function[Cr_nominal,Cec_nominal,Crco_nominal,Crcm_nominal]=
AxialFactoredResistanceA1R(h,b,t,Fy,Fc,KL_r,PhiR,PhiC,Es,Ec) % Factored resistance equation for
compression using nominal values

% Determine the axial factored resistance of RHS Beam-Columns

As = 2*t*(b+h-2*t)-(4-pi)*(((2*t)^2)-(t^2)); %cross sectional area of steel
Ac = (b-2*t)*(h-2*t)-(4-pi)*(t^2); %cross sectional area of concrete
alphaC = max(0.85-0.0015*Fc,0.73);
Cp = As*Fy+alphaC*Ac*Fc;  %Plastic section capacity
Ig = (1/3 - pi/16 - 1/(3*(12-3*pi)))*(2*t)^4;
Ag = (1-pi/4)*(2*t)^2;
hgh = h/2 - ((10-3*pi)/(12-3*pi))*2*t;
Ie = (1/3 - pi/16 - 1/(3*(12-3*pi)))*t^4;
Ae = (1-pi/4)*t^2;
heh = (h-2*t)/2 - ((10-3*pi)/(12-3*pi))*t;
Is = (b*h^3)/12 - ((b-2*t)*(h-2*t)^3)/12 - 4*(Ig+Ag*hgh^2)+4*(Ie+Ae*heh^2); %moment of inertia of
steel
Ic = ((b-2*t)*(h-2*t)^3)/12+4*(Ie+Ae*heh^2); %moment of inertia of concrete
```

```
r = sqrt(Is/As); %radius of gyration
EIe = (Es*Is+0.6*Ec*Ic); %effective flexural stiffness for the whole composite section
Cec_nominal  = (pi^2)*EIe/(r*KL_r)^2; %Euler buckling load
lambda = sqrt(Cp/Cec_nominal);
tau = 1;
taup = 1;
%resistance
Cr_nominal = (tau*PhiR*As*Fy + taup*alphaC*PhiC*Ac*Fc) / (1+lambda^(2*1.8))^(1/1.8); %axial factored resistance
Crco_nominal = (tau*PhiR*As*Fy + taup*alphaC*PhiC*Ac*Fc) / (1)^(1/1.8); %axial factored resistance with lambda=0
Crcm_nominal = 1.18*alphaC*0.65*Ac*Fc;
end

%BENDING RESISTANCE FUNCTION

function [Mr_nominal] = BendingFactoredResistanceA1R(h,b,t,Fy,Fc,PhiR,PhiC)

%Determine the axial factored resistance of RHS Beam-Columns

Ac = (B-2*t)*(H-2*t)-(4-pi)*(t^2); %cross sectional area of concrete
alphaC = max(0.85-0.0015*Fc,0.73);
fc = 1.18*alphaC*Fc;
%Required values to determine Zc
Ag = (1-pi/4)*(2*t)^2;
hgh = H/2 - ((10-3*pi)/(12-3*pi))*2*t;
Ae = (1-pi/4)*t^2;
heh = (H-2*t)/2 - ((10-3*pi)/(12-3*pi))*t;
Zs = B*H^2/4 - (B-2*t)*(H-2*t)^2/4 - (4*Ag*hgh) + (4*Ae*heh); %plastic modulus of the steel alone
Zc = (B-2*t)*(H-2*t)^2/4 - 0.429*t^2*(H-2*t) + 0.192*t^3; %plastic modulus of concrete alone
a = (H-2*t)/2 - (Ac*PhiC*fc)/(8*t*PhiR*Fy + 2*(B-2*t)*fc*PhiC); %depth of concrete compression zone
% resistance
Mr_nominal = Zs*PhiR*Fy - 2*t*((H-2*t)/2-a)^2*PhiR*Fy + Zc/2*PhiC*fc - (B-2*t)/2*((H-2*t)/2-a)^2*PhiC*fc; %Flexural factored resistance
end
%LOAD FUNCTION
```

```
function [L,D] = NominalLiveDeadLoadA1R(alphaD,alphaL,L_D,S)

% Determines nominal Live and Dead loads based on a given value and dead and live load combination

D = S/(alphaD + (alphaL*L_D));
L = D*L_D;
end
```